Uncovering Hidden Phenotypes to Accelerate Domestication in Perennial Ryegrass for Seed Production

A THESIS
SUBMITTED TO THE FACULTY OF
UNIVERSITY OF MINNESOTA
BY

Joan Barreto Ortiz

IN PARTIAL FULFILLMENT OF THE REQUIREMENTS
FOR THE DEGREE OF
MASTER OF SCIENCE

Eric Watkins and Nancy Ehlke
Advisors

October 2022

Copyright page

Table of contents

List of tables

List of figures

Chapter 1. Literature Review

Overview

Seed dispersion, shattering, shedding, and lack of retention, all refer to the same dispersal mechanism in which reproductive organs detach from plant inflorescences upon maturity. This separation, or disarticulation, is mainly attributed to the development of an abscission layer which is genetically programmed. However, such detachment is just part of the seed dispersal phenomenon determined by a network of interactions between biotic and abiotic agents allowing gene flow over space and time. Understanding the genetics underlying seed dispersal has ecological and agricultural implications; while this phenomenon grants an evolutionary advantage to wild plants, it affects crop productivity and domestication of species with economic potential by severely reducing seed yield. In consequence, variation for dispersal-related traits has been selected over millennia through improving seed retention and yield, thus allowing the development of agriculture and consequent human societies. Nevertheless, genetic correlations among traits can limit the progress of selecting for a dispersal trait and generate unfavorable trade-offs. The presence of these correlations can be attributed to (i) the univariate approach that characterizes both selection methods and the study of multivariate phenotypes like inflorescence architecture and seed dispersal, and (ii) our limited ability to perceive and quantify the multidimensional phenotypic reality. These are the two foci of this introductory chapter, in which I use perennial ryegrass (*Lolium perenne* L.) as an example to discuss the need for a holistic understanding of the relationships between inflorescence morphology and seed dispersal, with an ultimate goal to improve seed yield and plant domestication.

1.1 Introduction

Seed shattering is often acknowledged as the main cause of yield loss in perennial ryegrass and other recently domesticated plant species (Elgersma et al., 1988). This evolutionary mechanism triggers the formation of an abscission zone where seeds disarticulate before they can be harvested, severely affecting productivity and agronomic management (Tubbs, 2021). The availability of tools to quantify variation affecting seed retention has allowed an understanding of the genetics underlying the trait, and consequential yield improvement. Such tools are often unavailable for newly domesticated plants, including perennial ryegrass in which identifying phenotypic patterns is challenged by the inherent heterogeneity of the species (Brazauskas et al., 2011). Nevertheless, seed yield can still be improved by indirect selection on correlated traits of the spike architecture that are heritable and can be selected for (Elgersma et al., 1988).

Inflorescence morphology plays a fundamental role in the multidimensionality of seed dispersal and yield related traits. Its phenotypic complexity is a function of interspecific interactions across space and time that exert selection pressures on heritable traits. Variation for shape of plant structures and temporal dynamics as well as microscopic variation affecting spikelet morphology, abscission zones, seed metabolites, among others, have been selected over evolutionary time by humans and other dispersers. This has resulted in a network of correlated traits controlled by linkage and pleiotropy (Falconer, 1996; Saastamoinen et al., 2018), that can be potentially unfavorable (Keith & Mitchell-Olds, 2019; Oury & Godin, 2007; Wu et al., 2017). Because of the multidimensionality of spike architecture and dispersal, domestication is subject to human bias and indirect

selection; thus, improving dispersal traits such as shattering may not necessarily improve seed yield and growers' acceptability.

Recent computational and analytical tools provide potential for a comprehensive and less subjective characterization of complex traits which could accelerate domestication and crop improvement. Modern sequencing technologies can unveil the genomic basis of complex traits, bolstering our understanding of phenotypic variation and allowing major progress in plant breeding. This requires proper tools to effectively characterize substantial phenotypic variation across heterogeneous populations (Crowell et al., 2016), which could be accomplished with high throughput phenotyping. Nevertheless, this is still challenging for multidimensional phenotypes not only because of the innumerable traits that comprise them but because not all of them can be perceived. In this review chapter, I argue that focusing on characterizing the spike architecture and adopting a more comprehensive definition of "trait" could enable major improvements in seed yield for plants like perennial ryegrass. I focus on the importance of seed dispersal rather than shattering, for the improvement of seed yield and acceptability to seed growers.

1.2. Perennial Ryegrass as a Seed Crop

1.2.1. Perennial Ryegrass

Perennial ryegrass (*Lolium perenne* L.) is a multifunctional cool-season crop with significant economic and environmental importance around the globe. This bunch-type forage and amenity grass is native to Europe, temperate Asia, and North Africa, and has been introduced throughout the world (Terrell, 1968; Thorogood, 2003). It is one of the most widely sown forages worldwide because of its high digestibility and tolerance to

grazing (Wilkins, 1991). In Europe and North America, it is also important as a turf for athletic fields and lawns given its rapid germination and establishment, as well as high wear-tolerance (Sampoux et al., 2013; Shearman & Beard, 1975). Furthermore, perennial ryegrass has ecosystem benefits that include bioremediation of polluted water (Nduwimana et al., 2007; Xu et al., 2021) and soils (Nedunuri et al., 2000; Rezek et al., 2008), making it relevant for restoration and conservation programs.

Like other forage and amenity species with economic potential, perennial ryegrass' acceptance by seed growers depends on its ability to produce profitable seed yield (Elgersma, 1985; Heineck et al., 2020). This is a major concern to growers and breeders because the species is biologically inefficient at seed production being unable to produce more than 20% of its estimated seed yield potential (Abel et al., 2017; Elgersma, 1990b). Breeding efforts in perennial ryegrass have been going for less than a hundred years, and have focused on herbage qualities rather than seed yield (Wilkins, 1991). In consequence, wild morphological traits of the inflorescence that are associated with seed dispersal are still highly pronounced in perennial ryegrass. Changing wild traits through domestication is a slow process; identifying heritable patterns driving phenotypic variation for such traits is paramount to accelerate domestication.

1.2.2. Spike Architecture Determines Seed Yield

In grasses, the terms inflorescence, seed head, ear, and spike, all refer to the same modified panicle the morphology of which determines seed yield potential (Abel et al., 2017). Variation in inflorescence architecture is the main target to facilitate management and reliable seed yield during the domestication of sown grasses (Doust et al., 2014). The spikes in perennial ryegrass contain spikelets attached to the rachis by the pedicel that are

bundled by two glumes. Spikelets are comprised of florets attached by the rachilla where the glumes spread out as the seeds develop. The number and morphological aspects of these components interact with the environmental covariates to directly determine seed yield potential. The number of spikes per plant is highly dependent on crop management (Abel et al., 2017; Chynoweth et al., 2008; Elgersma, 1990b), supporting the importance of the spike architecture for breeding and genetics.

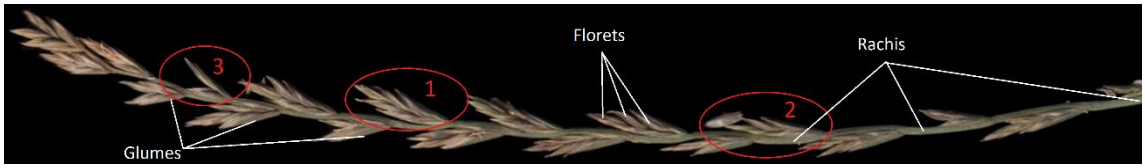

Figure 1.1. Architectural features of the spike in perennial ryegrass. Glumes, florets, and rachis are indicated in white. Circles in red represent 1: whole spikelet, 2: a spikelet beginning to shatter as shown by the detached seed, and 3: a fully shattered spikelet.

Not all the morphological properties of the spike affecting yield related traits are visible to naked eye. The spike architecture is comprised by infinite interacting traits driving morphological changes at micro and macroscopic levels. The interaction between such traits determines visible properties like flowering time and heterogeneity that impact characteristics that are more difficult to perceive such as pollen distribution, fertility, seed set, and floret site utilization (Friedman & Harder, 2004; Shah et al., 1990). Furthermore, microscopic dynamics affecting seed filling (Trethewey & Rolston, 2008), abortion (Kadkol et al., 1989), shattering (Elgersma et al., 1988; Fu et al., 2019), or seed quality, were arguably imperceptible by early domesticators and thus difficult to characterize in field conditions.

While the effect of the spike architecture on yield is indisputable, the way in which its components interact to determine economic seed yield is not fully understood. For

example, research has shown no correlation between yield and spike length, number, and thousand-seed-weight, possibly due to lack of seed development from nutrient deficiency (Elgersma, 1990b). There are also contrasting results regarding the effect of spikelet per spike on yield (Abel et al., 2017; Elgersma, 1990b). While economic seed yield depends on the final weight of saleable seed, genetic variation for yield depends more on the seed number rather than their weight (Elgersma, 1990a). The number of florets at anthesis that become viable seeds, i.e., the biological floret site utilization, is important to the theoretical yield potential; however, economic floret site utilization, i.e., the number of florets that become sealable seeds, determines realized yield (Elgersma, 1985). Growers' profitability depends on the number of harvested seeds, their weight, and ability to germinate conveniently. While poor seed yield in perennial ryegrass depends on infinite interactions that are hard to predict, identifying these interactions and their genetic basis may be essential to developing acceptable varieties.

1.2.3. Wild Traits Relate to Poor Yield

Perennial ryegrass has agricultural importance worldwide not only as a pasture and amenity grass, but also as a weed. As an obligate outcrosser with high self-incompatibility, its genetic diversity and phenotypic heterogeneity are reflected on wild traits that facilitate dispersal and colonization across space and time. This dispersal and its supreme resistance to herbicides cause severe yield reduction in cereal crops (Matzrafi et al., 2021). Because of its recent domestication and cultivation for seed production (Wilkins, 1991) identifying wild traits affecting seed productivity is essential to accelerating genetic gains in yield. Among the morphological, physiological and genetic changes during the domestication, commonly referred to as "domestication syndrome", the ability to retain seed in the

inflorescence is arguably the most important in sown grasses (Peleg et al., 2011). Increased retention, or reduced shattering, allowed early domesticators to have more reliable seed harvest.

The importance of seed shattering in perennial ryegrass is not limited to its reduction in yield potential but its intrinsic relationship with wild traits such as uneven flowering can challenge crop management. Whether perennial ryegrass is swathed or directly combined, growers must account for the overall maturity level of the crop to decide the best time to harvest. While swathing too early stops the seed fill process resulting in smaller and lighter seed, late cutting increases losses due to shattering (Klein & Harmond, 1971; Silberstein et al., 2007). Deciding the optimal time to cut is difficult due to uneven flowering and ripening, as well as the heterogeneity of the crop. Seed moisture content is a more reliable tool to determine time to harvest in perennial ryegrass (Klein & Harmond, 1971) and can be accounted for when estimating shattering. Similarly, the phenological stage can also be estimated using specialized developmental scales (Gustavsson, 2011; Moore et al., 1991). In contrast, there are no current methods with enough accuracy and precision that can evaluate shattering at large-scale which represent a problem for growers. The phenotypic and genetic characterization of shattering-related processes is necessary to improve retention in perennial ryegrass.

1.3. Seed Shattering

Seed shattering is acknowledged as a major cause of yield loss and hence is considered as a primary breeding target during plant domestication (Konishi et al., 2006). Seed shattering, shedding, or lack of retention, commonly refer to a dispersal mechanism

in which organs from plant inflorescences disarticulate upon maturity due to passive and active mechanisms. This disarticulation occurs before and during harvest, dramatically reducing the number of sellable seeds and increasing the number of volunteer plants (Tubbs, 2021). Active shattering is attributed to developmental stresses triggered by the abscission process whereas passive mechanisms require external force and mechanical disturbance (Kadkol, 2009). In perennial ryegrass, the abscission layers can start on the epidermis and extend across the rachilla where seed, attached by vascular bundles, disarticulates approximately five weeks after anthesis (Elgersma et al., 1988). Wind and rain can directly affect the mechanical disarticulation or provide conditions such as lodging that indirectly influence shattering.

Shattering losses in grasses like perennial ryegrass can be as high as 75% (Fu et al., 2019; Simon U et al., 1997) with approximately 10% of the florets lost before harvest (Warringa, 1997) and about 24% during swathing (Rolston et al., 2010). The seeds shed before harvest are commonly the heaviest, representing a substantial proportion of the potential economic yield (Elgersma, 1985). In addition, due to uneven flowering and ripening, more than half of the retained seeds are underdeveloped and thus lost after cleaning due to their light weight (Warringa, 1997). The real effect of shattering on yield is unclear due to its dependency on the interaction between morphological and environmental covariates under a much more complex evolutionary process: seed dispersal. Quantifying a complex trait like shattering depends on its genetic architecture and whether there are major patterns driving its variation.

1.3.1. Conventional Phenotyping

The phenotypic multidimensionality of dispersal traits has historically been simplified through univariate analyses (Saastamoinen et al., 2018). Shattering is often quantified based on the proportion of seeds lost per plant, per inflorescence, or the force required to disarticulate them from the spikelet (Tubbs, 2021). These measurements can be obtained from field observations, lab tests that simulate shattering conditions and measure the strength at the detachment zone, and indirectly by phenotyping morphological features associated with seed retention (Kadkol et al., 1989). Evaluation in field conditions can been accomplished at the plant and inflorescence level by using preestablished nets, containers, or any other material to capture the seeds that shed before harvest (Bitarafan & Andreasen, 2019). Seed could also be vacuumed from the ground and quantified either before and or after swathing (Anderson et al., 2019). The mechanical disturbance from harvest could be induced by physical impact from manual shaking, beating, or artificial winds. One could then measure the amount of shed and or retained seed in the standing crops. However, differences in weather conditions across seasons makes field evaluations inaccurate (Kadkol, 2009).

Laboratory tests simulating in-field detachment or measuring the strength at the disarticulation (abscission) area are suggested as better methods to quantify seed retention capacity (Kadkol, 2009; Zhang & Mergoum, 2007). Because uneven ripening can affect retention estimate, spikes can be classified a priori to minimize variation and properly stored to facilitate further analysis (Hampton & Hebblethwaite, 1985). Mechanical disturbance is then induced at the spike level to quantify the amount of shattering, at the abscission zone level to measure the force required for disarticulation, or both (Yao et al.,

2015). The former includes detaching seeds by shaking spikes with a shaker (Bonin & Goplen, 1963b; Harun & Bean, 1979; Lee, 2006) or manually (Larson & Kellogg, 2009). In addition, the proportion of detached seeds can also be quantified after dropping them from a given height (Yao et al., 2015) or rolling them on a surface (Tubbs, 2021). The most accurate methods measure the force required to dislodge the kernels, an approach widely used in rice that has contributed to characterizing the genetics of shattering in the species (Ji et al., 2006; Jiang et al., 2019). Because using these methods in field conditions is cumbersome, portable versions have been developed (Lamo et al., 2011).

1.3.2. Shattering and Abscission

While shattering is only a fraction of the dispersal phenomenon affecting yield, identifying genes involved in disarticulation is relevant to improving productivity. Shattering depends on abscission, a highly programmed phenomenon that is regulated by auxins, abscisic acid (ABA), and ethylene which are at the same time influenced by gibberellins and cytokinins (Addicott & Wiatr, 1977). Abscission occurs via biochemical reactions that disintegrate the middle lamella and cell walls leading to weak tissue and eventual disarticulation (Elgersma et al., 1988). The predetermined cell differentiation in the abscission zone is the first of this four-step process (Patterson, 2001; Roberts et al., 2002). Perennial ryegrass often initiates secondary (below the spikelet) abscission layers in addition to primary (below the rachilla), and both can be found before anthesis (Elgersma et al., 1988). Secondary abscission zones may be determined by cross-talk between ethylene and indole-2-acetic acid (IAA) that may determine the location for the secondary abscission zone (Roberts et al., 2002). Once the abscission zone has been differentiated, timing and environmental factors contribute to regulating the process. The second step

includes the development of the abscission zone's response to hormonal signals, which start and regulate the third step, the disarticulation progression. External ethylene sources can accelerate this process while auxins (IAA) can delay it (Patterson, 2001; Taylor & Whitelaw, 2001). Photoperiod can also play a role in regulating ethylene and auxin levels contributing to abscission (Taylor & Whitelaw, 2001). Similarly, high temperatures and water stress can elevate levels of ethylene and ABA while reducing those of gibberellins, cytokinins, and free auxins, creating optimal conditions for abscission (Nilsen & Orcutt, 1996). Levels of ABA may also increase during pathogen attack and the transcriptional activation of defense-related genes may involve jasmonates. In general, the influence of gibberellins, ABA, and cytokinins in abscission is related to their interaction with auxins or ethylene rather than a direct effect (Patterson, 2001). The fourth and last step in the abscission process involves the development of a protective layer over the separation surface.

1.3.3. Genetic Control

The genetic architecture of abscission has been widely studied across model and major crops. Pod shattering in Arabidopsis is determined by the interaction of several MADS-box and homeodomain genes (Liljegren et al., 2000). In particular, *SHATTERPROOF* (*SHP1*) and *SHATTERPROOF2* (*SHP2*) are closely related and redundant genes that promote cell differentiation and lignification in the dehiscence zone. These genes are positively regulated by the product of the *AGAMOUS MADS-box*, and negatively regulated by *FRUITFULL* (*FUL*), which also regulates *GT140* expression (Ferrándiz et al., 2000). In addition, *FILAMENTOUS FLOWER* (*FIL*) and *YABBY3* (*YAB3*) transcription factors control the expression of *FUL* and *SHP* (Dinneny et al., 2005).

Together, these genes interact to control the valve margin development in Arabidopsis, where the dehiscence zone forms. In dry and fleshy fruits, the molecular networks responsible for maturation and abscission appear to be highly similar (Dong & Wang, 2015). In general, a YABBY gene and an AP2-like genes have been reported to control abscission across several plant species (Bartlett & Patterson, 2019; Yu & Kellogg, 2018).

While some genes may be shared between the development of the abscission zone and the dehiscence zone, others regulate specific reproductive structures suggesting different processes (Yu & Kellogg, 2018). *APETALA2* (*AP2*), an essential gene for flower development in Arabidopsis (Jofuku et al., 1994), is a homologue of *SHATTERING ABORTION* (*SHAT1*) in rice and is closely related to Cleistogamy1 (*Cly1*) which is known to regulate lodicule development in barley (Zhou et al., 2012). The gene Q in wheat also encodes *AP2*-like transcription factor, and is associated with disarticulation, seed threshability, and other domestication traits (Li & Gill, 2006; Simons et al., 2006). Shattering1 (*Sh1*) is a YAB2 homologue, reported to have been under parallel selection during the domestication of sorghum, rice and maize (Lin et al., 2012). While independent mutations at orthologous loci are believed to have led to domestication of grasses, research suggests that there are multiple genetic pathways controlling abscission even within Poaceae (Li & Gill, 2006; Tang et al., 2013).

Shattering in grasses is mainly polygenic; nonetheless, single QTLs have been reported to control the process (Doust et al., 2014). In *Sorghum bicolor* (L.) Moench, for example, seed shattering is controlled by a single gene (*SH1*) that encodes a *YABBY* transcription factor (Lin et al., 2012). On the other hand, the *SpWRKY* controls seed shattering in a wild sorghum (*Sorghum propinquum*) and is substantially close (~300 kb)

to Sh1 which may imply that at least two genes are associated with the trait in the genus (Tang et al., 2013). Besides the *Q* gene in wheat, disarticulation in wheat ancestors is attributed to a dominant *Br* allele that produces brittle spikes (Li & Gill, 2006). In rice, *qSH1* is a major QTL on chromosome 1 that is reported to explain 68.6% of the variation in seed shattering (Konishi et al., 2006). Although just a single allele at *qSH1* (quantitative trait locus of seed shattering on chromosome 1) drastically changes the phenotype from shattering to non-shattering in rice, *qSH1* is epistatic to *qSH3* and *qSH4*, both of which are known to be important shattering genes in *Oryzae* species (Onishi et al., 2007). *qSH4* is essential for the activation and development of the abscission layer during early flowering and has been reported to explain 69% of shattering in rice (Li & Gill, 2006). In addition, *SH4* (grain shattering quantitative trait locus on chromosome 4) positively regulates the expression of *SHAT1* in the abscission zone and has even been reported to eliminate the shattering phenotype in rice with a frameshift-mutation (Zhou et al., 2012). Yoon et al. (2014) reported that *SH4* and *SHAT1* were positively regulated by *SH5*, a gene associated with lignin deposition and seed shattering. Later, Yoon et al. (2017) reported that *SH5* interacts with *OSH15* (a *KNOX* protein) to control seed shattering by repressing lignin biosynthesis. An additional example comes from the *OsLG1* in rice, which is regulated by the *SPR2* locus, modifying panicle shape and significantly influencing seed shattering (Ishii et al., 2013).

Compared to other grass species, the genetics of shattering in perennial ryegrass has not been well elucidated. A comparative phylogenetic analysis by Fu et al. (2019), using gene expression profiling during floret and seed development, identified putative sequences associated with seed shattering in the species and led to a proposal of the first

genetic model for shattering in *L. perenne* in which *LpSH1* appears to play an essential role in regulating genes associated with lignin deposition and consequential abscission (Fu et al., 2019). Nevertheless, the vast diversity in abscission zones in Poaceae indicates that lignification is not strictly necessary for abscission to occur (Yu et al., 2020). Furthermore, disarticulation in perennial ryegrass is associated with architectural traits that cannot currently be separated and measured in a high-throughput manner (Elgersma et al., 1988). The lack of proper methods to quantify shattering losses in perennial ryegrass are a hindrance to exploring whether homeologs found by Fu et al. (2019) are actual orthologs.

1.3.4. Challenges to Quantifying Shattering

Because abscission occurs at a microscopic level and shedding takes place before and during harvesting, shattering losses are difficult to predict and measure with accuracy. On one hand, inter- and intra-spike variation increases the labor inputs associated with phenotyping and, if done sparingly, may lead to incorrect measures of heritability and poor response to selection. On the other hand, the uneven flowering and ripening that characterizes perennial ryegrass contributes to confounding effects when estimating shattering (Bonin & Goplen, 1963b). While non-shattering phenotypes within the genus *Lolium* have been identified (Cai et al., 2011), along with homeologs associated with reduced shattering (Fu et al., 2019), entangled relationships with spike morphology at a micro and macroscopic levels hinder the separation of a singular trait to select for increased retention. Furthermore, selecting for univariate traits such as retention or yield, could lead to unintended selection for unfavorable correlations.

Arguably, any agronomic trait can be genetically improved through plant breeding only if it has a measurable variability. Unfortunately, for perennial ryegrass, there are no

current methods to accurately quantify the shattering phenomenon in a way that can be mapped to a genome or improved through selection. Hormonal imbalances affect morphological features of the inflorescence in a way that is not easy to measure or perceive with the naked eye. Fitness-related traits such as uneven flowering, ripening, and their duration, increase the complexity of hormone-morphology relationships. Furthermore, the interaction between traits, dispersal vectors, and environmental covariates affects phenotypes in cryptic ways. Large scale genetic and breeding designs with accurate and precise phenotyping can allow for the exploration of the components of phenotypic variances; however, such designs require accurate and precise phenotyping strategies that can identify heritable traits. Given the lack of improved germplasm and techniques to properly characterize dispersal traits in perennial ryegrass, retention improvement has focused on agronomic management more than genetic knowledge.

1.3.5. Management Practices

Given the lack of germplasm with increased seed retention and yield in perennial ryegrass, agronomic practices to indirectly influence productivity have been an important factor for the grass seed production industry. For example, Anderson et al. (2019) suggested that harvest management tools could have an effect on the shattering level in perennial ryegrass unlike in tall fescue. In their research, the authors concluded that the choice of swather or windrower may affect yield loss and such results may vary depending on seed moisture content (SMC). Research suggest that a 35 – 43 % SMC is recommended to determine cutting time and avoid shattering losses in perennial ryegrass (Silberstein et al., 2010). While the use of film agents has also been suggested to control shattering in the

species (Obraztsov et al., 2018), there needs to be more research to evaluate the potential of such practice.

Because the abscission process intrinsically depends on hormonal regulation, plant growth regulators (PGRs) have been a common agronomic practice to reduce shattering in grasses. Plant growth regulators are naturally occurring compounds that can be commercially produced and impact the development and metabolism in plants (Rademacher, 2015). Type I PGRs inhibit cell division while type II inhibit the synthesis of gibberellins and are most commonly used (Howieson, 2001). PGRs are often used to avoid head emergence but they have also shown promising applications for seed production (see Chapter 3). However, PGRs have inconsistent effects on shattering and productivity due genotype-specificity and environmental dependence (Mathiassen et al., 2007).

Breeding and agronomic management for seed retention in perennial ryegrass are challenging processes. The breeding efficiency depends on the heritability of the trait, which besides being unknown in perennial ryegrass, it is expected to be very low (Elgersma et al., 1988). Nonetheless, I argue that the major challenge to increasing seed retention and yield in perennial ryegrass is our simplistic approach to its phenotypic complexity. I suspect that plant domestication could be accelerated by selecting on highly heritable phenotypic patterns, or clusters of traits that may not necessarily be amenable to human perception. This, however, requires a more holistic approach to the multivariate nature of dispersal and perhaps a re-definition of "trait" in the context of breeding and genetics.

1.4. The Phenotypic Complexity of Shattering and Dispersal

The terms seed shattering and seed dispersal are often used interchangeably despite the former being only a component of the latter (Li & Olsen, 2016). Dispersal is an evolutionary phenomenon in which offspring distance from progenitors in a spatial and temporal manner to allow gene flow. A plant's ability to disperse depends on morphological patterns that emerge from its interactions with other species and environmental covariates (Spengler III, 2020). Interacting traits involved with dispersal are under anthropogenic selection through the domestication process, in which parallel selective pressures on desirable plant traits are exerted. It is important to acknowledge that domestication, rather than a human-driven process, is a natural consequence of herbivory that rapidly changes the plant's ability to disperse (Spengler III, 2020). Therefore, domestication-syndrome traits like shattering are only part of the perceived portion of the phenotypic multidimensionality affecting dispersal: remnant phenotypic patterns derived from selective pressures exerted by non-human dispersers are likely to be currently expressed and affecting seed yield. This implies that indirect selection for unknown trait correlations is inevitable during conscious selection for dispersal-related traits affecting fitness.

1.4.1. Dispersal: A Separation from Progenitors Across Space and Time

Seed dispersal is an evolutionary mechanism by which wild plants colonize diverse habitats and propagate their offspring. The dispersal process is characterized by initial departure from the progenitor, movement, and the settlement; it is predominantly passive in plants, i.e., dependent from external factors, even when active mechanisms such as

abscission are highly relevant. Seed dispersal across space as well as over evolutionary time depends on the morphological features of both the plant and the dispersers (Spengler III, 2020). Arguably, a good approximation of a plant's ability to disperse would require integrating the changes over time in inflorescence architecture that emerge from multidimensional selection pressures.

Dispersal mechanisms are determined by spatial and temporal interactions between biotic and abiotic vectors (Bello & Barreto, 2021; Robledo-Arnuncio et al., 2014). During dispersion, seeds often shed along with other parts of the inflorescence facilitating displacement, protection, and preconditioning the endosperm for germination (Bartlett & Patterson, 2019). The detached structure, referred to as diaspore, represents the dispersal unit; inflorescence and diaspore morophology have evolved to facilitate displacement. Biotic dispersers such as animals (zoochory), humans (hemerochory), and abiotic including wind (anemochory) and water (hydrochory) are important for plant fitness (Hintze et al., 2013). In general, short-distance movement is associated with ballistic, unassisted methods such as active shattering and insects, whereas long-distance dispersal relies on wind, water, and vertebrates (Thomson et al., 2010). Temporal changes in landscape and climate conditions are relevant to the dispersers distribution and behavior, affecting the plant's ability to disperse and persist (Robledo-Arnuncio et al., 2014).

1.4.2. Dispersal Traits Result from Coevolution

The genetic and phenotypic basis of seed dispersal are difficult to investigate because they depend on unmeasurable spatial and temporal interactions between biotic and abiotic agents. Seed dispersal effectiveness is a function of the quantity and quality of dispersed seeds as they interact with phenotypic properties of the disperser vector (Valenta

& Nevo, 2020). As an example of this complexity, consider seed dispersal by birds. Wing morphology interacts with climate conditions to determine the bird's displacement capability (Claramunt, 2021). Seed dispersal thus depends on the birds' bones and tissues comprising their wing architecture, the environment preferred by both plants and birds, and the architectural characteristics from plants that attract dispersers (Nathan et al., 2008). The biotic components in the example can be infinitely subdivided to molecular levels where mutations ultimately determine the genetic contribution to their phenotypic variation (Saastamoinen et al., 2018). While those mutations (or polymorphisms) are physical entities that can be measured, the phenotypic multidimensionality they generate cannot be exhaustively quantified or even contemplated by human perception (Chitwood & Topp, 2015; San-Miguel et al., 2016). Ultimately, these interactions exert different selection pressures that change the phenotypic multidimensionality of the plant (Valenta & Nevo, 2020). Arguably, those genetic alterations get passed through generations and across geographic regions to generate the phenotypes that we currently observe.

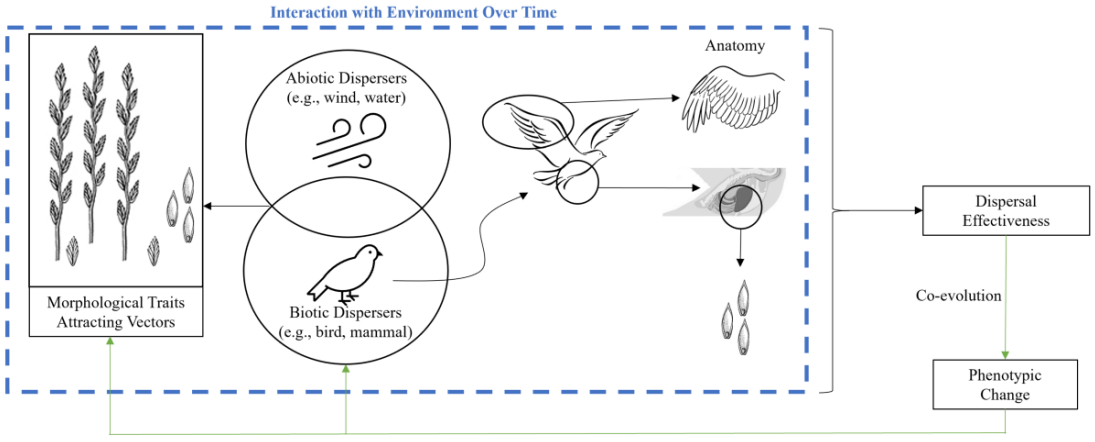

Figure 1.2. Example of the coevolutive process driving morphological changes across space and time under environmental conditions. From left to right: spikes evolved morphological features that facilitate dispersal under changing environmental conditions (represented by blue dashed line). Biotic and abiotic vectors (and a combination of both,

represented by arrow towards spikes) exert selective pressures on the spike traits. The first arrow pointing right represents a bird dispersing across space and time while carrying seeds. The circles focus on their wing (upper) and stomach (lower) morphology. The former facilitates its own dispersal; the latter indicates seed and stomach morphology traits that benefit both species and facilitate their dispersal. This mutualistic relationship results in coevolution and phenotypic changes that iterate the same process. The totality of an individual's phenotypes that results from these interactions could be referred to as a holophenotype (Chitwood & Topp, 2015).

Environmental covariates can also affect the phenotypic multidimensionality of the plant and dispersers. For example, nitrogen and protein levels, while not quantified by early domesticators, could have still been perceived as some form of energy, driving changes in selective pressure and dispersion (Donati et al., 2017). Light reflectance on specific tissues can also change due to light conditions potentially affecting vertebrates' capacity to detect and consequently disperse fruits (Valenta & Nevo, 2020). More severe conditions could also change fruit morphology and chemical composition (Teramura & Sullivan, 1994) and may affect vertebrates behavior as a disperser. This implies that that the relevance of genotype by environment interaction (GxE) increases for every single disperser, environmental covariate, and interaction contributing to dispersal at a given time.

1.4.3. Indirect Selection is Inevitable During Domestication

Plant domestication is considered the most important event in human history (Ross-Ibarra et al., 2007). This evolutionary process involves selection on specific traits that differentiate plants from their wild progenitors; these traits are collectively referred to as "domestication syndrome" (Hammer, 1984; Harlan et al., 1973). Although these traits vary according to the species, seed shattering has been the most important in grasses as it allows a more reliable harvest and greater yield, and consequently the development of human societies. In the process, other traits such as asynchronous flowering and seed dormancy

are also under high selective pressure to facilitate plant cultivation. Interestingly, instead of an exclusively anthropogenic process, domestication is better explained as a natural consequence of herbivory; neither humans domesticate plants nor plants domesticate human, they coevolved based on their biological needs (Spengler III, 2020). This implies that organisms exert selective pressures that change plant phenotypes whether humans can or not perceive them. Therefore, indirect selection for unobservable traits is inevitable during domestication or artificial selection.

Multiple genetic variants are commonly associated with spike architecture and dispersal traits such as uneven flowering, seed dormancy, and shattering, indicating pleiotropic effects or linkage (Kantar et al., 2017). While these phenotypic relationships can originate from common environmental covariates, they share a genetic architecture that is subject to correlated evolution (Saastamoinen et al., 2018). These genetic correlations can be disentangled with proper statistical methods if the phenotypic variation is heritable and depends on multiple genes of small effect (Korte et al., 2012). Nevertheless, as discussed earlier, characterizing such phenotypic complexity and its effect on seed yield is extremely difficult, particularly for species like perennial ryegrass which lack proper phenotyping tools.

Understanding the nature of genetic correlations between traits could help to determine strategies for crop improvement. Correlations due to chromosomal linkage can be, at least in theory, separated with enough recombination events; conversely, pleiotropic relationships are more difficult to undertake. It is speculated that the relationships between spike morphology and dispersal traits might be pleiotropically controlled (Zhang et al., 2009). While some pleiotropic relationships can be beneficial others are unfavorable (Keith

& Mitchell-Olds, 2019; Law, 1979; Oury & Godin, 2007; Schulthess et al., 2017; Thorwarth et al., 2019; Wu et al., 2017). Arguably, the greatest challenge is to know whether a gene is controlling more than one trait given that we are bounded by human perception. For example, selection against abscission increases the number harvestable seeds while selection for uniform flowering and ripening could favor pollination, seed set, and improved harvest management. Nevertheless, these indirect effects on productivity are not exclusively favorable, as increasing the number of harvested seeds does not necessarily represent additional weight. Therefore, the genetic correlation from historical selection among dispersal traits may produce phenotypes with increased seed retention but not necessarily higher seed yield. Unveiling these phenotypic correlations depends on our ability to measure the phenotypic multidimensionality. Exploiting them in the context of domestication depends on the power to detect their associations to genomic loci.

1.5. Uncovering Meaningful Phenotypes Hidden in the Spike Architecture

All plant phenotypes are the product of unfathomable physicochemical processes creating abstract shapes at micro- and macroscopic levels. From protein complexes formed during translation to the reactions creating a metabolite or morphological trait, three-dimensional shapes drive the phenotypic reality that we may or not contemplate. This implies that the idea of a trait is exclusive to the observer and not all traits within the spectra of a multivariate phenotype can be selected for and hence changed by humans. Nevertheless, it is possible to achieve tangible genetic gains for complex phenotypes if the trait under selection is heritable enough.

All plant traits are multivariate, and their phenotypic complexity is reflected in their genetic architecture. While advancements in sequencing technologies have driven substantial progress in genomic characterization of biological phenomena, measuring the phenotypic reality remains challenging; this is often referred to as a phenotypic bottleneck (Furbank & Tester, 2011). Understanding the multidimensionality of complex phenotypes such as spike architecture, dispersal, and yield, is paramount to interpret the growing abundance of genetic and genomic information (Chitwood & Topp, 2015), and its potential for breeding and domestication. Because of its relevance to dispersal and seed yield capacity, I argue that a comprehensive characterization of the spike architecture in perennial ryegrass could reveal major patterns that can be selected for to accelerate its domestication.

1.5.1. Inflorescence Morphology Determines Dispersal Capacity

Inflorescence features are highly diverse across Poaceae species and their variability determines dispersal and disarticulation patterns affecting seed yield (Doust et al., 2014). During dispersion, seeds often shed along with other parts of the inflorescence facilitating displacement, protection, and preconditioning the endosperm for germination (Bartlett & Patterson, 2019). Changes in the inflorescence-morphology at micro- and macroscopic levels through interactions with dispersers have been paramount to the spatial dispersal and to maintain germination capacity over time.

For example, panicle length and width have shown both negative and positive relationships with shattering in *Phalaris aquatica* L. (Kelman & Culvenor, 2003). Rigid heads and densely packed spikelets are reported to increase retention in the species (McWilliam, 1963). Glume morphology and dynamics affect seed shattering in reed canary

grass (Bonin & Goplen, 1963a). In wheat, glume strength and angle are also highly correlated with shattering and less environmentally dependent than spike density and plant height (Vogel, 1941; Zhang et al., 2009). This also applies to dicots such as Brassica spp. in which the number of branches, their angle, and their relationship with the siliqua all affect disarticulation (Kadkol et al., 1989). Such architecture has not been elucidated in perennial ryegrass because the heterogeneity in the species requires large sample size and proper methods to effectively quantify morphological patterns, which are currently non-existent. Nonetheless, classifying dispersal mechanisms based on diaspore morphology can produce misleading findings as the interaction among and between environmental factors plays an essential role in the dispersal potential (Tackenberg et al., 2003). This implies that that the relevance of genotype by environment interaction (GxE) increases for every single trait contributing to the spike architecture and dispersal.

1.5.2. Comprehensive Phenotyping the Spike Architecture

Given its relevance to seed production and dispersal, a comprehensive characterization of the spike architecture in perennial ryegrass could reveal major patterns that can be selected for to accelerate its domestication. Some of the spike properties to quantify include geometry (e.g., spike length, shape, curvature), color (e.g., brightness, greenness, yellowness), and structural relationships (e.g., spikelets per spike, florets per spike, along with their distances, angles, shapes, etc.). This phenotypic characterization could be even more comprehensive if compiled with dispersal related traits such as flowering time, yield/fitness, and seed morphology traits including size, shape, moisture, dormancy, and quality. The combination of such traits could provide major information of the degree in which they are correlated but could also help build phenospaces where such

correlations are inexistent, for example, through dimensionality reduction and eigenvalue decomposition (Chitwood & Topp, 2015; Feldmann et al., 2021). This requires re-considering our idea of plant trait as rather an abstract, multidimensional, group of interacting phenotypes that are not necessarily observable.

Because the inflorescence morphology determines seed dispersal and yield in grasses, its architecture has been a main selection target throughout domestication. The study of inflorescence morphology has allowed the identification of pleiotropic genes controlling its architecture as well as yield, domestication traits (Larson & Kellogg, 2009; van Nocker, 2009; Wolde et al., 2019; Yu & Kellogg, 2018). The development of semi-automated image analysis pipelines has led to further elucidation of the genetic architecture of inflorescence morphology in rice (Agata et al., 2020; Crowell et al., 2014; Crowell et al., 2016; Rebolledo et al., 2016), sorghum (Li et al., 2020; Zhou et al., 2019), and wheat (Wang et al., 2019). Some of these efforts have detected major effects when using multivariate traits in the context of domestication (Crowell et al., 2016). In perennial ryegrass, the genetic basis of spike architecture has been studied using conventional phenotyping of univariate traits defined a priori (Sartie et al., 2018; Studer et al., 2008): while major QTLs were detected for flowering time, the relationships between spike architecture and yield were not easy to characterize. Such characterizations require intensive labor, time, and other resources; they are also limited by population size, which should be large enough in perennial ryegrass to account for its vast heterogeneity.

Applications of high-throughput phenotyping several traits have helped to reduce the time commitment, and labor intensity of measuring phenotypes in perennial ryegrass (Gebremedhin et al., 2020; Heineck et al., 2021; Heineck et al., 2019; Jayasinghe et al.,

2019; Wang et al., 2019). Furthermore, machine learning techniques have allowed the implementation of imaging tools to facilitate crop management (Smith et al., 2020; Yu et al., 2019). More sophisticated methods have recently been proposed to holistically explore the inflorescence architecture and its relationship to shattering in perennial ryegrass (Tubbs, 2021). Nevertheless, these approaches are limited to researchers selection of traits to explore which may hamper the ability to explore the actual phenotypic reality (Chitwood & Topp, 2015; Feldmann et al., 2021).

1.5.3. Seeking Meaningful Phenotypes

A better approach to characterize phenotypic multidimensionality is to dissect a complex trait into components or clusters that represent chronological or morphological dynamics that compose it (Sparnaaij & Bos, 1993). Such components are not necessarily observable as the traits from which they are derived: they represent their cumulative interaction and are independent from other latent component. Chitwood and Topp (2015) suggested the term *cryptotype* to represent hidden traits that maximize the separation between patterns comprising the phenotypic reality, or *holophenotype*. This involves the use of mathematical tools to identify hidden features controlling complex shapes. Remote sensing technologies are able to numerically quantify morphology through signals and pixel values in a rapid and large scale. The raw variables can then be dimensionally reduced to a phenospace where each new component is orthogonal to another.

Studying hidden phenotypes has allowed the discovery of genomic loci controlling unobservable, yet robust phenotypes controlling complex plant morphology. While defining plant shape is inherently difficult and prompt to human bias the use of mathematical and geometrical approaches could help to overcome such challenges and

unveil major drivers of phenotypic variation. Grafius (1964) suggested a geometrical approach to characterize yield using components, which mitigated the correlation between conventional yield components. Other approaches include the use of Generalized Procrustes Analysis, Principal Component Analysis, and Elliptical Fourier Descriptors, and machine mearning, among others (Chitwood & Otoni, 2017; Chitwood & Topp, 2015; Feldmann et al., 2020). Recently, Feldmann et al. (2021) reviewed most of the current methods seeking hidden and meaningful phenotypes, and highlighted the potential of latent phenotyping (Ubbens et al., 2020) in the context of breeding and genetics.

The combination of flexible multivariate methods and geometric definitions of shape has been applied to the context of quantitative genetics (Klingenberg & Monteiro, 2005). Li et al. (2018) found pleiotropic basis to variation in tomato shoots and roots, using persistent homology, a mathematical tool to measure persistent topological features across scales. Fu et al. (2018) identified QTLs controlling leaf shape in *Populus szechuanica* var tibetica using radius centroid contour and statistical curve modeling, the novelty being characterizing shape as a function rather that a combination discrete principal components. Topp et al. (2013) demonstrated the potential of multivariate phenotypes in identify QTL controlling root architecture in rice that could not be identified with multivariate approaches.

1.5.4. The Potential of Hidden Phenotypes

Multidisciplinary research has contributed to unveiling the genetics of complex agronomic traits through genomics and phenomics. Accordingly, genomic selection has emerged as an approach to reducing the breeding cycle by predicting phenotypes using genome-wide markers. Current genomic resources in perennial ryegrass include expressed

sequences tag (ESTs) (Sawbridge et al., 2003), a reference transcriptome (Farrell et al., 2014), and high-quality reference genomes (Byrne et al., 2015; Frei et al., 2021). On the other hand, as mentioned earier, high-throughput phenotyping has helped to reduce the subjectivity, time commitment, and labor intensity of measuring traits in this species. Moreover, machine learning techniques have allowed the development of imaging tools to facilitate crop management (Smith et al., 2020; Yu et al., 2019). Genomic selection has promising potential for the improvement of complex traits in perennial ryegrass and accelerates its domestication (Faville et al., 2018; Lin et al., 2016; Pembleton et al., 2018). However, these tools are yet to be implemented for the characterization and improvement of spike architecture, dispersal related traits, or seed yield.

Genomic selection has promising potential for the improvement of complex traits in perennial ryegrass and accelerate its domestication (Faville et al., 2018; Lin et al., 2016; Pembleton et al., 2018). Yet these approaches usually focus on single traits, overlooking the potential benefit from exploiting trait correlations (Jia & Jannink, 2012). An alternative approach would use multiple traits or, even better, multivariate phenotypes measured in an unbiased way. The latter strategy could take advantage of the genomic resources available for a given species and apply them to complex traits such as inflorescence morphology and root architecture, along any related trait. Research in rice has shown that multivariate traits are more heritable and have greater power to detect marker-trait associations (Crowell et al., 2016; Topp et al., 2013). Perhaps the genetic gain from genomic selection could be increased by using such phenotypes.

Indirect selection is inevitable under domestication, thus using multivariate phenotypes that account for more trait interaction could represent an opportunity to

accelerate domestication. This would involve identifying a phenospace where conventional traits with unfavorable correlation, e.g., seed yield and quality, have favorable directionality even if the response to selection is slower. Such approaches should be tested by comparing their expected genetic against those that would result from selection on conventional traits in less domesticated crops. Nevertheless, lack of functional resources in recently domesticated plant may be a barrier, which emphasizes the importance of developing phenotyping tools that are cost-effective and can match the low cost of modern sequencing technologies.

Even with abundant genomic and phenomics resources, introgressing loci controlling robust multivariate phenotypes could require several breeding cycles. There could be major potential for the combination of latent phenotyping and genetic engineering to accelerate crop improvement. The Clustered Regularly Interspaced Short Palindromic Repeats/CRISPR-associated endonuclease 9 (CRISPR/Cas9) system have been successfully used to introduce mutations in perennial ryegrass (Zhang et al., 2020). While CRISPR/Cas9 could be less efficient in quantitative traits such as those affecting dispersal, spike architecture, and yield, it could potentially work for hidden phenotypes affecting those traits and that have a simpler genetic basis. Furthermore, genetic transformation in combination with latent phenotyping could also introduce diversity from related species (Stewart & Hayes, 2011).

Finally, I infer that hidden phenotypes are not only useful to accelerate domestication but to understand adaptation to a rapidly changing climate (Ubbens et al., 2020). For qualitative phenotypes that are easy to quantify, multivariate approaches may not necessarily be pragmatic: they would require resources such as high throughput

screening that have no significant advantage over visual phenotyping. Nevertheless, while such traits may be controlled by major genes, the phenotypic expression under dramatically different climate may not be easily predictable. Therefore, the potential of hidden phenotyping may even benefit qualitative traits and such application could be transferred to other species with higher complexity. Identifying molecular markers controlling major phenotypic patterns with little genotype by environment effect could be used in comparative approaches for species that lack adaptability of plasticity.

Conclusion

Seed shattering is dispersal trait that depends on abscission, a highly programmed mechanism that avoids retaining seed in the inflorescence at harvest. Nevertheless, shattering is only a fraction of a complex evolutionary process that impedes high economic seed yield: seed dispersal. Because spike architecture genetically determines seed dispersal and yield, specific attributes have been selected through the domestication process to obtain reliable yield, allowing the thrive of agriculture and hence human societies. Both the dispersal process and the spike architecture are the result of coevolution: biotic and abiotic vectors exerted selective pressures over space and time that generate the current phenotypes we may or not be able to perceive. These has resulted in convoluted trait correlations that have a complex genetic basis and challenge domestication and crop improvement overall. A thorough characterization of the spike architecture could reveal phenotypic patterns, i.e., multivariate traits driving major changes in seed yield potential that could be selected for. Modern sequencing technologies have enabled the genomic characterization of traits promising a significant reduction in breeding through genomic

selection. Concurrently, advances in computer vision and machine learning facilitate the phenotypic characterization of large populations and simultaneous traits. Maximizing the benefit from such technologies requires thinking differently about agronomic traits, if we are to seek a comprehensive understanding of the phenotypic reality. The use of hidden, or latent phenotypes, as multivariate traits, could serve this purpose by identifying holistic and robust phenotypic patterns that have stronger association to loci than conventional phenotypes. By doing so, not only do we expect to improve the current traits we desire but identify core phenotypes that can facilitate adaptation under a rapidly changing climate.

Chapter 2. SpykProps: An Imaging Pipeline to Quantify the Spike Architecture of Perennial Ryegrass

(This chapter has been written in preparation for submission to the Plant Methods Journal)

Overview

Spike (inflorescence) morphology comprises a plethora of interacting traits at micro- and macroscopic levels, some of which may not be perceived. In recently domesticated species like perennial ryegrass, some of such traits preserve wild (or weedy) characteristics that have detrimental effects on seed yield and the seed growing industry. Breeding these spike architectural traits is difficult given the lack of proper tools and the need for large sample size in such highly heterogeneous species. To facilitate, I developed *SpykProps*, a semi-automated imaging pipeline aimed to detect spikes in images, extract color and shape properties including spike length, and count spikelets in perennial ryegrass. The system was tested on images of spikes from field plots that were treated to induce variation in spike morphology. *SpykProps* detected most spikes (99.8%) and generated significant Pearson correlations with manual measures for spike length ($r = 0.97$) and spikelet count ($r = 0.78$). I also identified unexpected differences in imaging hardware, a potential source of confounding and misleading results, using high-dimensional color descriptors. Both conventional geometric and elliptical Fourier descriptors (EFD) allowed for the grouping of spikes into otherwise imperceptible clusters. *SpykProps* has potential

to rapidly and inexpensively generate spike properties to facilitate research on yield components in perennial ryegrass.

2.1. Introduction

Inflorescence architecture, comprised by innumerable interactions among traits, genetically determines the yield potential across grasses. Variation in morphological patterns influence the number and size of their reproductive organs directly affecting seed yield (Kellogg et al., 2013). Similarly, the architecture can indirectly affect productivity by influencing important yield determinants such as flowering time, pollen availability, and seed retention (Elgersma et al., 1988). Understanding the importance of inflorescence components to yield is essential to develop productive varieties.

Lacking proper tools to measure large sample sizes, quantifying the multidimensionality of inflorescence morphology represents a challenge for yield improvement. Breeding pipelines involve selecting on several traits across numerous lines in different environments, requiring extensive resources in labor, time, and funding. High throughput phenotyping (HTP) often implements imaging techniques to rapidly quantify plant traits, which allows better heritability estimates in the context of plant breeding when used properly (Araus et al., 2018). Combined with genomic resources, HTP has facilitated the genetic characterization of complex traits such as root (Topp et al., 2013) and inflorescence architecture (Crowell et al., 2014; Crowell et al., 2016; Li et al., 2020), bolstering the potential for increased genetic gains (Mir et al., 2019). Furthermore, modern sequencing and computational techniques have enabled breeders to select earlier for heritable traits by predicting expected phenotypes using genomic selection, which may

speed up crop improvement (Cabrera-Bosquet et al., 2012). However, the potential application of such technologies for seed yield is limited by the low heritability of the trait. Furthermore, while indirect selection for inflorescence features with higher heritability could increase yield, the pleiotropic nature of the features of the inflorescence could generate unfavorable trade-offs affecting the crop's economic potential.

Plant phenotypes are derived from physicochemical processes that create shapes at micro and macroscopic levels. Unlike genes, which are physical entities, traits are an arbitrary subset of the phenotypic reality (Chitwood & Topp, 2015). While implementation of HTP tools in plant breeding can measure myriads of traits simultaneously, researchers commonly decide the traits to be measured, inevitably adding bias (Feldmann et al., 2021). Alternatively, parameters from a trait could be projected into a reduced space whose components would represent chronological or morphological dynamics comprising the trait's complexity (Sparnaaij & Bos, 1993). Therefore, novel techniques such as persistent homology (Li et al., 2018) and latent space phenotyping (Feldmann et al., 2021; Ubbens et al., 2020) have been proposed as alternatives to reduce subjectivity plant phenotyping. These techniques commonly use HTP to generate high-dimensional datasets which can be reduced using multivariate methods such as principal component analysis (PCA), partial least squares (PLS), factor analyses, etc., to generate latent variables and relate to a genome (Jannink et al., 2010; Momen et al., 2021). In general, the use of HTP with multivariate methods to detect associations between loci and latent phenotypes has proven to be promising in major grasses (Crowell et al., 2016; Momen et al., 2021; Topp et al., 2013) but its potential is yet to be explored in less domesticated species.

Better selection methods and definitions of traits could facilitate improving yield and domestication of species with economic potential. Perennial ryegrass (*Lolium perenne* L.), for example, is a multifunctional seed crop with high economic importance but biologically inefficient seed yield (Anjo Elgersma, 1990). Like other forage and amenity grasses, its acceptance to seed growers and thus commercial stability around the globe depends on its ability to produce profitable yields (Elgersma, 1985; Heineck et al., 2020). Because of its recent domestication, inflorescence-related traits such as asynchronous flowering and seed shattering dramatically affect yield (Wilkins, 1991). Currently, at most 20% of the estimated biological seed yield potential can be harvested in perennial ryegrass (Abel et al., 2017). Given the lack of selection tools to improve inflorescence traits affecting yield in less domesticated species, I sought to develop a HTP platform to characterize the inflorescence architecture in perennial ryegrass. This approach has great potential to derivate latent phenotypes aimed to accelerate the species domestication.

2.2. Materials and Methods

2.2.1. Image Collection

This imaging pipeline was developed in Python using 40 images of 7016 pixels in height by 5104 pixels width obtained with flatbed scanners model CanoScan Lide 300 at 600 dpi. A summary of the workflow can be found in Figure 2.1. The images (Figure 2.2) contained perennial ryegrass spikes from a field trial of a single commercial variety (Galactic Green) that had maximized spike morphology due to hormonal treatments. This pipeline segments the spike and spikelets before extracting features describing variation in

spike morphology. The system includes functions to visualize, compare, and extract data for a single spike, but it is meant to be used on set of images containing multiple spikes. Ideally, such images contain inflorescences of the same plots, replication, or plant. The most complete datasets are obtained by running the *SpykBatch* function, which only requires the path to the images in a Python list. Once finished, the function returns different datasets containing spikes and spikelets color and shape descriptors.

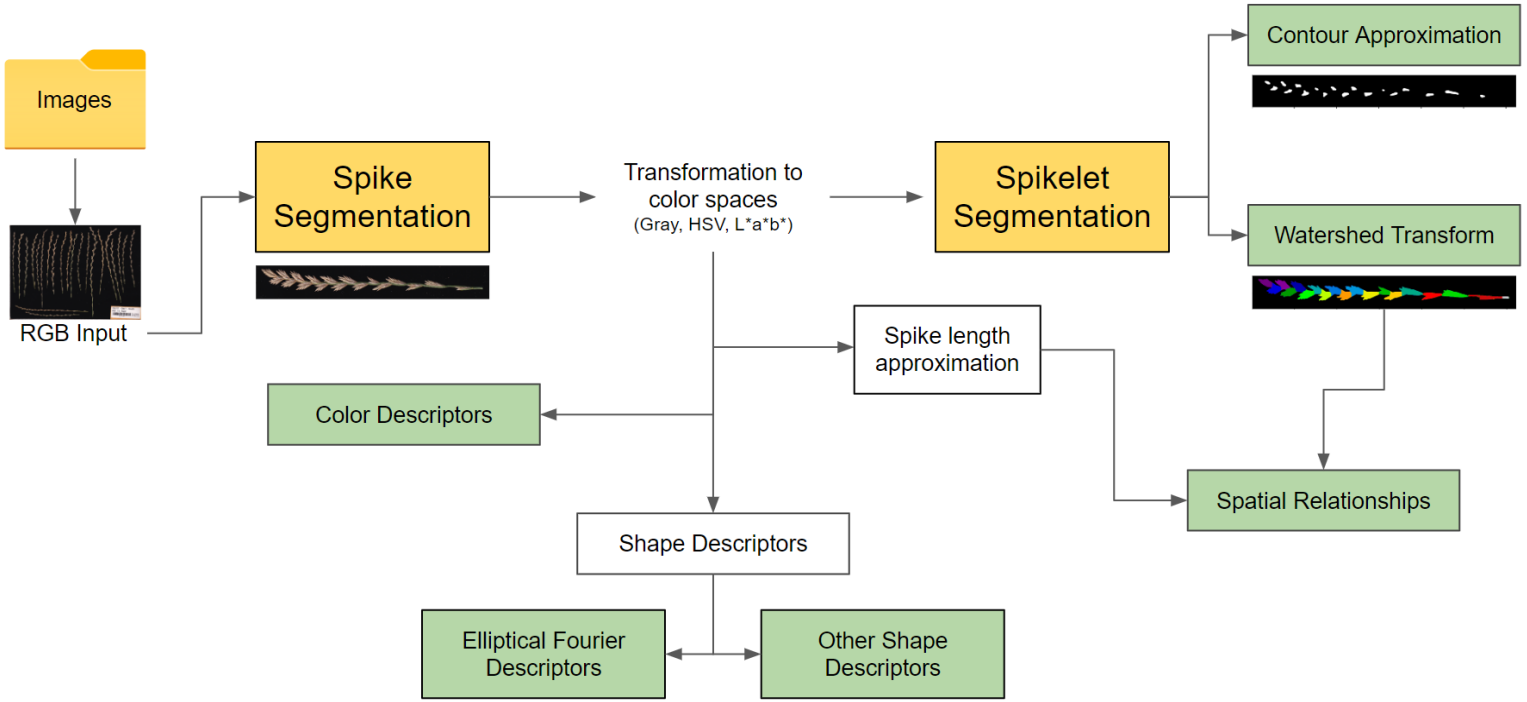

Figure 2.1. Workflow of *SpykProps* imaging pipeline. The pipeline starts with a folder containing the images to process (top left), followed by segmentation processes (yellow boxes). Once the spike has been segmented, it can be transformed to other color spaces to generate the color and shape descriptors. Similarly, the spikelet segmentation can be performed using either contour approximations, watershed transform, or both methods (default). The final output are six datasets (green boxes) in comma separate value format.

Figure 2.2. Example of images used to develop *SpykProps*. The spikes were purposedly arrange to avoid touching each other. Some images included fully shattered spikes (horizontally placed) that were included for further machine learning functionality but are ignored in the current study.

2.2.2. Segmentation

The first function (*ListImages*) gathers all the images in each directory and subdirectories if recursive=True, that have a particular format (default is imgformat=".tif"). Once listed, the images can be manipulated for specific purposes or automatically processed with the *SpykBatch* function. The initial step in the pipeline is to segment the spikes from the input image, i.e., to remove the background.

2.2.2.1. Spikes

The spikes are automatically segmented using the *RemoveBackground* function which takes a red-green-blue (RGB) image (or its path) and returns versions of the image in different color spaces without the detected background. This is accomplished by automatically detecting a threshold on the image's grayscale version using the Otsu algorithm (Otsu, 1979), which can be too stringent on the spikes but can be adjusted with the *OtsuScaling* parameter (Figure 2.3).

A

B

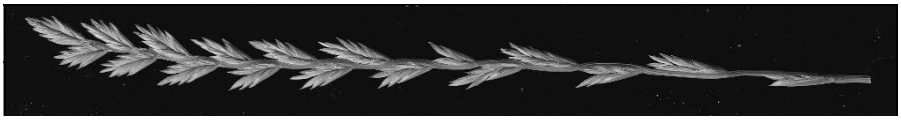

C

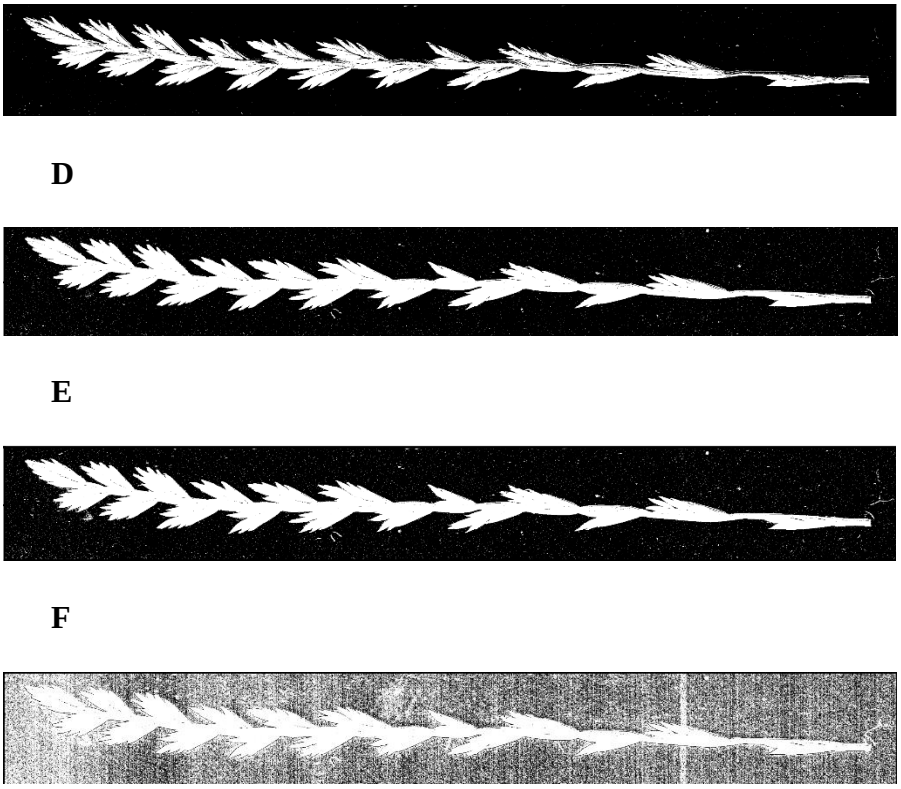

Figure 2.3. Spike segmentation using different Otsu levels. **A)** Original RGB. **B)** Gray scale image segmented at: **C)** 100%, **D)** 30%, **E)** 25%, and **F)**. 20%, of the estimated Otsu threshold. Values across x and y axes are in pixel units.

Thresholding is necessary to create an initial binary mask comprising the contour of the spike. Scaling the Otsu value up to a half (i.e., 1 to 0.5) can keep edges within the spikelets that required additional morphological operations to fill holes. For several spikes, values closer to 0.3 could remove parts of the rachis or spikelets. Values approaching 0.2 can also affect the spike's integrity and include dirt, fingerprints in the scanner, or other source of noise. Empirical experimentation led to choosing 0.25 as the best scaling value for all images; nonetheless, other values or thresholding type (e.g., color thresholding, edge detection) could be more appropriate for other type of inflorescences. In any case, the binary mask will most likely require additional filtering, which in this approach was

conducted using the *remove_small_objects* function (Van der Walt et al., 2014) with a minimum size equal to the 1% of the image's area in pixels.

The output is a list of images containing the final mask applied to the original RGB image along with data for the hue-saturation-value (HSV) and CIELAB (L*a*b*) domains (Figure 2.4). The images in different color spaces provide additional channels that serve to better describe the color properties of the spike. While some of these channels are highly similar, variation in their pixels could provide valuable information that is lost when images are only treated as RGB. In consequence, exploring differing quantiles as well as the variation within and across channels is one of the main strategies used in this system to explore spike architecture.

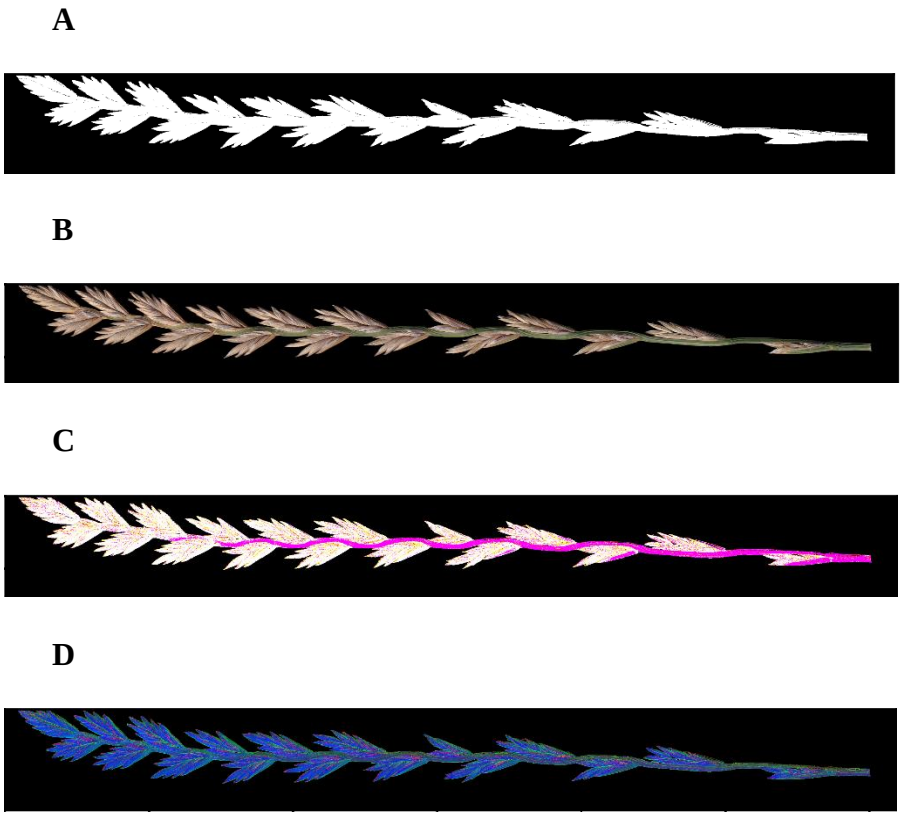

Figure 2.4. Example of spike projected onto different color spaces. **A)** Black and white mask applied to: **B)** RGB (red, green, blue); **C)** CIELAB or L*a*b* (L*: luminosity, a*:

red to green, b*: blue to yellow); and **D)** HSV (hue, saturation, value/brightness) color spaces. Values across x and y axes are in pixel units.

2.2.2.2. Spikelets

The pipeline includes two segmentation approaches to detect spikelets. The first approach uses several morphological operations to fit contours on the predicted spikelets, whereas the second approach uses the watershed transformation (Beucher, 1992). Both methods were compared against visual spikelet counts on 641 spikes. I estimated the mean absolute percentage error (MAPE) as a measure of accuracy (Equation 2.2-1) and the root mean squared error (RMSE) as a measure of precision (Equation 2.2-2).

Equation 2.2-1

$$MAPE = \frac{1}{n}\sum_{i=1}^{n}\left|\frac{O_i - P_i}{O_i}\right|$$

Equation 2.2-2

$$RMSE = \sqrt{\frac{\sum_{i=1}^{n}(O_i - P_i)^2}{n}}$$

where n is the total number of spikelets, O_i and P_i are the observed and predicted values for the i^{th} spike respectively

2.2.2.2.1. Contours

A following step in *SpykBatch* isolates and labels a given spike from the segmented RGB image to detect its spikelets (Figure 2.5). This is accomplished with the *SpkltThresh* function which takes an RGB mask of the spike along with a resizing factor, a threshold, and a minimum object size, as arguments. The spike is converted to grayscale, shrunk by the resizing factor, and returned to its original size to obtain a blurred image that is then

and enhanced using histogram equalization. The *SpkltThresh* function then applies a Gaussian filter with sigma=1 and equalize once again with a Contrast Limited Adaptive Histogram Equalization (CLAHE). The blurred image is then thresholded with the value given as input (default thr2=0.8) leaving connected elements that are kept only if their area is at least the specified minimum size (default MinSize=1000). This mask is eroded with a structural element to disconnect objects representing more than one spikelet and opened to smooth out the edges.

A

B

C

D

E

Figure 2.5. Spikelet detection using contour approximations. **A)** Gray image from RGB mask. **B)** CLAHE equalized image after blurring; **C)** Mask images with objects greater than MinSize. **D)** Following mask after erosion with a disk (radius = 3). **E)** Following mask after opening with a disk (radius = 10). Values across x and y axes are in pixel units.

The analysis of contours aims to approximate the relative area and direction from the rachis in which the spikelet grows (Figure 2.6). The angle is determined by the major axis of a fitted ellipse whose area acts as a subsample of properties within each estimated spikelet. This is a challenging task because the major axis of the ellipses highly depends on its area, therefore, the contour's angle must be corrected by its size. A solution for this challenge is defining a penalizing function, discarding angles and/or areas when they do not meet a criterion, for example, a given area or circularity.

A

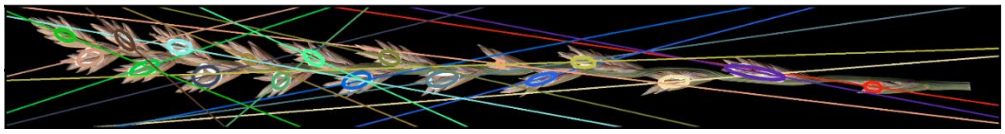

B

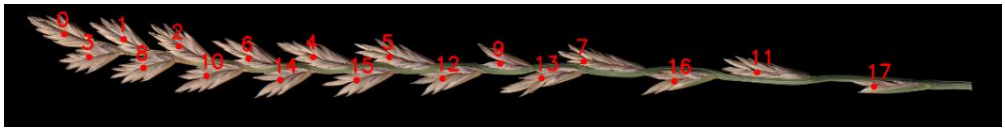

Figure 2.6. Example of spikelet and angle approximation using contours as subsamples. **A)** Detected spikelets, each has an ellipse and a line with a unique color, representing its sampled area and angle, respectively; **B)** Observed spikelets enumerated from 0 to 17 in red. In this example, 17 out of 18 spikelets were detected; spikelet 6 was not detected. Values across x and y axes are in pixel units.

The returned dataset contains color and shape properties of the contours as a relative approximation to spikelets. Smaller contours often represent shattered spikelets (9 and 17 in Figure 2.6) and have a directionality that do not necessarily follow the growth of the

spikelet. Given that intact spikelet could also have a wrong angle (e.g., yellow, and light blue contours) characterizing the real angles in which spikelets develop requires further analysis. For example, one could create a matrix of relationships between each contour indicating their angle, area, or a combination of both, followed by a cluster analysis to identify the two most common angles in a straight spike.

2.2.2.2.2. **Watershed**

The watershed transformation facilitates segmentation and object detection by separating adjacent regions. This algorithm is implemented in the function *LabelSpklts* to approximate each spikelet in each RGB mask of a spike. The function first rescales the RGB mask to 10% of its size to rapidly perform erosion with a 3x3 cross-shaped kernel followed by an iteration of opening before returning the image to its original size. The opened image is converted to gray and binarized to keep intensity values above 50. The resulting mask is used to get the distance of each white pixel from its nearest black pixel, allowing to determine pixels with the highest local maxima that are distanced by the specified minimum distance (default MinDist=50). Those peaks are labeled and used as markers for the watershed function (Van der Walt et al., 2014), which returns the approximated spikelets (Figure 2.7).

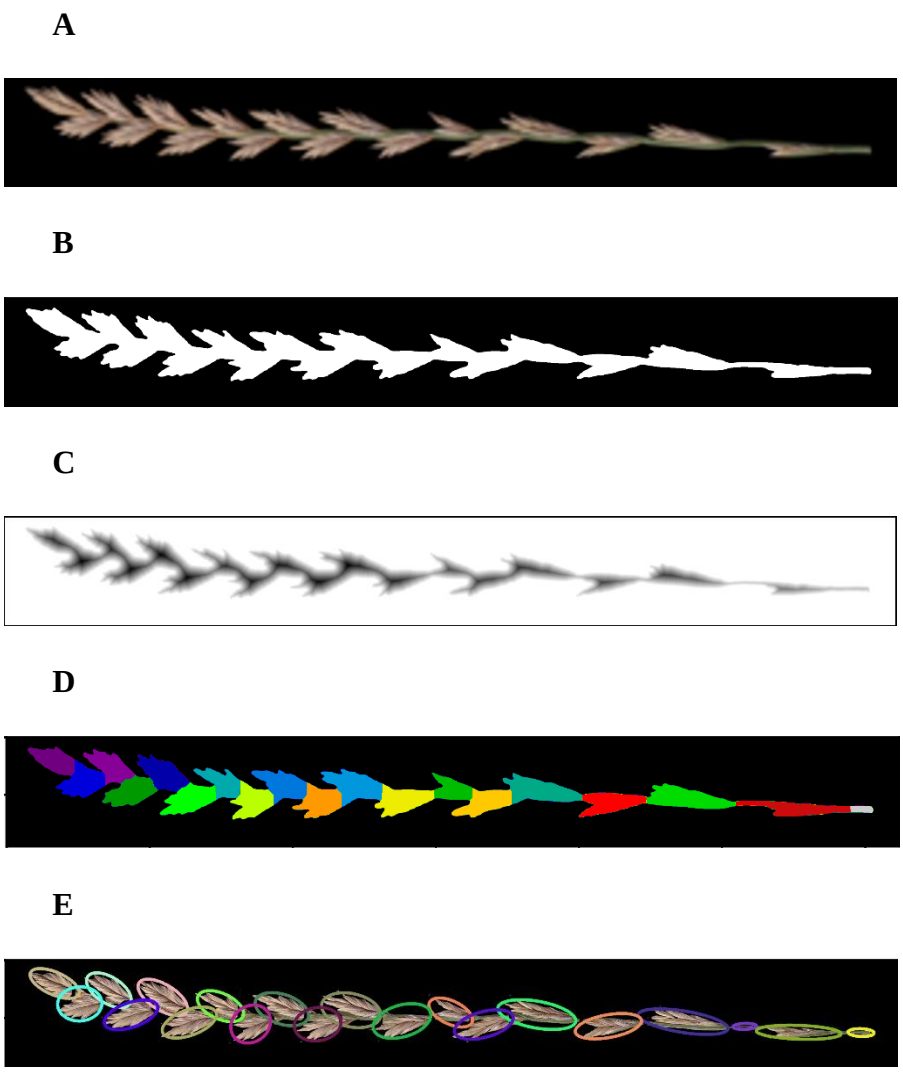

Figure 2.7. Spikelet segmentation using watershed transform. **A)** Blurred RGB mask as input. **B)** Binarized input. **C)** Distance to the background (from nearest nonzero pixel) in gray intensity values. **D)** Output from watershed segmentation. **E)** Ellipses circling the detected spikelets. Values across x and y axes are in pixel units.

As in the example above, most spikelets are often detected with *LabelSpklts*. Minor misdetections can be filtered out from the resulting dataset by setting a threshold on area or any other geometrical property that deviates from a normal spikelet size. This could also be adjusted at the image level with a potential cost in reproducibility. The parameters used by default are those who better match most of the tested images.

2.2.3. Spatial Relationships

Our pipeline includes an approach to explore the spatial relationship between spikelets across the rachis. This involves estimating the spike length and its ratio to the number of spikelets, which are indicator of productivity in perennial ryegrass (Sartie et al., 2018).

2.2.3.1. Spike Length Approximation

I approximate the length of a spike using a custom function (*spk_length*) that uses a skeletonization algorithm (Lee et al., 1994) and includes alternative options. Conventionally, the length of an object of interest is estimated by the major axes of a fitted ellipse or a convex hull (Das Choudhury et al., 2019), which are not always applicable to a spike because of its curvature. Instead, I blurred the spike with a 100x100 kernel, retaining values greater than 0.1, and then skeletonized the mask with the *medial_axis* and *skeletonize* functions from *scikit-image* (Van der Walt et al., 2014) and compared them to the bounding box and convex hull method, which are also included as *bbox* and *chull*, respectively. Because the result in pixels may contain small branches (Figure 2.8), I validated the methods with manual measurements from 812 spikes that were collected using the freehand tool in ImageJ (Ferreira & Rasband, 2012).

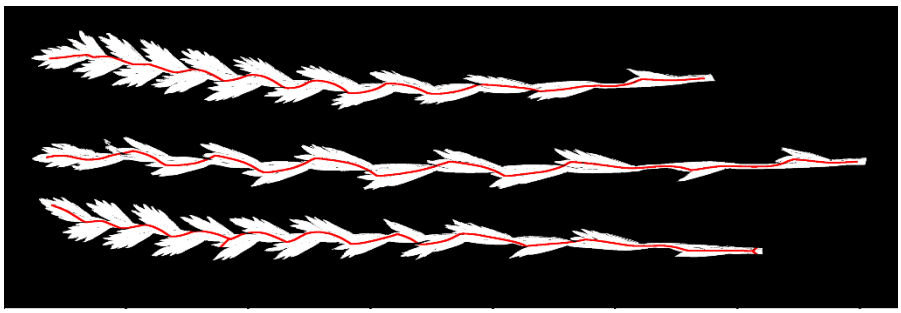

Figure 2.8. Spike length approximation. Spike length approximation using *medial axis*. Binary mask of three spikes with their length approximation (red) using the default method (skeleton of a medial axis). Values across x and y axes are in pixel units.

2.2.3.2. Distances Among Spikelets

Once the spike length is estimated and the spikelets are detected, I estimated their relative distance across the rachis. This could potentially help to understand not only spatial but physiological relationships along the rachis that affect yield components. After detecting the spikelets through contours or watershed transform, I used their center coordinates to estimate *d*, their Euclidean distance (Equation 2-3) using the *DistAll* function.

Equation 2-3

$$d = \sqrt{(x_2 - x_1)^2 + (y_2 - y_1)^2}$$

where (x_1,y_1) are the coordinates of one spikelet, (x_2,y_2) are the coordinates of another spikelet, and *d* is the distance between (x_1,y_1) and (x_2,y_2).

DistAll returns a diagonal matrix with the distances among spikelets which can be visualized as in Figure 2.9. The distance can be expressed in pixels or relative to the spike length, if passed as an argument.

A

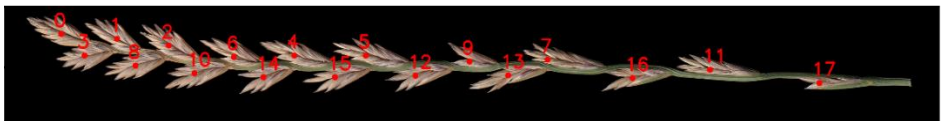

B

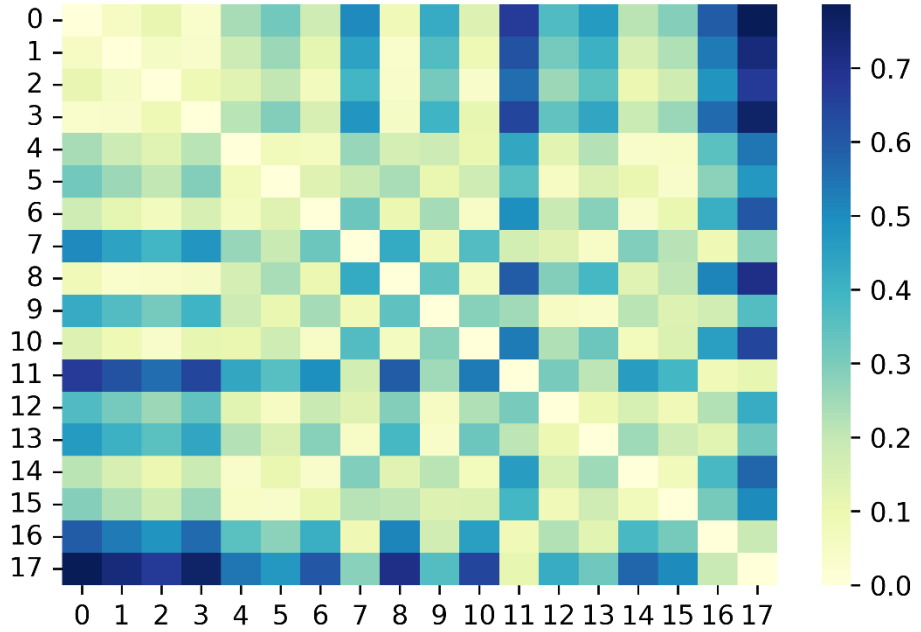

Figure 2.9. Distance between spikelets relative to the spike length. **A)** Segmented RGB spike with spikelets enumerated (red) using the *EnumerateSpkCV* function. Values across x and y axes are in pixel units; red dot indicates the spikelet's centroid (x,y) in (1). **B)** Heatmap of the relative distance among spikelets obtained using the *DistAll* function. Values across x and y axes represent the spikelet number in A. Color scale (green to dark blue) indicates their distance (d in (1)) as a proportion from the spike's length.

2.2.4. Color-Based Properties

I characterized each color channel as a probability distribution rather than obtaining averages or other single values from the original red (R), green (G), and blue (B) channels. I used different percentiles across channels and color spaces and included descriptors of their variation, thus generating over a hundred color descriptors out the three initial R, G,

and B variables. This is based on the idea that several spikes could have similar mean intensity values but different distributions; this would not necessarily be visible across all color spaces. Such information could be advantageous when assessing variation for spike phenology, particularly in perennial ryegrass, where spikes within the same plant often have different maturity (and color) levels at a given point. Data of the color descriptors are generated with the function *channel_percentiles* which considers all non-zero pixel values in each spike and returns the minimum, maximum, mean, standard deviation, coefficient of variation, percentiles 5, 25, 50, 75, 95, and quantile-based coefficient of variation across nine channels (R, G, B, H, S, V, L*, a*, b*). In addition, it estimates the same parameters for negative and positive values in a* and b*.

Because of its high redundancy, I projected the high-dimensional color descriptors into a reduced space using principal component analysis (PCA). The resulting eigenvectors are treated as latent variables that represent a linear combination of interacting traits describing a spike's color profile. I included a tool (*PixelHist*) to explore the basis of such color profiles using histograms and areas of the spikes in an image (Figure 2.10). Besides providing insight into the main drivers of variation in color and maturity channels, the tool could help identify outliers skewing a channel's distribution.

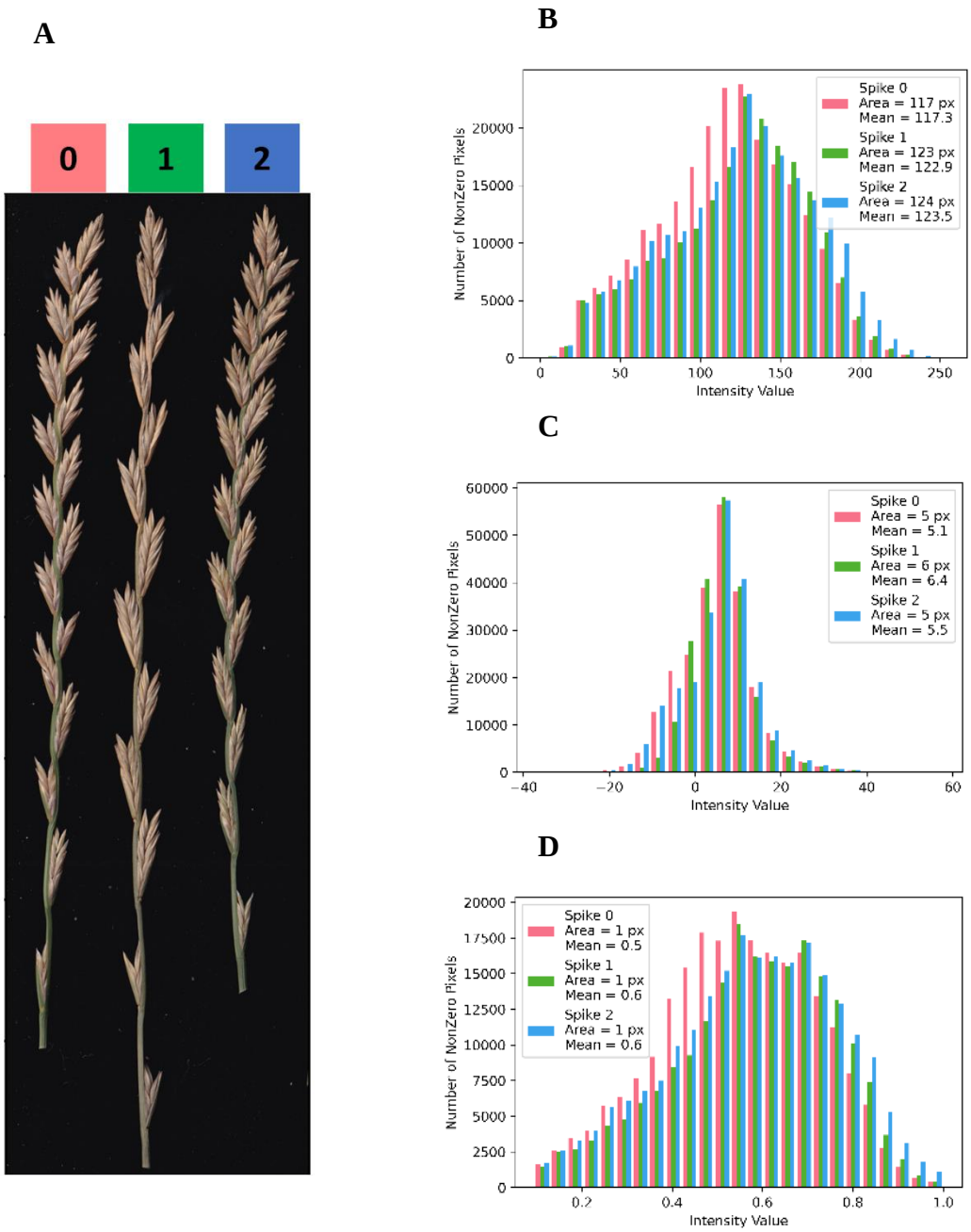

Figure 2.10. Differences in pixel distribution in channels across color spaces. **A)** Example of an RGB mask with three spikes with their respective color and number above them. **B)** Channel *G* from RGB. **C)** Channel *a** from CIEL*a*b*. **D)** Channel *V* from HSV. Axes in B,C, and D, represent the intensity value of their channel (x) and the number of nonzero pizels standarized by spike area. The box in the upper right corner the area and mean intensity value for the color-coded spikes.

2.2.5. Shape-Based Properties

The spike's shape was quantified using two different sets of descriptors, based on the Fourier Transform, and common geometrical properties used in image analysis. I generated latent variables from both datasets using dimensional reduction.

2.2.5.1. Elliptical Fourier Descriptors

The spike's outline is treated as a wave and decomposed into a specified number of harmonic series using the Fourier Transform (Chitwood & Otoni, 2017; Li et al., 2018). The resulting Elliptical Fourier Descriptors (EFD) are the coefficients a_n, b_n, c_n and d_n, which are derived from the elliptic loci $x_i = a_i \cos\theta + b_i \sin\theta$ and $y_i = c_i \cos\theta + d_i \sin\theta$, for a point ($x_i$, y_i) with n number or harmonics (Kuhl & Giardina, 1982). The coefficients are obtained using the 'CalculateEFD' function from the 'spatial_efd' package (Grieve, 2017) which is built upon the 'pyefd' module. To do so, I first provide a binary mask of the spike and fill any using the *binary_fill_holes* function from *SciPy* (Virtanen et al., 2020). I then execute the 'findContours' function using the 'RETR_CCOMP' mode and the 'CHAIN_APPROX_SIMPLE' method (Bradski, 2000) to extract the outline of the spike as paired x and y coordinates. Once obtained, the a_n, b_n, c_n, and d_n, are normalized to be rotation and size-invariant.

The outline representation of the spike depends on the number of harmonics chosen. The more harmonics included, the more accurate the shape representation (

Figure 2.11). I arbitrarily computed 100 harmonics for each spike and reduced the 400 resulting coefficients using PCA. As in the color-based descriptors, this generates latent variables describing the spikes' outline. It is worth mentioning that the EFD can also

be used to describe more features including symmetric (b_n and c_n harmonics) and asymmetric (a_n and d_n harmonics) sources of variance (Chitwood & Otoni, 2017).

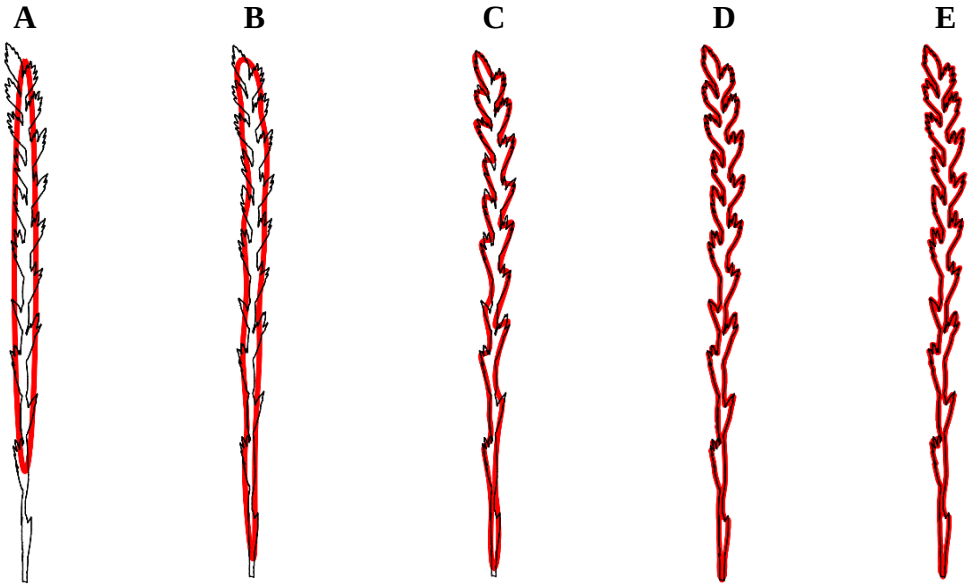

Figure 2.11. Spike shape reconstruction using Fourier series with different number of harmonics (n). **A)** n = 1. **B)** n = 10. **C)** n = 25. **D)** n = 100. **E)** n = 1000. The shape of the spike is outlined in black, and the outline approximation is fitted in red.

When computing the EFD, the pipeline uses the *FourierPower* function (Grieve, 2017) to estimate the number of harmonics needed to exceed a 0.9999 threshold Fourier power. This value, from now on referred to as "OptimalNH", along with the number of spikelets per spike (NSS), were combined with other geometric descriptor as an additional set of shape properties.

2.2.5.2. Additional Shape Descriptors

Given the complex basis of the EFD, I generated an extra set of shape properties that includes conventionally used geometric descriptors, which in addition to OptimalNH and NSS, include:

*Area and Perimeter**:*** The area is estimated as the number of pixels that compose the 2D spike. The perimeter is computed as the distance in pixels around the boundary region of the spike's mask.

*Width**:*** Rather than being the actual width, this variable represents the relative thickness of a spike. It is estimated as the ratio of the area to the spike length.

Circularity: This parameter indicates the similarity between a spike and a circle. It is calculated as 4π times the ratio between the area and the squared perimeter. Spikes with higher values are more curved than straight spikes whose values tend to zero.

Roundness: This variable also indicates the similarity to a circle for a given spike and is often estimated as $4\frac{Area}{\pi(major\ axis)^2}$ after fitting and ellipse. I replace the major axis of a fitted ellipse by an estimate of spike length, which resulted in $4\frac{Area}{\pi(spike\ length)^2}$.

Eccentricity: Eccentricity of an ellipse that has the same second central moment as the spike. It is calculated as the ratio of the distance between the foci of the ellipse over the length of its major axis and has value ranges between 0 and 1, with 0 being a circle and 1 being a line segment.

2.3. Results

I developed an imaging pipeline in Python (SpykProps) that extracts thousands of spike properties in perennial ryegrass. This approach also estimates the number and spikelet location along the spike and their relative distance from each other. I transformed those features into latent variables to comprehensively describe the spike architecture with

less human bias. Besides providing a basis for classifying spikes into latent types, the analysis unveiled unexpected sources of error.

2.3.1. Spike and Spikelet Segmentation

Using a 0.25 of Otsu threshold resulted in highly accurate spike segmentation. Most spikes (99.98 %) across images were accurately segmented and separated from the background; only two objects were incorrectly segmented, corresponding to smudges in the scanner. Although spikelet segmentation was more challenging, the watershed algorithm was still highly accurate at counting spikelets (

Figure 2.12). A significant Pearson correlation coefficient r = 0.78 indicated a strong relationship between the predicted and actual number of spikelets across 784 spikes. On average, the absolute difference between observed and detected was 1.43 ± 1.38 spikelets. Furthermore, the MAPE was 8.89% and the RMSE was 1.99, indicating a high accuracy and precission, respectively. The contour method did not perform as well as watershed. The significant Pearson correlation coefficient r = 0.68 indicated that the strength of this relationship was lower than with the previous method. Nonetheless, the accuracy and precision were just slightly different from the watershed methods (1.95 ± 1.71), with a MAPE = 11.48% and the RMSE = 2.6.

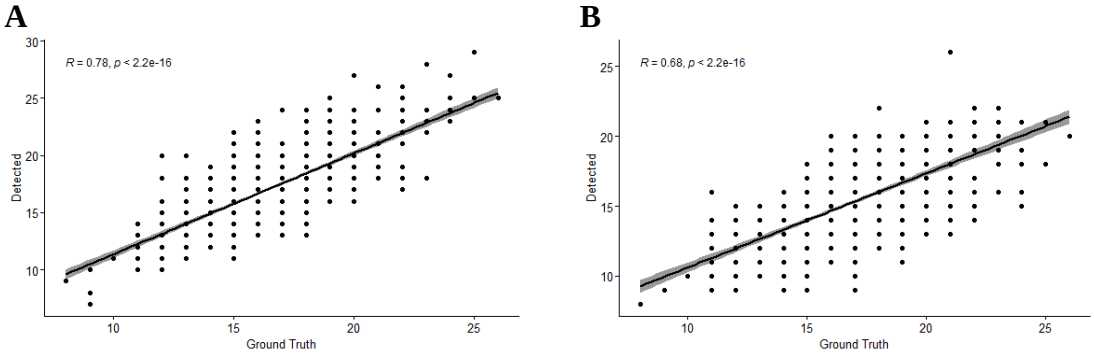

Figure 2.12. Validation of two spikelet detection methods. **A)** Watershed transform. **B)** Contour approximation. Scatter plots show the fitted line (black) and confidence interval (gray) for number of spikelets manually counted (ground truth) in the x-axis versus detected with *SpykProps* in the y-axis. Values in the top left represent Pearson coefficient (*R*) and p-value (*p*).

2.3.2. Spike length

There were significant correlations between observed spike length and the four approximation methods from *spk_length* ($p < 0.001$). The medial axis method (*skel_ma*) had the highest Pearson correlation ($r = 0.97$) with ground truth values. While this method appeared to be better than alternative skeletonization (*skel* $r = 0.95$), bounding box (*bbox* $r = 0.95$), and convex hull (*chull* $r = 0.90$) methods, it was also more computationally intensive. On average, *skel_ma* approximated the length in 0.42 ± 0.48 seconds, whereas *chull* (0.25 ± 0.15) and *bbox* (0.03 ± 0.02) were much faster and less variable. *Skel_ma* was also more variable than *skel* (0.51 ± 0.23) but slightly faster. In general, the bounding box and convex hull methods are recommended if the spike are straight. Such methods will not work properly for curved spikes; the medial axis will be preferred but will increase the computational time.

2.3.3. Latent Variables

Latent descriptors derived from color and shape properties were able to separate the spikes into relatively well-defined groups. The separation was further improved with the use of a second-order interaction set to derive latent variables.

2.2.3.1. Color-Based

Mean R, G, and B (or L*a*b*) values and subsequent dimensional reduction are often used in plant research to explore spectral properties (Ahmad & Reid, 1996; Yadav et al., 2010); nevertheless, transformation of the original RGB values can be beneficial for pattern identification in plant phenotyping (Philipp & Rath, 2002). I derived 125 variables from the R,G, and B pixel values, that represent the probability distributions of channels across color spaces. I also generated a larger dataset that includes the 125 variables and their second-order interaction resulting in 7503 descriptors after removing those with zero variance. Principal component analysis (PCA) then reduced the descriptors to a few eigenvectors, or latent descriptors, that characterize the color dynamics across the sampled of spikes.

Unexpectedly, plotting the first two eigenvectors of both the first and second order interaction datasets revealed differences across the two flatbed scanners used in this study. The conventional approach using PCA of mean RGB or L*a*b* values (Figure 2.13A) was unable to separate the two scanners. Reducing the first (Figure 2.13C) and second order dataset (Figure 2.13E) showed clear distinction between the imaging devices scanner used despite them being the exact make and model. This implies that minor differences in the imaging hardware, including the background, could affect the data quality in a way that cannot be often observed.

A

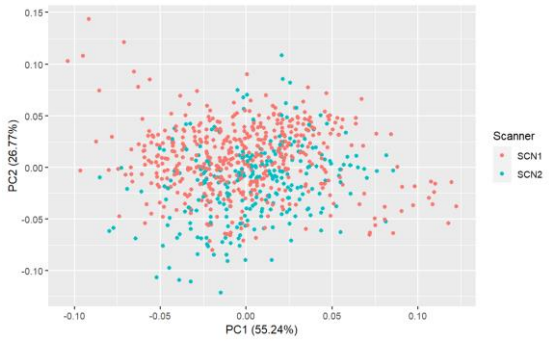
PC2 (26.77%)
PC1 (55.24%)
Scanner
SCN1
SCN2

B

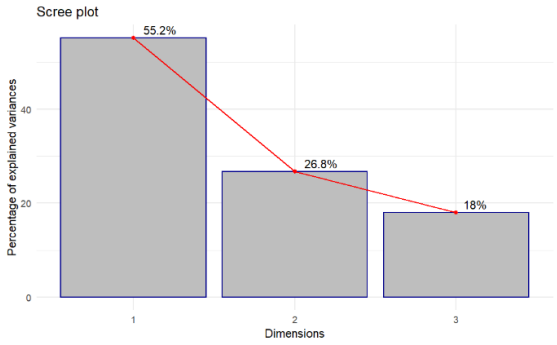
Scree plot
55.2%
26.8%
18%
Percentage of explained variances
Dimensions

C

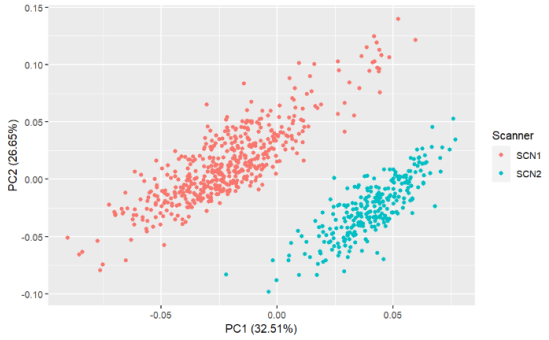
PC2 (26.65%)
PC1 (32.51%)
Scanner
SCN1
SCN2

D

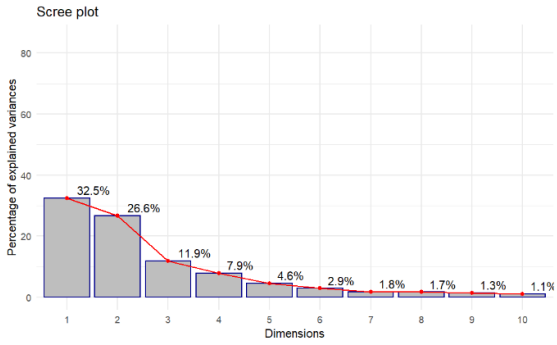
Scree plot
32.5%
26.6%
11.9%
7.9%
4.6%
2.9%
1.8%
1.7%
1.3%
Percentage of explained variances
Dimensions

E

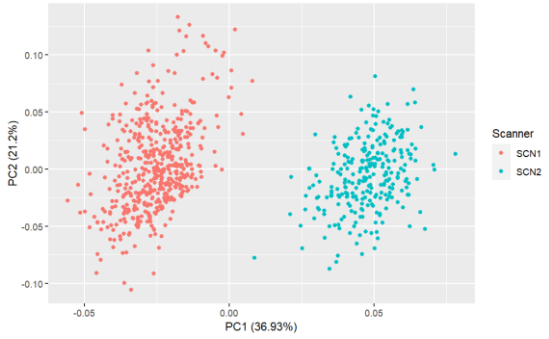
PC2 (21.2%)
PC1 (36.93%)
Scanner
SCN1
SCN2

F

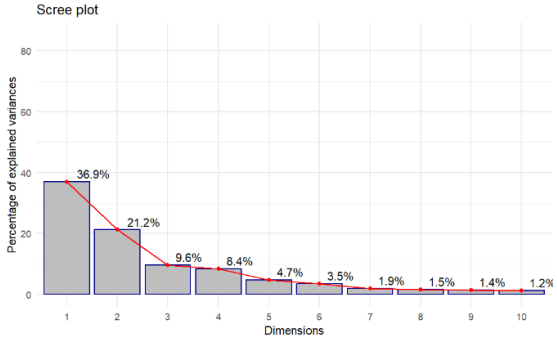
Scree plot
36.9%
21.2%
9.6%
8.4%
4.7%
3.5%
1.9%
1.5%
1.4%
Percentage of explained variances
Dimensions

Figure 2.13. Unveiled differences in imaging hardware based on color descriptors. Figures on the left column plot the variance explained by the first (x-axis) and second (y-axis) principal components of: A) Three (L*a*b*) color descriptors; C) First-order of all color descriptors; E) Second-order of all color descriptors; B, D, and E, are the their scree plots, repectively, indicating the variance explained by their eigenvectors (dimensions). Colors differentiate the scanners used for this experiment. Figures on the right are the scree plots showing the percentage explained (y-axis) by principal components (x-axis) of the color descriptors for A in B, C in D, and E in F.

2.2.3.2. Shape-Based

I performed PCA on the 400 EFD and kept the first 10 eigenvectors as Fourier-based descriptors of shape. As with the color-based descriptors, the EFD revealed two well-defined clusters, but they were unrelated to the differences in imaging hardware shown in Figure 2.14.

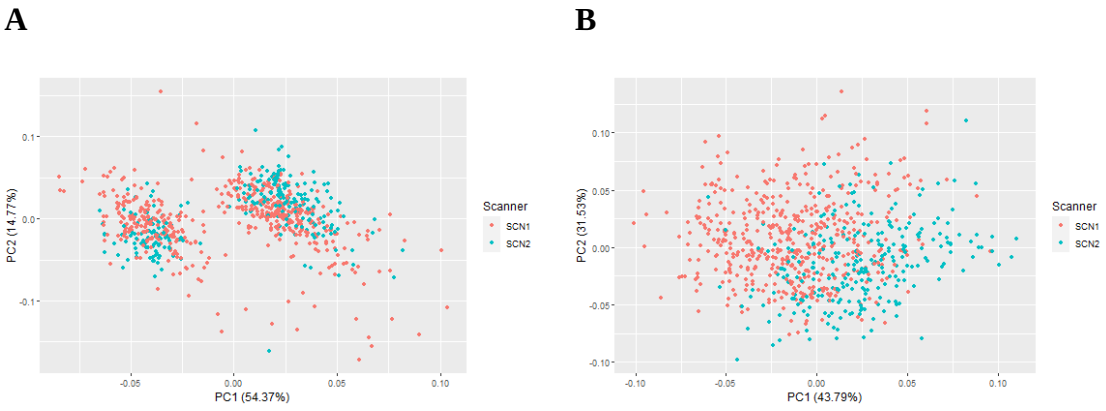

Figure 2.14. Shape descriptors do not capture differences in imaging hardware. Figures plot the variance explained by the first (x-axis) and second (y-axis) principal components of **A)** Elliptical Fourier Descriptors (EFD), and **B)** Additional geometric descriptors. Colors indicate the two identical scanners used for this experiment.

2.4. Discussion

Inflorescence architecture is difficult to quantify and comprehend. The problems of selecting limited and subjective traits as well as the lack of proper tools to overcome these challenges causes unconscious indirect selection for unfavorable phenotypic correlations. The main objective of this research was to use computer vision to quantify such architecture by generating latent phenotypes from thousands of spike properties in perennial ryegrass.

2.4.1. Implications

Breeding and genetic populations are often large and require extensive resources, limiting the quantity and quality of possible data collection. While imaging techniques can provide large amounts of accurate and precise data, they may also require investment in imaging hardware and trained personnel. In addition to economic cost, time to phenotype could also be increased due to manual and specific sample preparation. However, this approach proves possible to inexpensively collect large number of phenotypes that cannot be manually measured, in a timely manner. Furthermore, continuous advancements in machine learning and computational techniques bolster improvements in the imaging pipeline and hence the data quality, without necessarily having to gather samples or images again. Moreover, by collecting numerous traits breeders and geneticist can explore phenotypes that are not necessarily detectable to human perception.

Research has shown that such latent phenotypes describing architecture can be more heritable than univariate (Li et al., 2018), implying the possibility of higher genetic gains through selection. Molecular marker-based technologies enable to shorten the

breeding cycle through early selection upon loci controlling highly heritable phenotypes. This is difficult to apply on low heritable traits in perennial ryegrass such as asynchronous flowering, seed retention, and yield, which are affected by the spike architecture (Elgersma et al., 1988; Wilkins, 1991). Furthermore, there may be unfavorable relationships that can be indirectly selected when choosing a subset of the multidimensional phenotypic nature of the inflorescence. Accordingly, I suggest seeking and selecting loci controlling a holistic (latent) phenotype that account for such relationships. I suspect that such approach has potential to identify traits with high heritability to avoid unfavorable relationships. While I was unable to test such hypothesis without sequencing data, I encourage investigators with such resources to do so.

2.4.2. Spike and Spikelet Segmentation

While spike and spikelet segmentation were highly accurate there are important factors to consider when applying these methods. This includes imaging hardware, as well as the image background, size, and resolution. As shown in these results, identical models of imaging hardware can generate unexpected differences in color profile. This variation in pixel values could also be introduced by different computers, outlets, or any other energy source powering the same imaging device. In addition, the background's color and texture can affect the segmentation thus should be considered cautiously, especially if the spike or object of interest shares similar hues with the background. Furthermore, the ratio of the areas between the background and the spikes and thus the image size, could affect the segmentation. In some cases, segmentation based on color thresholding, edge detection, with additional convolutions (e.g., sharpening, smoothing, etc.) could be more efficient than an Otsu-based algorithm, depending on the image resolution. These parameters are

even more important and will require extra consideration when studying other plant species, especially if their inflorescences are not flat as in perennial ryegrass. These challenges can be tackled by testing the images devices before gathering input images; color scales can be very useful in such case as they could help standardize the imaging hardware. Monitoring any potential variation in power supply should also prevent these issues; in cases where the scanners are powered by the laptop, like in this study, using the same laptop would be ideal.

The watershed algorithm was more accurate at detecting spikelets than the contour-based method. Several observations deviating from the fitted value were observed in longer spike, yet no statistical significance supported a potential relationship between spike length and detection accuracy. Such deviation appeared to more related to twisted spikes and spikelets with lower seed retention. Machine learning algorithms could be more accurate; however, they often require extensive manual annotation making them potentially impractical. Nevertheless, deep learning models could be more robust and facilitate spike and spikelet detection in field condition, which could be also accomplished with my method but would be more cumbersome.

2.4.3. Latent phenotypes

Our approaches aim towards the identification of latent patterns within the spike architecture, which could potentially be stronger drivers of seed productivity. Though I encourage efforts to reduce human bias in phenotyping core components of seed yield, I acknowledge that human input cannot be fully eliminated. For example, I used PCA to reduce the multidimensionality of imaging data to a lower latent space, but this is limited by the assumption of linearity and distorts non-linear relationship within the spike. There

are other such techniques that accomplish this as well as non-linear methods (Feldmann et al., 2021), which could return different relationships to genomic loci. Nevertheless, my focus centers on the methods to generate the basis for, rather than deriving, the proper latent variables; PCA is just an example. This emphasizes the need to validate the association between molecular markers with latent phenotypes as well as conventional components of seed yield.

A clear challenge from using latent phenotypes centers on the difficulty of interpretation. Differences in grams per plant or area are easier to understand and visualize than unitless values from a latent space. The latent components from color descriptors were able to identify a potential confounding factor by clustering the two scanners used for this study. The shape descriptors also clustered the data in two well-defined groups, but their technical or biological meaning is not fully understood. This could reasonably create skepticism among the scientific and breeding community, but that is also what drives us to validate and improve our technologies. Despite being a recent field, latent phenotyping is rapidly growing in plant genetics, and I suspect it will continue to increase as modern computational tools become are more accessible.

Conclusions

While spike architecture determines seed productivity it is difficult to quantify not only because of the infinite traits that comprise it but because some of them are imperceptible. I developed *SpykProps*, an imaging pipeline in Python that accurately detects properties of the spike architecture in perennial ryegrass from which latent phenotypes could be derived. Integrating this approach with molecular breeding has great potential for understanding the

genetic basis of the spike architecture and the rapid domestication of forage and amenity grasses like perennial ryegrass.

Chapter 3. The Effect of Plant Growth Regulators on Seed Shattering, Yield, and Spike Architecture in Perennial Ryegrass

Overview

Among all agronomic practices, the use of plant growth regulators (PGRs) has played an important role in perennial ryegrass seed production despite having inconsistent effects across environments. Inhibitors of gibberellins biosynthesis are widely used PGRs for lodging control, but they may also have potential to increase in shattering and yield. Aminoethoxyvinylglycine (AVG) is an ethylene inhibitor that increases retention across different crops, yet its potential effect in perennial ryegrass seed production has been widely explored. The goal of this study was to evaluate the effect of GA and ETH inhibition in greenhouse and field conditions on seed shattering, yield, and spike architecture. I used a custom imaging approach to rapidly collect and measure spike length, spikelet number, and other shape descriptors. While extenuating circumstances affected the data collection process, PGRs showed a clear effect on plant height and significant differences on spike architecture. Nevertheless, I did not find statistical differences on agronomic traits attributed to PGRs. The results of this experiment require further validation with greater sample size and proper replication across environments. Nevertheless, trends from the analyses suggest that PGR may not be a reliable practice to increase seed retention or yield in perennial ryegrass.

3.1. Introduction

Plant growth regulators (PGRs) are naturally occurring compounds that can be artificially synthesized and affect the development and metabolism in plants (Rademacher, 2015). Type I PGRs inhibit cell division while type II inhibit the synthesis of gibberellins, and thus, cell expansion (Howieson, 2001). These phytohormones are commonly used in the turf industry to control head emergence on mowed swards, however, their inhibitors are also commercialized and have been reported to increase perennial ryegrass seed retention and yield (Chynoweth et al., 2008; Joaquin et al., 2007; Lee, 2006). Given the intrinsic dependence of abscission on hormonal regulation (Addicott & Wiatr, 1977), PGRs could potentially be used to overcome to the lack of germplasm with improved seed retention and yield in perennial ryegrass.

Inhibitors of gibberellin (GA) biosynthesis are the most economically important and used PGRs (Rademacher, 2015) and have been inconsistently reported to affect seed retention in grasses. These type II PGRs are known to reduce internodal length and increase stem strength which helps to keep grass crops upright. Trinexapac-ethyl (TE) is a widely used GA inhibitor in perennial ryegrass seed production despite its inconsistent effect on productivity (Chastain et al., 2014). TE is reported to delay lodging, increase harvest index, and reduce shattering, altogether resulting in greater seed yields in perennial ryegrass (Chynoweth et al., 2008; Chynoweth et al., 2014; Rolston et al., 2010). However, studies have shown variable effects of TE in perennial ryegrass' growth (Ervin & Koski, 1998) and other grass species (Hare et al., 2008). Paclobutrazol [(αR,βR)-*rel*-β-[(4-

chlorophenyl)methyl]-α-(1,1-dimethylethyl)-1H-1,2,4-triazole-1-ethanol], for example, was shown to significantly increase seed retention at harvest in a two-year study in perennial ryegrass (Hampton & Hebblethwaite, 1985); in the study, GA inhibition modified the inflorescence morphology, redistributing the number of florets and seeds per spikelet compared to untreated plants. Nonetheless, this can also be accomplished by mechanical control of lodging (Burbidge et al., 1978). Prohexadione-calcium (calcium salt of 3,5-dioxo-4 propionylcyclohexanecarboxylic acid; Pro-Ca) another GA inhibitor, has also shown increased yield in grasses in perennial ryegrass because of reduced lodging, increased seed set, and improved canopy architecture (Silberstein et al., 2001). Lee (2006) found a positive effect between spike length and seed shattering by evaluating GA inhibition rates but avoid suggesting it for agronomic management strategy due to inconsistent effects.

Other hormonal inhibitors have shown promising results in reducing shattering in grass species. Given that the abscission timing is regulated by a balance and interaction between auxin (IAA) and ethylene (Taylor & Whitelaw, 2001), studies have evaluated their potential use to reduce shattering. In Guinea grass (*Panicum maximum* Jacq.) treatment with IAA increased retention 32% in controlled conditions and up to 40% in field conditions (Weiser et al., 1979). While ethylene induction is expected to decrease seed yield, in some cases it has increased it; for example, Joaquín et al. (2007) showed increased seed retention and yield in Guinea grass by effect of salicylic acid and the steroidal hormone cidef-4. Ethylene inhibition, and in particular, the use of aminoethoxyvinylglycine (AVG) has shown delayed maturation and increased retention in fruits (Wood et al., 2009; Yuan & Carbaugh, 2007) but its potential in grasses has not been

widely investigated. Through greenhouse and field experiments using AVG, Lee (2006) found a negative relationship between the level of ethylene inhibitor and shattering in perennial ryegrass Despite not having statistically significant effects, such results suggest a potential effect of to increase retention.

The effect of PGRs on shattering and yield in perennial ryegrass is highly variable and depends on different factors. The inconsistent effects of the phytohormones are mainly attributed to genotype-specificality as well as interaction between inhibition levels with the phenology of the crop and environmental conditions such as temperature and humidity (Mathiassen et al., 2007). In consequence, isolating the effect of phytohormones on yield-related traits is challenging not only due to the myriad of variables and interactions at play but because of the lack of proper phenotyping tools for the species. Furthermore, differences in flowering time and duration as well as the species heterogeneity can be confounding variables and their effect is difficult to separate. It is possible for type II inhibitors to affect seed shattering indirectly by altering inflorescence morphology to compact shapes that are less susceptible to disarticulation (Lee, 2006); however, this requires proper experimentation that carefully consider the way in which shattering is measured, sample size, genotype-specificity, and environmental interaction.

The objective of this study was to evaluate the effect of inhibiting ETH and GA biosynthesis at different rates, on seed shattering, yield, and spike architectural traits. To do so, I conducted experiments in controlled and field conditions using a single variety.

3.2. Materials and Methods

3.2.1. Controlled Experiment

Greenhouse experiments took place in 2021 at the Minnesota Agricultural Experiment Station Plant Growth Facility in St. Paul, Minnesota, United States. The average temperature, relative humidity, and dew point in the greenhouse were 23.3 ± 3.8°C, 57.6 ± 14.5%, and 13.9 ± 3.9°C, respectively (monitored with a HOBO by Onset MX2301A data logger). Light was supplied for 16-h photoperiod with 400-watt high pressure sodium lamps at 0.8 meters from the plants. Seedlings were moved to the greenhouse after 20 weeks of primary induction at 6°C. Each seedling was transplanted to pots with 4 cm in diameter and 35 cm containing a 2:1 ratio of Metro-MIX 852 RSI Professional Growing Mix and Turface Athletics MVP, 4.9 g Osmocote Plus, and were weekly fertigated. The concentrated solution for fertirrigation was made from 906 g of ammonium sulfate, 950 g of Peat-lite, and 38 g of Sprint 330 mixed into 5 gallons of water, and a tablespoon of granular "Green Clean" to prevent algae growth in the stock solution; the nutrient level of the applied solution is 200 ppm N, 22 ppm P, 83 ppm K, 114 ppm S, 2.5 ppm Fe, 750 ppb Mg, 100 ppb B, 50 ppb Cu, 280 ppb Mn, 500 ppb Mo, and 81 ppb Zn. The pots were interleaved on 6x3-cell trays where each tray contained each of the initial nine treatments once (Figure 3.1A). These plants were staked and loosely tied throughout their development to avoid lodging and shading.

The experiment was originally designed with randomized complete blocks (RCB) comprising three blocks, 20 reps (trays), and nine treatments, for a total of 540 experimental units (Figure 3.1B). Three inhibition rates along with positive controls for each of the two inhibitors were compared with untreated pots, using the cultivar ‘Galactic

Green'. Trinexapac-ethyl [4-(cyclopropyl-α-hydroxy-methylene)-3,5-dioxocyclohexanecarboxylic acid ethyle ster] (*Palisade*), hereafter referred to as TE, was used as a gibberellin (GA) inhibitor at three rates: 0.29 (low), 0.73 (mid), and 1.09 (high) liters per hectare. Aminoethoxyvinylglycine (*PinCor*), hereafter referred to as AVG, was used as an ethylene (ETH) inhibitor and included three rates: 0.29 (low), 0.58 (mid), and 0.88 (high) liters per hectare. Positive controls for ETH and GA were Ethephon (*Proxy*) at 1.7, and GA3 (*ProGibb T&O*) at 0.04 liters per hectare, respectively. All PGRs were mixed with 0.25% V/V solution of nonionic surfactant and sprayed in an isolated chamber at two time points to guarantee an effect on the plants. The first application took place on April 05, 2021, at spike initiation and the second was 21 days later, when the first spikelet was visible in most untreated plants. The plants were placed in a tray and sprayed for less than a second with an XR 8002XR sliding nozzle at 30 PSI located 0.5 m above the canopy.

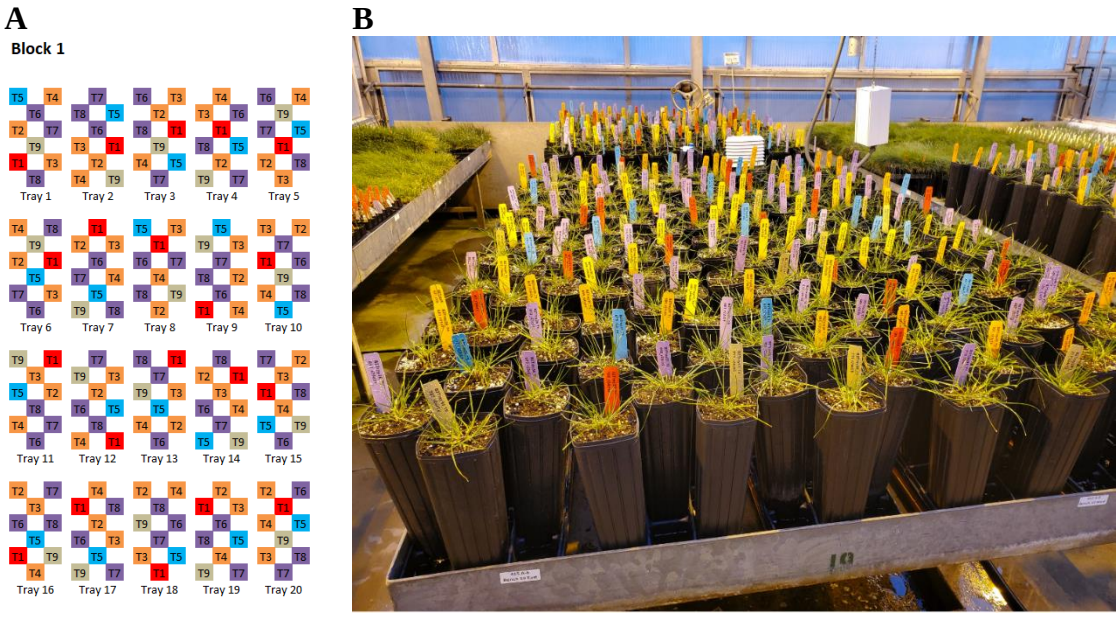

Figure 3.1. Experimental design for controlled experiment. **A** Greenhouse layout of one of the three blocks. Each of the 20 trays per block contained all nine treatments, colored by type of hormonal treatment. Red: untreated (T1); purple: ethylene inhibitor (T2, T3, T4); blue: ethylene inducer (T5); orange: gibberellin inhibitor (T6, T7, T8); tan: gibberellin inducer (T9). **B** Actual image of a block from the experiment in controlled conditions.

3.2.2. Field Experiment

Two farms located near Roseau, Minnesota, separated by approximately 6.5 km, and planted with the cultivar Galactic Green were used for this experiment. Perennial ryegrass was planted in the fall of 2020 as a double crop with spring wheat. Differences in maturity levels across locations were present when the experiment was demarcated: plants from Site 1 had 2-3 nodes while those from Site 2 were closer to booting. Nutrition management was adjusted based on results from soil analyses and following best agronomic practices for perennial ryegrass seed production in northern Minnesota (Heineck et al., 2018; Koeritz et al., 2013). The experimental design at both locations was

the same RCB with four replicates, five treatments, and therefore, 20 experimental plots of ~39 m^2 (3x13 m) with borders around the blocks as shown in **Error! Reference source not found.**B. For this experiment, only a low and a high concentration of each inhibitor were compared against untreated plots. Prohexadione-calcium (calcium salt of 3,5-dioxo-4 propionylcyclohexanecarboxylic acid) was used as a GA inhibitor at a rate of 0.29 (low) and 0.73 (high) liters per hectare, and AVG (*PinCor*) was used as an ETH inhibitor at a rate of 0.37 (low) and 0.95 (high) liters per hectare. The treatments were mixed with a 2.34 liters per hectare of 28%N + 0.25% V/V solution of nonionic surfactant (*Preference*) and applied using a 3-meter-wide bike sprayer. As in the greenhouse experiment, PGRs were sprayed twice to guarantee an effect on the crop; the first application took place on June 03, 2021, and the second was 20 days later during anthesis.

A **B**

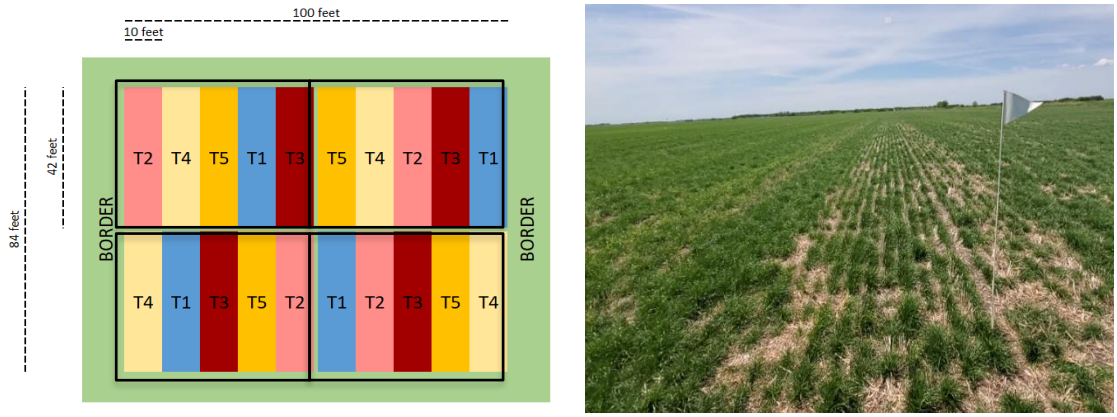

Figure 3.2. Experimental design for field experiment. **A** Field layout of one of the two sites with its respective dimensions in feet. Each of the four replicates (black squares) contains all five treatments, colored by type of hormonal treatment. Blue: untreated (T1); red tones: ethylene inhibitor (T2: low, T3: high); yellow tones: gibberellin inhibitor (T4: low, T5: high). **B** Partial view of the actual site from the field experiment in Roseau, MN.

Table 3.1**.** Summary of plant growth regulator treatments in controlled and field experiments.

Molecule	Biosynthesis	PGR	Brand name	Rate	Concetration (lt/ha)	
					Greenhouse	Field
Water	Control	--	--	--	--	--
Ethylene	Inhibitor	Aminoethoxyvinylglycine	PinCor	Low Medium High	0.29 0.58 0.88	0.37 -- 0.95
	Inducer (Positive Control)	Ethephon	Proxy	Recommended	1.7	--
Gibberellins	Inhibitor	Prohexadium Calcium Trinexapac-ethyl	Apogee Palisade EC	Low Medium High	0.29 0.73 1.09	0.29 -- 0.73
	Inducer (Positive Control)	GA3	ProGibb T&O	Recommended	0.04	--

PGR = plant growth regulator
lt/ha = liters per hectare

3.2.3. Harvest and Sampling

Plant height was measured in both experiments at harvest, followed by spike sampling and immediate storage at ~6°C for further processing in a dry lab. Pots from the greenhouse were harvested on different days when approximately 75% of the spikes were filled with matured seeds. Field plots were harvested at ~40% seed moisture content on July 15, 2021 (S2_W) and July 22, 2021 (S1_S). Approximately 20 spikes were harvested per plot and carefully placed in long envelopes keeping approximately 10 of the less shattered spikes from both the greenhouse and field experiments. In addition, two samples from two different 1 m^2 area within field experiment plots a quadrant were collected to better estimate the effect of PGRs at the field level. These plants were cut at ~8 cm and weighed after drying for two weeks at room temperature, then threshed to estimate seed yield ($g \cdot m^2$) and harvest index (% sellable grain from the total dry matter).

3.2.4. Dry Lab Processing

Several variables were measured from the detached and retained seed before and after shaking sampled spikes from 2021 with a wrist action shaker. A summary of the

process can be found in Figure 3.3. The first step was to weight the seed at the bottom of each envelope, i.e., detached before shaking (DBS) and divide it by the number of sampled spikes (NSS). The spikes were then carefully scanned on a flatbed scanner and assigned a visual shattering estimate (VSE) as the percentage of seed lost from the harvested sample. Once imaged, the spikes were placed upside-down in a cylindrical container of 25 cm length and 5 cm diameter with a mesh at the bottom. A container per sample was placed on the shaker to induce seed disarticulation for 5 min at 385 rpm. The weights for the seed detached after shaking (DAS) and retained after shaking (RAS) upon following hand-threshing were recorded. The seed retained before shaking (RBS) was recorded as the sum of DAS and RAS, therefore, the remaining weight corresponded to that of the rachis. The sum of RBS+RAS+DBS+DAS referred to as Wet, was placed in an oven at 95°C for two weeks to obtain the dry weight before and after threshing (DryBT and DryAT, respectively) and estimate the agronomic variables in Table 3.2.

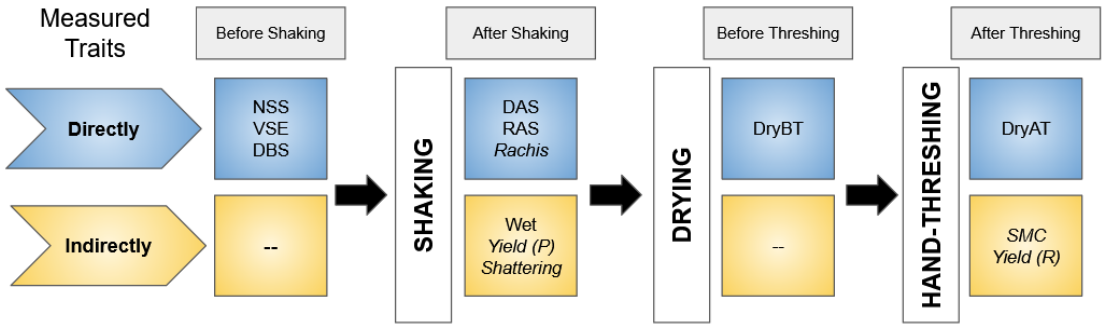

Figure 3.3. Schematic representation of the variables measured during the dry-lab processing to estimate the agronomic traits (italic).

Rachis: weight of seedless rachis; *Wet*: wet weight of dried seed; *Yield (P)*: yield potential; *Shattering*: percentage lost from yield potential. *SMC*: seed moisture content; *Yield (R)*: percentage of sellable seed from yield potential. NSS: number of sampled spikes; VSE: visual shattering estimate; DBS: detached before shaking; DAS: detached after shaking; RAS: retained after shaking; Rachis: weight of seedless rachis; Wet: wet

weight of dried seed; Yield (P): yield potential; Shattering: percentage lost from yield potential, DryBT: weight of the dried seed before threshing; DryAT: weight of the dried seed after threshing.

Table 3.2. Agronomic traits evaluated in this study.

Trait	**Description**	**Equation**
Yield (P)	Yield Potential: Represents the weight of all sealable seed per spike in the absence of shattering.	$Yield\ (P) = \frac{Wet\left(\frac{100 + VSE}{100}\right)}{NSS}$
Shattering	Seed Shattering: Percentage from the yield potential lost due to mechanical seed disarticulation.	$Shattering = 100 - \frac{\frac{RBS}{NSS}}{Yield\ (P)} \times 100$
Yield (R)	Realized Yield: Percentage from the yield potential that could be sold as seed.	$Yield\ (R) = (100 - Shattering)\left(\frac{Wet - DryBT}{DryBT}\right)$
DR	Developmental Rate: Sum of six phenology scores using Gustavsson's scale. Higher values indicate faster development.	$Gust = \sum_{i=1}^{6} G_i$ G = score from Gustavsson's scale on date *i*.
SMC	Seed Moisture Content: Percentage of water in seed at harvest (only in Chapter 4)	$SMC = \frac{Wet - DryBT}{ToDry} \times 100$
Rachis	Rachis Weight: Weight of the remaining spike stem after hand-threshing all seed.	$Rachis = spike\ weight - Wet$

VSE: visual shattering estimate; Wet: wet weight of dried seed; NSS: number of sampled spikes; RBS: retained before shaking; DryBT: weight of the dried seed before threshing; G: score on phenological scale (Gustavsson, 2011); SMC: seed moisture content.

The images gathered during the dry-lab processing were curated and analyzed using *SpykProps* a custom imaging pipeline described in Chapter 2. The RGB images were collected at 600 dpi without using any type of filters. The following spike architectural traits were generated: area, eccentricity, perimeter, circularity, length, width, roundness,

number of spikelets per spike, and minimum number of optimal elliptical Fourier descriptors describing the spike's outline.

3.2.5. Analysis

Differences in treatments were evaluated based on analysis of variance using a 0.05 level of significance (P). Pearson correlation coefficients (R) were used for comparisons between agronomic traits. The developmental rate (DR) was visually classified in the greenhouse experiment using a scale (Gustavsson, 2011) designed cool season perennial grasses; all plants scored a "10" when moved from primary induction to the greenhouse.

3.3. Results

Limitations due to logistics dramatically reduced the amount of data collected for the controlled and field experiments. While all plots in the field experiments were evaluated, a maximum of 15 pots per treatment were collected from the greenhouse for dry-lab processing. Developmental rate (DR) was the only trait that was recorded on most experimental units of the original greenhouse design. Accordingly, I modified the analysis to treat the greenhouse experiment as an additional environment, GH, to Site 1, and Site 2. Furthermore, I excluded the positive controls and medium rates from the greenhouse. In summary, I analyzed the effect of all initial treatments from greenhouse and field experiments on developmental variables, however, the measurements from dry-lab processing were limited to low and high concentrations of inhibitors in three environments (GH, Site 1, and Site 2).

3.3.1. Development

Plants in the greenhouse experiment were scored a "10" developmental rate (DR) value at the end of primary induction on March 15, and additionally scored seven times after. Values included "45" at booting, "55" at spike initiation, "61" at the beginning of anthesis and "69" at the end (Gustavsson, 2011). Higher DR values indicate faster growth, lower indicate a delayed development. On April 07, 23 days after primary induction, the control treatments had the highest DR, and particularly those with ETH inducer which were already at booting. In contrast, GA and ETH inhibitors at high and medium rates showed delayed growth (**Error! Reference source not found.**).

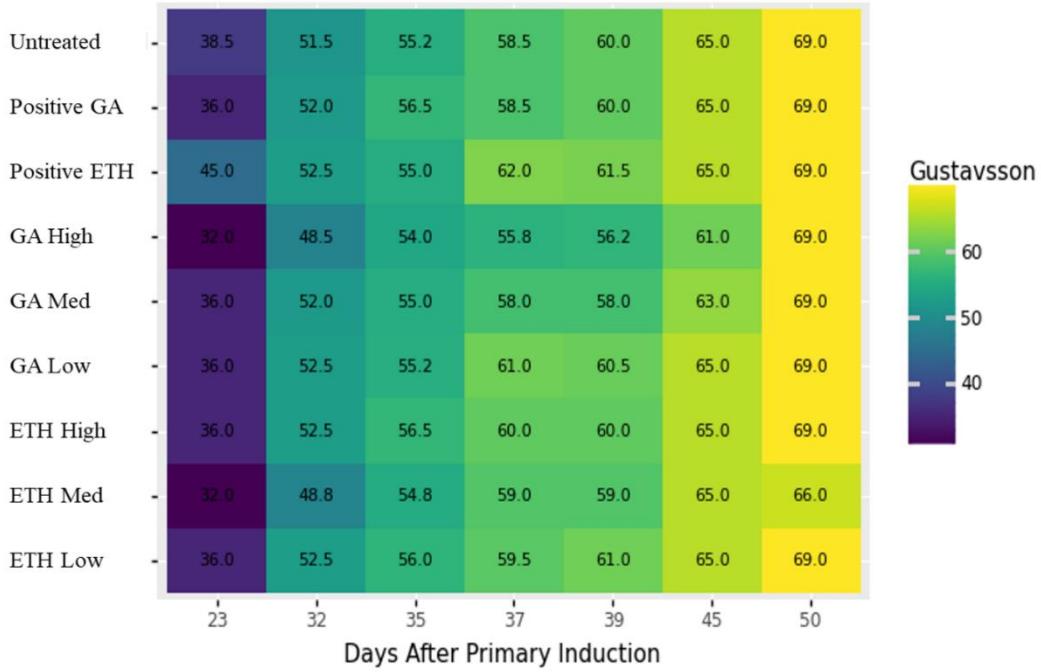

Figure 3.4. Developmental variation over time across hormonal treatments in controlled conditions. Axes represent the days after primary induction (x) across treatments (y). Values indicate means across blocks of the median phenological values per treatment, based on Gustavsson (2011) phenological scale (right); darker an lighter values indicate slower and faster growth, respectively.

The area under de curve for the first five measurements (**Error! Reference source not found.**) was used to represent changes in maturity: higher values indicate faster development while lower values indicated slower. Untreated plants developed faster (+0.46 SD) than those treated with inhibitors, and positive ETH control, respectively. Besides the positive ETH control, high GA (-1.54 SD) and medium ETH (-1.48 SD) levels of inhibition were the most deviant. The coefficient of variation (CV) was highest on the first date (0.16) and dramatically dropped for the second (0.09). The growth rates across treatments continued decreasing slowly until it reached CV=0.05 on May 03.

There was substantial variation across treatments including the untreated pots which had the highest CV on the first date (0.17) after ETH med (0.18). While the growth rate steadily decreased in untreated and the GA3 pots, the rate oscillated in all PGR treatments but ETH high. Interestingly, GA high had a CV as high as 0.09 on the last scoring date, which could be the effect of strong genotype by environment interaction. The CV for GA med on the last date (0.08) supports the premise of strong growth retardance by inhibition of gibberellins.

Plants in the greenhouse were attached to a grounded stick and tied with a wire to avoid lodging. This allowed to observe differences in height due to hormonal regulation (

Figure 3.5). There was a direct negative relationship between GA inhibition and plant height. Inducing gibberellin biosynthesis produced a 44 – 82 cm range and mean increase of 11.8 cm compared to untreated pots. As expected, external ETH, dramatically reduced plant height and avoid flowering. However, inhibiting the synthesis of ethylene did not have a clear effect on plant height, instead it matched the 36-69 cm range found in untreated plants. This pattern was similar in field conditions, where plots with high and low GA inhibition rates were on average 6.5 cm and 3.6 cm shorter than untreated (mean

= 21.5 cm). Low (22.2 cm) and high (21.5 cm) levels of ETH inhibition were not different from untreated field plots in terms of plant height.

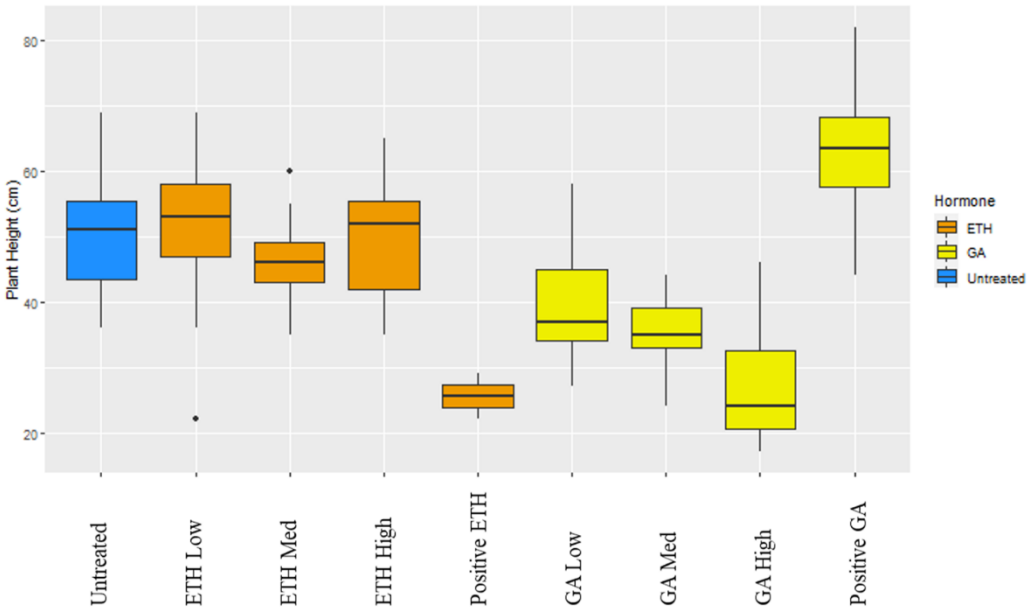

Figure 3.5. Differences in plant height by plant growth regulators in controlled conditions. Axes indicate the rate (x) and plant height (y) in centimeters. Colors represent hormonal treatments. Blue: untreated; orange: ETH inhibition; yellow: GA inhibition.

3.3.2. Agronomic Traits

Analysis of the reduced data sets indicated no significant effect of PGR inhibitors on agronomic traits. While average levels of shattering across environments were greater on untreated plots (80.02 %) and those with low inhibition rate, differences were not significant from high concentrations of ethylene (78.83 %) or gibberellin (78.45 %) inhibitors. The main effect of the environment was statistically significant in all agronomic traits but shattering; the interaction between treatment and inhibitor was more relevant (Table 3.3). Yield potential was statistically different across GH (1.87 g/spike), S1_S (3.04

g/spike), and S2_W (5.13 g/spike). The same pattern was found on realized yield, which had a significant correlation with yield potential (R = 0.37) at the alpha 0.05. Rachis weight was the highest on S2_W (0.94 g) followed by S1_S (0.86 g), both statistically similar but different from GH (0.04 g). Rachis had a significant correlation with yield potential (R= 0.64) and realized yield (R = 0.46), and seed moisture content (R = 0.40), but not with shattering.

Table 3.3. Significance values (P values) and model statistics of the main effects on agronomic traits across environments.

Trait	Main Effects Significance			Model Statistics	
	Environment	Inhibitor	Interaction	R^2	P value
Yield (P)	0	0.18	0.03	0.76	0
Shattering	0.84	0.67	0.02	0.21	0.09
Yield (R)	0	0.08	0.01	0.49	0
SMC	0	0.33	0.84	0.34	0
Rachis	0	0.13	0.01	0.77	0

R^2: coefficient of determination.
YLDpot: yield potential; *SHATTE*: yield potential lost to shattering, *ReaYld*: realized yield, *SMC*: seed moisture content, *rachis*: weight of the spike rachis.
p-values smaller or equal to 0.05 indicate no significant effect.

3.3.3. Architectural Traits

In contrast with agronomic traits, spike architectural traits appeared to be significantly affected by plant growth regulators (Table 3.4). While the spike area was only affected by the environment, its perimeter was affected by differences in environment and inhibitors. Spikes tended to be longer with low inhibition of ethylene and shorter with high gibberellin inhibition; the spikes in the greenhouse were significantly shorter than those from field conditions. High GA inhibition was also different from other treatments in the effect on overall shape (minimum Fourier coefficients) and number of spikelets per spike.

On average, high GA inhibition produced less spikelets (15.24) than other treatments, low ethylene inhibition produced more (18.13).

Table 3.4. Significance values (P values) and model statistics of the main effects on spike architectural traits across environments.

Trait	Main Effects Significance			Model Statistics	
	Environment	Inhibitor	Interaction	R^2	p-value
Area	0	0.18	0.29	0.56	0
Perimeter	0.01	0.04	0.15	0.3	0
Length	0	0	0.38	0.54	0
Roundness	0.07	0	0.25	0.51	0
Min_Coeffs	0	0	0.65	0.34	0
Spikelet number	0.36	0	0.32	0.31	0

R^2: coefficient of determination.
Min_Coeffs: optimal number of harmonics (ellipses) to decompose the spike's outline using Fourier Transform.
p-values smaller or equal to 0.05 indicate no significant effect.

3.4. Discussion

The results from this study agree with previous reports on the inconsistencies that plant growth regulators have on shattering and yield in perennial ryegrass. Lee (2006) found that ethylene and gibberellin inhibitors did not reduce shattering losses at a statistically significant level. This may be because despite the genetic control of abscission, shattering is highly environmentally dependent (Elgersma et al., 1988). As part of a dispersal mechanism, other wild traits that also have a hormonal basis may be affecting seed dispersal in cryptic ways (Saastamoinen et al., 2018). Nevertheless, the limited sample size analyzed, and subsequent low statistical power, in this experiment represents a barrier to making concrete conclusions or even detect significant effects on agronomic traits. Yet, the use of imaging techniques allowed finding differences in architectural traits due to

inhibitors under the same experimental limitations. The potential of high throughput phenotyping techniques to overcome sample-size limitations should be validated in further studies.

While sample size for the analysis of the field experiment was also smaller than planned, its results shared similarities with those obtained in previous studies. For example, Chynoweth et al. (2008) found that gibberellin inhibition in perennial ryegrass increased harvest index, reduced internode length and thus lodging, overall increasing yield. I found similar results: clear statistical differences in plant height and differences between GA inhibitor rates (high: 38.1 cm, low: 45.1 cm) and untreated (54.6 cm). In addition, high ethylene inhibition rates were not statistically different from untreated plots, however, low rates differed and had the tallest plants (56.5 cm). I also found statistical differences in harvest index but the values for untreated plots (600) were rather higher than those treated by gibberellin inhibitors (high: 453.12, low: 523.62), which were even lower than in ethylene inhibitors (high: 520, low: 547). Moreover, while I also found significant differences in seed yield attributed to inhibition rates, the environment and interaction with treatment had a much stronger effect (

Figure 3.6**Error! Reference source not found.**). Nevertheless, because PGR experiments often include combinations of years, locations, and different varieties (Rolston et al., 2010), the results from this study require further validation with proper replication.

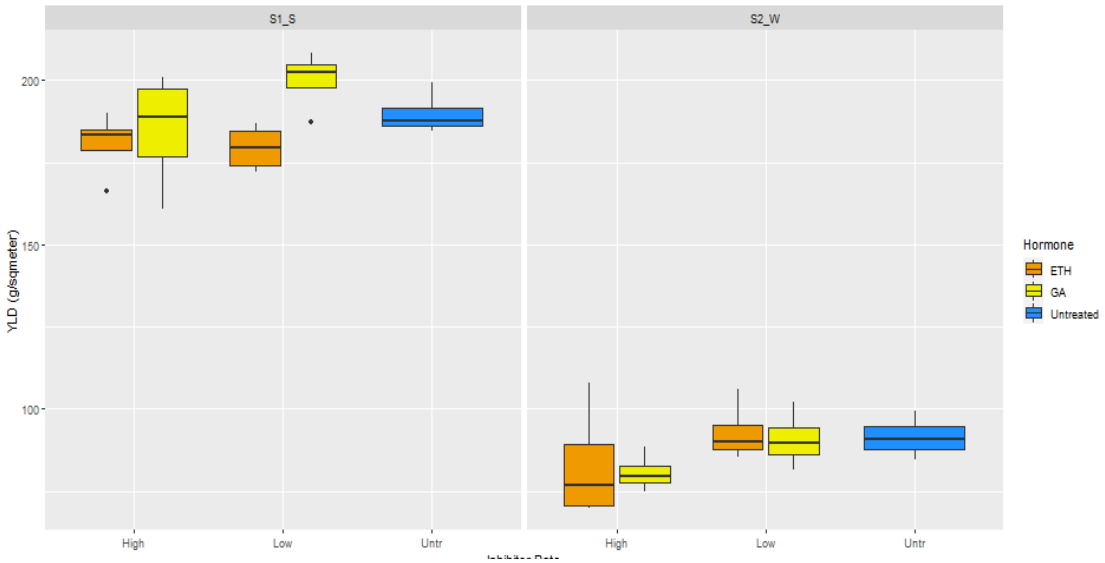

Figure 3.6. Boxplots of the seed yield distribution by inhibition rates in two field sites in Roseau, MN. Site 1 (S1_S) on the left, Site 2 (S2_W) on the right. Axes indicate the rate (x) and seed yield (y) in grams per squared meter. Colors represent hormonal treatments. Blue: untreated; orange: ETH inhibition; yellow: GA inhibition.

Despite the limitations of these studies, their general results support the need to strengthen breeding and genetic efforts focusing on seed retention and yield in perennial ryegrass. It is possible for agronomic management to increase production costs and decrease profitability even if they produce greater yields. While the use of plant growth regulators can occasionally show positive results on yield, seed growers need more stable and long-term solutions. Because perennial ryegrass is rather a recently domesticated species, there needs to be a major focus on heritable components affecting seed productivity and unfavorable characteristics resembling wild ancestors. Perhaps, as speculated from this study, some of those components may be hidden within the spike architecture and could be elucidated using holistic phenotyping tools.

Conclusions

Perennial ryegrass has been predominately a forage crop; higher seed retention and yield have not been a major breeding focus during its recent domestication. Agronomic management and particularly the use of plant growth regulators has therefore played an important role in the seed producing industry. The objective of this study was to evaluate the effect of low and high rates of ethylene and gibberellin inhibitors on seed shattering, yield, and spike architecture, in greenhouse and field conditions. I found no statistical difference in shattering and yield, but on spike architectural traits when evaluating plots at the plant level, across environments. At the plot level, gibberellin inhibition produced higher seed yield on average but lower harvest index. Furthermore, most differences were attributed to environmental differences and interaction with treatments. Plant growth regulators had only clear effects on plant height and their inconsistencies on yield performance suggest that they may not be a sustainable approach to increasing retention and yield in perennial ryegrass. Nonetheless, the results from this study should be considered in the context of the experimental limitations and must be validated in further research.

4. Genetic Variation of Spike Architecture, Seed Shattering, and their effect on Yield in Perennial Ryegrass

Overview

Seed yield in perennial ryegrass is highly affected by spike architectural traits that are also related to seed dispersal capacity. Breeding for increased seed yield in this species is challenging due to genetic correlations among such wild traits and the lack of accurate phenotyping tools to characterize populations at a large scale. In this paper, I measured yield-related traits across several perennial ryegrass families, and I used *SpykProps*, an imaging pipeline to rapidly derive multivariate descriptors of spike architecture including color, shape, and spikelet features. I estimated the broad (H) and narrow sense (h_2) heritability across traits and evaluate the predictive power of spike architectural traits on agronomic traits. Shape descriptors had the strongest association with agronomic traits, as well as highest broad and narrow sense heritabilities overall. Among agronomic traits, rachis weight was the most heritable ($h_2 = 0.95$) despite having low repeatability ($H = 0.52$). Shape descriptors had the highest predictive ability for rachis weight and yield potential, whereas spikelet descriptors were best at predicting seed shattering. I found two multivariate traits that represent examples of selection targets to improve seed yield in perennial ryegrass while potentially decreasing unfavorable genetic correlations. These results suggest the use of more accurate and less biased phenotyping methods to characterize and identify patterns affecting yield that could be selected for molecular breeding.

4.1. Introduction

The domestication of perennial ryegrass as a forage grass is relatively recent (Brazauskas et al., 2011), and more so is its cultivation for seed production. In consequence, spike-related traits such as asynchronous flowering and seed shattering that did not affect its use for animal feed (Wilkins, 1991), are a major problem to researchers and seed growers. Because of differences in swathing, the harvested seed includes a large proportion of light seed. Furthermore, the heaviest seed is often lost before harvest due to abscission. Agronomic practices could address these issues but can also be inconsistent due to its dependency on variety, weather conditions, and could increase. Therefore, the genetic improvement of perennial ryegrass is essential to obtaining high-yielding cultivars.

The rate at which a given trait is improved through breeding depends on the heritability of the trait given a selection differential (Falconer, 1996). In other words, the response to this selection, i.e., the genetic gain from breeding for seed retention, yield, or any other trait, depends on whether the variation for the trait is controlled by genetics. Broad-sense heritability (*H*) of a trait refers to the total genetic variance contributing to the phenotypic variance within a population. The narrow-sense heritability (h_2) of such trait indicates the proportion from the total genetic variance, that is additive, i.e., it is transmitted through generations.

Heritability is a function of the accuracy and precision with which the trait is quantified during experimentation. Inaccurate measurements of the trait lead to inaccurate estimates of heritability, thus affecting the response to selection across related traits. Conceptually, quantifying the variation for a single trait is arguably impossible given its inseparable entanglement with other traits, some of them imperceptible, within a

multivariate phenotypic spectrum. For example, seed disarticulation may be controlled in large part by the development of an abscission zone but also as a function of spikelet morphology. However, accurate measurements of a strong phenotype with a large enough sample size could capture substantial phenotypic variation to better estimate its additive component. Therefore, improving retention (or reducing shattering) in perennial ryegrass depends on how one measures the phenotypic multidimensionality of seed dispersion.

Correlations among yield components have led to selection upon inflorescence morphology traits driving higher productivity in major crops; however, the inevitable effect of indirect selection could also cause unfavorable trait correlations (Keith & Mitchell-Olds, 2019; Law, 1979; Oury & Godin, 2007; Schulthess et al., 2017; Thorwarth et al., 2019; Wu et al., 2017). The genetic basis of such correlations can be due to closely linked loci or pleiotropy (Falconer, 1996), the latter which may be common in grasses inflorescence architecture (Doust et al., 2005; Simons et al., 2006; Zhou et al., 2012). Understanding the nature of trait correlations within spike architecture is a challenge not only because of the difficulty in quantifying complex morphology, but also because as in yield and quality, not all traits are necessarily perceivable by humans (Chitwood & Topp, 2015; San-Miguel et al., 2016).

As a sown grass, the varieties developed for different markets must have profitable seed yield to be accepted by growers. This represents a major concern given that perennial ryegrass can only produce up to 20% of its theoretical yield potential (Abel et al., 2017). Seed yield is a complex trait whose potential is determined before anthesis by the interacting components of inflorescence morphology (Heineck et al., 2020). Although yield is highly affected by environment the structures comprising spike architecture are

more heritable and can be selected for (Byrne et al., 2009; Sartie et al., 2018). In addition, the number of spikes per plant is known to have low heritability and effect on seed yield implying that spike architecture has major implications for breeding (Studer et al., 2008). Because domestication in perennial ryegrass has been recent, wild traits such as seed shattering and uneven flowering are still retained and severely affect productivity.

Despite being the major cause of seed yield loss in perennial ryegrass, seed shattering is a difficult trait to quantify. Because abscission occurs at a microscopic level and seed shedding takes place before and during harvesting, shattering losses are difficult to accurately predict and measure with accuracy. This problem is exacerbated by the uneven flowering and maturity that characterizes perennial ryegrass (Bonin & Goplen, 1963a). Hence, in addition to flowering, seed retention is an essential target of plant improvement efforts (Sartie, 2006). The genetic and phenotypic characterization of seed shattering is critical to increasing seed retention and yield. While non-shattering phenotypes within the genus *Lolium* have been identified (Cai et al., 2011), along with homologues associated with reduced shedding (Fu et al., 2019), entangled relationships with spike morphology and flowering time hinder selection for the higher retention. Some of these relationships may be problematic causing detrimental yield via unintended indirect selection for unfavorably correlated traits. In consequence, selection and further breeding for non-shattering perennial ryegrass requires proper phenotyping and statistical tools accounting for its complex multivariate architecture.

Computer vision techniques offer high-throughput capabilities to increase precision and accuracy of complex phenotypes. This allows for better estimates of heritability that can facilitate breeding decisions. Nevertheless, it is important to define proper traits for

selection to avoid potentially unfavorable genetic correlations. In this study, I used *SpykProps* (described in chapter 2 of this thesis) to characterize the spike architecture across several clones and families and compare its repeatabilities and heritabilities with such values for agronomic traits. I sought to identify phenotypic patterns as examples of potential selection targets to improve seed yield and reduce shattering in perennial ryegrass

4.2. Materials and Methods

4.2.1. Shattering Nursery

I established a shattering nursery in 2020 using a subset of half-sib families originated from cross-pollinating 25 clonal genotypes in the University of Minnesota turfgrass breeding program. The clones were selected for having the best performance after two years of screening families varying on winter survival, stem rust, and crown rust, that were derived from MSP3973 (MSP x Arctic Green/ Royal Green). Five tillers from a single clonal parent per genotype were grown in greenhouse conditions after approximately 13 weeks of primary induction (cooler at 6°C). The design resulted in five blocks containing the 25 genotypes each arranged in a square of 5 by 5 pots, which were shaken during pollination to allow random mating. The seed from each genotype across blocks was bulked and germinated after cold stratification. The seedlings remained in a cooler for ~13 weeks until transplanted to field conditions along with their clonal parents. I used a randomized complete block design with four reps, each containing 3 clonal parents and seven half-sibs per each of the 20 families, for a total of 800 spaced plants (200 per rep).

4.2.2. Agronomic Traits

Phenological scores were given in spring and summer 2020 during the reproductive stage using a phenological scale for cool-season grasses (Gustavsson, 2011). All plants were scored a "10" when transplanted, "55" at spike initiation, "61" at the beginning of anthesis and "69" at the end. The sum of values at different points was defined as the developmental rate (DR): higher values indicate faster development. Spikes were harvested during the first year after establishment (2021). Matured spikes were cut at 5 mm below the basal spikelet, carefully placed in 23 cm-long envelopes, and stored at ~6 °C for further analysis. Dry lab processing was conducted as described in the Materials and Methods section of Chapter 3 (Figure 3.3). In addition to the agronomic traits collected in Chapter 3, the current chapter included seed moisture content (SMC), derived with Equation 4-1, where Wet is the weight of the total seed to dry and DryBT is its dry weight before hand-threshing (Table 3.2)

Equation 4-1

$$SMC = \frac{Wet - DryBT}{Wet} \times 100$$

4.2.3. Spike Architecture

The spike architectural traits for this chapter were also derived using *SpykProps* (Chapter 2) and followed a similar protocol as in Chapter 3. I used four different data sets representing different descriptors of the spike architecture as shown in Table 4.1, that were used to predict the agronomic traits; the number of descriptors were reduced, using principal component analysis to a set of multivariate traits (eigenvectors) of color, shape, spike's outline (elliptical Fourier Descriptors), and spikelets.

Table 4.1. Descriptors of spike architecture

Dataset	Features	Number of Descriptors
Spike Color	Mean, standard deviation, coefficient of variation, percentiles 5, 25, 50, 75, 95, and quantile-based coefficient of variation across nine color channels (R, G, B, H, S, V, L*, a*, b*).	86
Spike Shape	Area, eccentricity, perimeter, circularity, length, width, roundness, minimum number of optimal EFD coefficients, number of spikelets per spike.	8
Spike EFD	Elliptical Fourier Descriptors (EFD) are the coefficients a_n, b_n, c_n and d_n, with n=100 harmonics for every (x,y) coordinate representing the spike outline	400
Spikelet Color	Same as in "Spike Color" but in spikelets detected per spike	86

4.2.4. Models

Because color descriptors capture patterns corresponding to the imaging hardware (Figure 2.13), the equipment used to collect the images was considered a random effect in a mixed model approach when predicting agronomic traits. The type of germplasm (either parent or offspring) within family was also considered as a random effect so that only the spike properties were fixed. I evaluated the marginal and conditional coefficient of determination; the former indicates the variance explained by the fixed predictor while the conditional refers to the variance explained by the whole model. I also used mixed models to estimate the variance components across families and offspring, considering block as a random effect and family as fixed.

The best linear unbiased estimators were extracted from mixed models for each type of germplasm and used to regress offspring on parents. Narrow-sense heritability (h_2) was estimated by multiplying the resulting linear regression coefficients by two (Elgersma,

1990a; Falconer, 1996). Broad-sense heritability (*H*), also known as repeatability, was estimated by extracting the components of variance from analysis of variances using the "anovaVCA" package in R (Team, 2013). All mixed models were fitted using the "lmer" function from the "lme4" package (Bates et al., 2014) in R.

4.3. Results

4.3.1. Variation in Agronomic Traits

Most agronomic traits were statistically significant across families and no genotype by block interaction (Table 4.2). Shattering and realized yield were the only traits with no significant effect by block; realized yield was also the only trait with no differences across families. Average yield potential ranged from 0.151 g ± 0.08 in family P17 to 0.322 g ± 0.1 in P19. However, the latter had the lowest realized yield (1.19 g ± 1.37) and slowest growth, while P24 had the highest realized yield (4.73 g ± 5.52). Shattering losses for families P13 and P15, were the lowest (76.9 % ± 2.95) and highest (81.2 % ± 5.09), respectively; interestingly, they also had the heaviest (0.113 g ± 0.03) and lightest (0.06 g ± 0.02) rachis weight, respectively. Seed moisture content at harvest was on average higher than the 35 - 43 % that has been suggested (Silberstein et al., 2004) and ranged from 49.8 % ± 3.19 in family P23 to 54.8 % ± 5.45 in P02.

Table 4.2. Analysis of variance for agronomic traits in half sib families of perennial ryegrass.

Trait	Mean Square		
	Family	Block	Family x Block
Yield (P)	0.04 ***	0.06 ***	0.01 NS
Shattering	27.38 ***	0.91 NS	12.8 NS
Yield (R)	12.54 NS	12.12 NS	12.48 NS
DR	29.57 **	68.48 ***	18.38 NS
SMC	29.55 ***	120.87 ***	14.15 NS
Rachis	0 ***	0 ***	0 NS

Yield (P): yield potential; *Yield (R)*: realized yield; *DR*; developmental rate; *SMC*: seed moisture content. Significance codes: '***' < 0.001; '**' < 0.01; 'NS' > 0.05

4.3.2. Agronomic Trait Correlations

All traits approximated a normal distribution, and some had statistically significant ($P < 0.05$) correlations though at medium to low levels (Figure 4.1). Yield potential and realized yield were negatively related and had the strongest correlation among all traits ($R = -0.43$). SMC also had comparatively strong and positive associations with yield potential, rachis weight, and in a negative direction with developmental rate. At a lower but significant level ($P < 0.05$), increased shattering was associated with decreased realized yield, however, it had no relationship to yield potential. On the other hand, the decreased shattering was more associated with increased rachis weight and faster development. Overall, these results suggest multidimensionality in the correlations between traits, i.e., the association between yield related traits can change its direction depending on what trait is being changed.

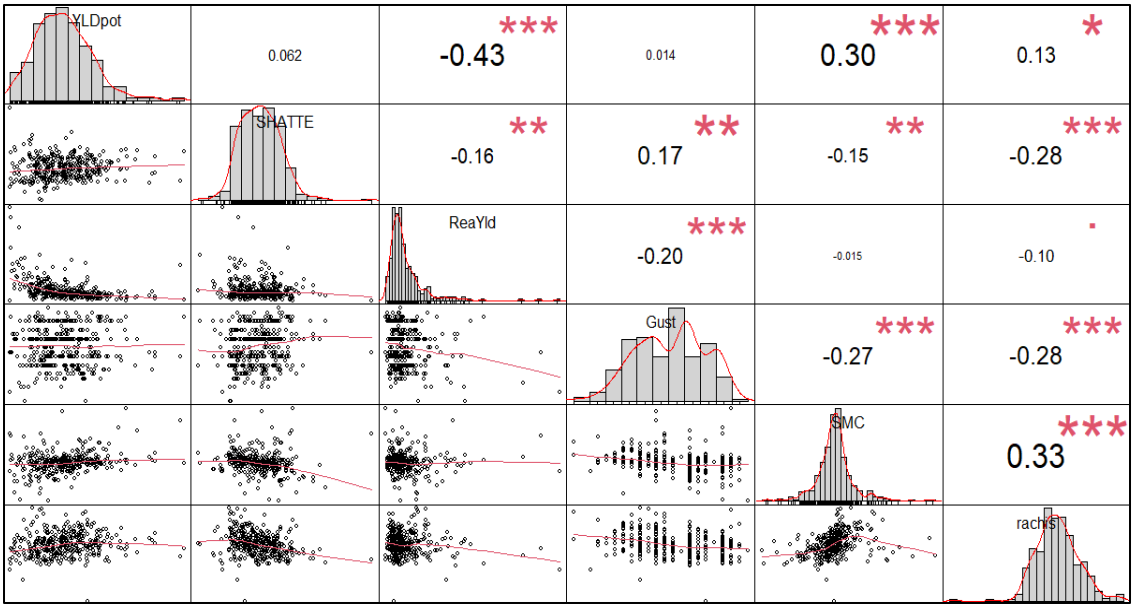

Figure 4.1. Correlations between agronomic traits in half sib families of perennial ryegrass. *YLDpot*: yield potential; *SHATTE*: seed shattering; *ReaYld*: realized yield; *Gust*; developmental rate; *SMC*: seed moisture content; *rachis*: rachis weight. Diagonal: histogram and probability densities for each trait; upper off-diagonal: Pearson correlation coefficients with their associated significance codes; lower off-diagonal: bivariate scatterplots with a fitted line. Significance codes: '***' < 0.001; '**' < 0.01; '*' < 0.05; '.' < 0.1.

4.3.3. Spike Architecture

The first 30 principal components of the color, EFD, and spikelet datasets, as well as the nine eigenvectors derived from the shape dataset, were evaluated as linear predictors of the agronomic traits. The imaging hardware, i.e., combination of laptop and scanner, and the germplasm (either parent or offspring) nested within family, were defined as random effects in the mixed linear models; the eigenvectors of each dataset were modeled as fixed effects. Table 4.3 shows the variance explained by each model (R^2_{Cond}), as well as by predictors (R^2_{Marg}) and their percentage from the whole model (%), across spike properties. The four spike architectural groups differed in their ability and agronomic trait to predict. Color features explained 42% of the variance in yield potential and in rachis

weight; over 75% and more than 90% of these variabilities, respectively, was attributed to the 30 multivariate descriptors of color (Table 4.3). Shape descriptors were also relatively good predictors of rachis weight, explaining 45% of the total variation for the trait. EFD explained about a fourth of the variation in potential yield, and a fifth of that in developmental rate and shattering. Spike and spikelet color were the best predictors for seed shattering despite explaining only a fourth of the trait's variation. Nevertheless, and unlike other descriptors, spikelet features could not contribute even half of the variation in any agronomic trait.

Table 4.3. Variance in agronomic traits explained by four different linear combinations of spike architecture.

Trait	Spike Color			Spike Shape			Spike EFD			Spikelet Color		
	R^2_{Marg}	R^2_{Cond}	**%**	R^2_{Marg}	R^2_{Cond}	**%**	R^2_{Marg}	R^2_{Cond}	**%**	R^2_{Marg}	R^2_{Cond}	**%**
Yield (P)	0.42	0.55	76.36	0.33	0.56	58.93	0.24	0.40	60.00	0.22	0.62	35.48
Shattering	0.26	0.54	48.15	0.21	0.56	37.50	0.19	0.57	33.33	0.25	0.51	49.02
Yield (R)	0.18	0.53	33.96	0.16	0.57	28.07	0.13	0.51	25.49	0.18	0.46	39.13
DR	0.17	0.64	26.56	0.22	0.34	64.71	0.20	0.31	64.52	0.22	0.48	45.83
SMC	0.24	0.48	50.00	0.13	0.50	26.00	0.14	0.31	45.16	0.15	0.56	26.79
Rachis	0.42	0.46	91.30	0.45	0.52	86.54	0.14	0.64	21.88	0.14	0.79	17.72

Yield (P): yield potential; *Yield (R)*: realized yield; *DR*; developmental rate; *SMC*: seed moisture content. *EFD*: Elliptical Fourier Descriptors.
R^2_{Marg}: marginal coefficient or determination; R^2_{Cond}: conditional coefficient of determination; *%:* Percentage from R^2_{Cond} explained by R^2_{Marg}, color-coded within spike descriptor.

4.3.4. Variance Components

Estimates of broad and narrow sense heritability were highly variable across agronomic and spike architectural (Table 4.4). Broad-sense heritability, also referred to as repeatability, was highest in clones and particularly in shattering, yield potential, and rachis weight; SMC had the lowest repeatability (H = 0.33). These estimates were even lower in half sib families, especially for realized yield (H = 0.1) and developmental rate (H = 0.18). Rachis weight had the highest heritability (h_2 = 0.95) and repeatability (H = 0.52) estimates

suggesting a potential control by additive genetic effects. In contrast, shattering and realized yield appeared to be highly environmentally dependent. However, these heritability estimates could be highly inflated and unreliable given the lack of environmental replication and thus need to be approached cautiously.

The repeatability and heritability estimates for each of the four types of spike descriptors was limited to their most relevant linear combinations (eigenvectors). Within type of spike descriptor, except for shape, I selected the up to five eigenvectors with the greatest and significant ($P < 0.01$) regression coefficient for the agronomic trait they predicted the best based on Table 4.3. Because the shape data set comprised nine instead of 30 linear combinations, I kept all of which were statistically significant ($P < 0.01$). Overall, most (seven) of the multivariate descriptors of shape, which were best at predicting rachis weight, had the highest repeatability across parents and offspring and highest narrow-sense heritability (Table 4.4). Descriptors of spike color were also good predictors of rachis weight and had high repeatability (0.8 – 0.87) and medium to high heritability (0.52 – 0.75). In contrast, the top five spikelet color descriptors that were best predictors of shattering had relatively low repeatability across families even though their heritability values also ranged from medium to high (0.45 – 0.72). Only two multivariate descriptors of the spike outline (EFD) significantly explained variation in yield potential, and their repeatability and heritability were also in the medium to high end.

Table 4.4. Heritability estimates for agronomic and spike architectural traits in perennial ryegrass

Trait		Broad-Sense Heritability		Narrow-Sense Heritability
		Parents	Offspring	
Agronomic	Shattering	0.86	0.25	0.33
	Yield (P)	0.79	0.38	0.56
	SMC	0.33	0.35	0.58
	Yield (R)	0.57	0.1	0.33
	DR	0.67	0.18	0.63
	Rachis	0.79	0.52	0.95
Spike Color (Rachis)	PC3	0.92	0.8	0.52
	PC4	0.94	0.84	0.59
	PC5	0.95	0.87	0.55
	PC7	0.93	0.84	0.74
	PC16	0.9	0.8	0.75
Spike Shape (Rachis)	PC1	0.96	0.9	0.79
	PC2	0.96	0.91	0.81
	PC3	0.93	0.86	0.63
	PC4	0.75	0.76	0.76
	PC5	0.94	0.81	0.68
	PC6	0.9	0.75	0.72
	PC9	0.88	0.74	0.75
Spike EFD (Yield Potential)	PC5	0.85	0.76	0.81
	PC7	0.85	0.73	0.59
Spikelets (Shattering)	PC9	0.63	0.56	0.52
	PC11	0.44	0.36	0.72
	PC17	0.86	0.8	0.53
	PC18	0.4	0.38	0.62
	PC26	0.8	0.65	0.45

Yield (P): yield potential; *Yield (R)*: realized yield; *DR*; developmental rate; *SMC*: seed moisture content.
Columns are color-coded blue (low), white (medium), and red (high).
Significance codes: '***' < 0.001; '**' < 0.01; '*' < 0.05; '.' < 0.1.

4.4. Discussion

Seed yield in perennial ryegrass is low and depends on multiple spike architectural traits that also affect variables of agronomic importance. Determining whether there is any additive genetic variance associated with complex agronomic traits is important to define selection criteria for the development of successful cultivars. At least in the families and using the phenotyping methods described here, additive genetic variance may be partly responsible for variation in agronomic traits, and no block or microenvironment interaction was detected (Table 4.2). This implies that, except for realized yield, selection upon any of the other agronomic traits could have an effect in the offspring. Similar analysis in clonal material supported these results, except for a genotype by block interaction effect on realized yield ($P < 0.05$) and seed moisture content ($P < 0.01$), with only a significant effect by microenvironment on the latter (Table S4.1). These findings agree with previous studies on perennial ryegrass where variation in yield was attributed to genetic variance with little genotype by environment interaction (Elgersma, 1990a). While repeatability estimates were relatively high in clone material, in half sib they were very low, indicating potential issues with phenotyping methods. This is expected because unlike in half sib families all variation in clone material is assumedly attributed to non-genetic effects. While it is very likely that the heritability estimates in this study were inflated given the lack of environments and replicates, highest repeatability and heritability values for rachis weight suggest that this trait might be under additive genetic control. Further studies should validate these results and explore the breeding effectiveness of selecting for rachis weight. In parallel, such studies must validate its relationship to shattering and evaluate its effect on other agronomic traits to avoid unfavorable genetic correlations.

Correlations between traits can have unknown and potentially unfavorable consequences for crop improvement during selection and domestication (Gregory, 2009). For example, yield potential had no relationship to shattering yet it was strongly related to realized yield in a negative way; this implies that selecting for greater yield potential in perennial ryegrass would not necessarily represent greater profitability, yet higher retention could potentially do. Shattering was directly proportional to developmental rate which could explain previous approaches to delay growth and general interest in using plant growth regulators (Chynoweth et al., 2008; Lee, 2006). Because realized yield did not appear to have a strong genetic basis it could be possible to select based on higher yield potential and complement with proper agronomic management. Rachis weight had significant correlation with most traits at the alpha 0.05 and with realized yield at the alpha 0.1. Further studies should aim to better understanding rachis morphology in perennial ryegrass and its relationship to dispersal and seed yield.

From the total variation explained by the models predicting agronomic traits (R^2_{Cond}), at least half was attributed to spike architectural traits (R^2_{Marg}). Color and shape features were good predictors of rachis weight and yield potential, they could not explain much variation in developmental rate or realized yield (Table 4.3). The latter was the most difficult trait to predict across data sets which coincides with lacking a genetic basis in the analyses of variance (Table 4.2). Elliptical Fourier descriptors (EFD) were good predictors of yield potential but not of rachis; this is not unexpected given that the EFD are size invariant meaning that the rachis length, thus weight, should be independent. Nevertheless, EFD had the lowest repeatability and heritability estimates among spike architectural traits; this could be explained by the large number of harmonics (default = 100 Fourier harmonics,

i.e., ellipses) used is the imaging pipeline to describe the spike shape. Strawberry fruit, for example, has a simple shape so that a subset of the outline coordinate and fewer harmonics could quantify its shape (Zingaretti et al., 2021). EFD has been successful at identifying leave morphology (Chitwood & Otoni, 2017; Neto et al., 2006), and canopy in soybean (Jubery et al., 2017) but its application to spike architecture is rather more complex. Nonetheless, my results provide examples (PC5 and PC7) of the potential use of EFD to identify repeatable and heritable components of the spike shape affecting yield potential. The spikelet data set contrasted the results from the spike descriptors and while it did not predict much of the previously mentioned traits it explained a larger proportion of shattering. I speculate that this could be related to differences in the amount and possibly ratio between green and brown pixels that often distinguish less from more ripe spikelets, respectively. These patterns may be more difficult to identify when looking at the whole-spike color descriptors because unlike in the spikelet data set, they consider the rachis. The number of spikelets per spike in perennial ryegrass have been identified as an heritable yield component (Abel et al., 2017); the study of their morphology could broaden our understanding of their relationship with other patterns that could be more visible. For example, some of those color and geometrical patterns could also detect differences in flowering dynamics which explains its association with developmental rate (Table 4.3). This emphasizes the need for a comprehensive understanding of the relationship between rachis morphology and spikelet number rachis from a multivariate approach. Nevertheless, these results also show that there need to be much more progress on imaging techniques to improve trait acquisition and definition if they are ever meant to complement or substitute conventional agronomic traits. In general, I hypothesize that multivariate traits like the ones

illustrated in here cannot have very high coefficients of determination in such models because of their latent nature; while agronomic traits are defined based on human perception of the phenotypic reality, the spike architectural traits attempt to derive phenotypic patterns of clusters from combinations -linear, in this case- of multiple traits.

Overall, shape descriptors of the spike architecture appeared to be more reliable than other traits and could have a great potential for breeding perennial ryegrass seed production. Multivariate traits have shown higher heritability and potential to identify unique phenotypic patterns in other grasses (Li et al., 2020; Topp et al., 2013). In this study, multivariate descriptors of shape have significant correlations to all agronomic traits, higher repeatability, and higher heritability. Because all the descriptors are independent from one another, they could have a significant importance in breeding for increased yield in perennial ryegrass with lesser concern about genetic correlations. For example, because of pleiotropic relationships, improving selection on spike architectural traits to improve yield may lead to unfavorable relationships affecting overall agronomic performance. These results suggested that to some extent, it is possible for higher yield potential to represent lower realized yield (Figure 4.1); making decisions on what to select for is therefore challenging. On the other hand, multivariate descriptors of shape could potentially help to overcome this challenge by allowing selection on linear combinations that are correlated to yield potential and realized yield in the same direction or affect one trait without having major effect on the other (Grafius, 1964). For example, PC1 and PC2 appeared to be highly heritable, but while selecting on them could theoretically represent greater genetic gains on yield potential, realized yield could be consequently lower (Figure 4.2). Selecting on multivariate trait PC3 (or PC9), which has lower heritability could

possibly help to overcome such limitation. In addition, selecting for PC1 could be problematic given that in such phenospace, potential and realized yield vary in opposite directions; nevertheless, this multivariate trait aligns with and has a stronger effect on rachis weight, developmental rate, shattering, and yield potential, in a way that could potentially mitigate the negative effect on realized yield. If validated, these approaches could result in increased in genetic because of selection would act on traits higher heritability and that consider more trait interactions, possibly lowering trade-offs from genetic correlations during domestication.

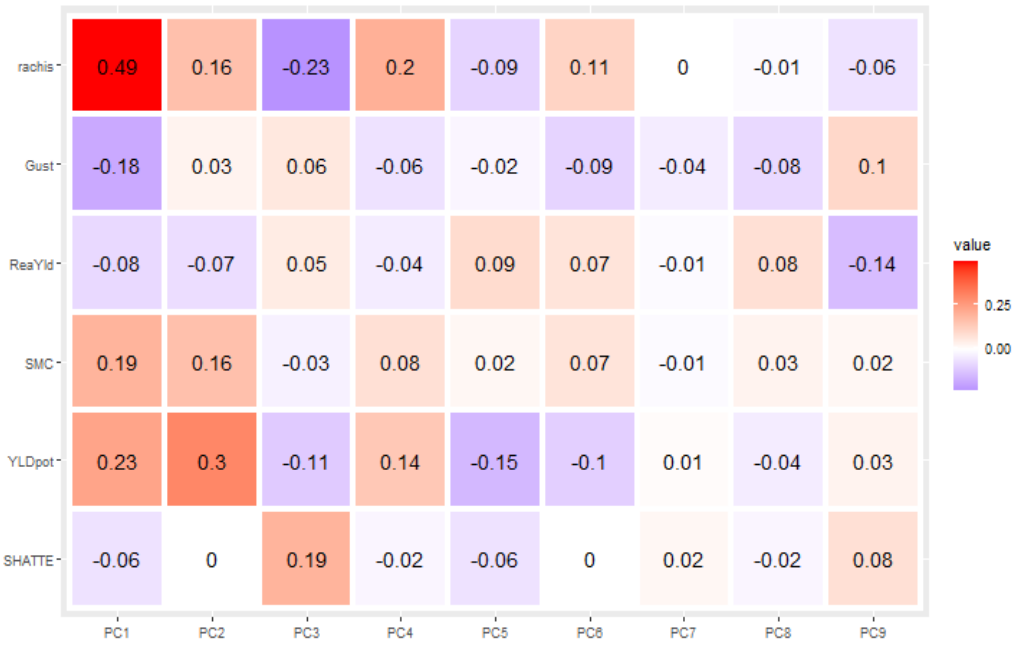

Figure 4.2. Correlations between multivariate descriptors of shape (x axis) and agronomic traits (y axis). Values indicate Pearson correlation coefficients and are color-coded from blue (low) to red (high). *YLDpot*: yield potential; *SHATTE*: seed shattering; *ReaYld*: realized yield; *Gust*; developmental rate; *SMC*: seed moisture content; *rachis*: rachis weight.

Conclusion

There is evidence suggesting additive genetic control on agronomic traits affecting seed yield in perennial ryegrass. Trait correlations between agronomic traits could be potentially unfavorable when selecting for such traits, thus identifying uncorrelated and heritable traits could be advantageous in the context of breeding. By using an imaging pipeline to characterize the spike architecture, I found multivariate descriptors with higher repeatability and heritability than conventional agronomic traits. Different architectural descriptors were associated with different agronomic traits indicating exclusive contribution to the multidimensionality of the spike architecture and yield. While there were correlations between agronomic traits, I found a multivariate descriptor of shape (PC3) with high repeatability and heritability as an example of how multivariate descriptors could address the challenges of genetic correlations. Further studies should explore the genomic basis of such multivariate traits and evaluate their potential for improving seed yield in perennial ryegrass using molecular breeding. More research combining high throughput phenotyping and multivariate (latent) phenotypes could potentially help breeders to accelerate the domestication of economically important species with pronounced wild traits associated with dispersal.

Supplemental

Table S4.1. Analysis of variance for agronomic traits in clonal families of perennial ryegrass.

Trait	Mean Square			p-value		
	Family	Block	Family x Block	Family	Block	Family x Block
Yield (P)	0.06	0.02	0.00	0	0.0178	0.5814
Shattering	87.36	2.06	4.68	0	0.6321	0.4165
Yield (R)	42.03	13.31	12.72	0	0.1576	0.0131
DR	61.44	49.69	9.18	0	0.0045	0.4055
SMC	27.10	39.34	17.86	1.00E-04	0.0122	0.0025
Rachis	0.00	0.00	0.00	0	0.0032	0.824

Yield (P): yield potential; *Yield (R)*: realized yield; *DR*; developmental rate; *SMC*: seed moisture content. Significance codes: '***' < 0.001; '**' < 0.01; 'NS' > 0.05

Bibliography

Abel, S., Gislum, R., & Boelt, B. (2017). Path and correlation analysis of perennial ryegrass (Lolium perenne L.) seed yield components. *Journal of Agronomy and Crop Science*, *203*(4), 338-344.

Addicott, F., & Wiatr, S. (1977). Hormonal controls of abscission: biochemical and ultrastructural aspects. In *Plant growth regulation* (pp. 249-257). Springer.

Agata, A., Ando, K., Ota, S., Kojima, M., Takebayashi, Y., Takehara, S., . . . Matsuoka, M. (2020). Diverse panicle architecture results from various combinations of Prl5/GA20ox4 and Pbl6/APO1 alleles. *Communications biology*, *3*(1), 1-17.

Ahmad, I. S., & Reid, J. F. (1996). Evaluation of colour representations for maize images. *Journal of Agricultural Engineering Research*, *63*(3), 185-195.

Anderson, N. P., Goussard, M., Donovan, B. C., Garbacik, C. J., & Chastain, T. G. (2019). Seed yield and seed shattering with different windrowers in Oregon grass seed crops. Proceedings of the 10th International Herbage Seed Conference,

Araus, J. L., Kefauver, S. C., Zaman-Allah, M., Olsen, M. S., & Cairns, J. E. (2018). Translating high-throughput phenotyping into genetic gain. *Trends in plant science*, *23*(5), 451-466.

Bartlett, M., & Patterson, E. (2019). Many ways to drop a fruit: the evolution of abscission zones in the grasses. *New Phytologist*, *225*(4).

Bates, D., Mächler, M., Bolker, B., & Walker, S. (2014). Fitting linear mixed-effects models using lme4. *arXiv preprint arXiv:1406.5823*.

Bello, C., & Barreto, E. (2021). The footprint of evolution in seed dispersal interactions. *Science*, *372*(6543), 682-683.

Beucher, S. (1992). The watershed transformation applied to image segmentation. *Scanning Microscopy*, *1992*(6), 28.

Bitarafan, Z., & Andreasen, C. (2019). Harvest weed seed control: seed production and retention of fallopia convolvulus, Sinapis arvensis, Spergula arvensis And Stellaria media at spring oat maturity. *Agronomy*, *10*(1), 46.

Bonin, S., & Goplen, B. (1963a). A histological study of seed shattering in reed canary grass. *Canadian Journal of Plant Science*, *43*(2), 200-205.

Bonin, S., & Goplen, B. (1963b). Evaluating grass plants for seed shattering. *Canadian Journal of Plant Science*, *43*(1), 59-63.

Bradski, G. (2000). The openCV library. *Dr. Dobb's Journal: Software Tools for the Professional Programmer*, *25*(11), 120-123.

Brazauskas, G., Lenk, I., Pedersen, M. G., Studer, B., & Lübberstedt, T. (2011). Genetic variation, population structure, and linkage disequilibrium in European elite germplasm of perennial ryegrass. *Plant Science*, *181*(4), 412-420.

Byrne, S., Guiney, E., Barth, S., Donnison, I., Mur, L. A., & Milbourne, D. (2009). Identification of coincident QTL for days to heading, spike length and spikelets per spike in Lolium perenne L. *Euphytica*, *166*(1), 61-70.

Byrne, S. L., Nagy, I., Pfeifer, M., Armstead, I., Swain, S., Studer, B., . . . Hentrup, S. (2015). A synteny-based draft genome sequence of the forage grass Lolium perenne. *The Plant Journal*, *84*(4), 816-826.

Cabrera-Bosquet, L., Crossa, J., von Zitzewitz, J., Serret, M. D., & Luis Araus, J. (2012). High-throughput phenotyping and genomic selection: The frontiers of crop breeding converge F. *Journal of integrative plant biology*, *54*(5), 312-320.

Cai, H., Stewart, A., Inoue, M., Yuyama, N., & Hirata, M. (2011). Lolium. In *Wild crop relatives: genomic and breeding resources* (pp. 165-173). Springer.

Chastain, T. G., Young III, W. C., Silberstein, T., & Garbacik, C. J. (2014). Performance of trinexapac-ethyl on Lolium perenne seed crops in diverse lodging environments. *Field Crops Research*, *157*, 65-70.

Chitwood, D. H., & Otoni, W. C. (2017). Morphometric analysis of Passiflora leaves: the relationship between landmarks of the vasculature and elliptical Fourier descriptors of the blade. *GigaScience*, *6*(1), giw008.

Chitwood, D. H., & Topp, C. N. (2015). Revealing plant cryptotypes: defining meaningful phenotypes among infinite traits. *Current opinion in plant biology*, *24*, 54-60.

Chynoweth, R., Rolston, M., & McCloy, B. (2008). Plant growth regulators: a success story in perennial ryegrass seed crops. *NZGA: Research and Practice Series*, *14*, 47-57.

Chynoweth, R. J., Trethewey, J. A., Rolston, M., McCloy, B., & NZArable, P. (2014). Reduced stem length increases perennial ryegrass seed yield. *Agronomy New Zealand*, *44*, 61-70.

Claramunt, S. (2021). Flight efficiency explains differences in natal dispersal distances in birds. *Ecology*, *102*(9), e03442.

Crowell, S., Falcão, A. X., Shah, A., Wilson, Z., Greenberg, A. J., & McCouch, S. R. (2014). High-resolution inflorescence phenotyping using a novel image-analysis pipeline, PANorama. *Plant Physiology*, *165*(2), 479-495.

Crowell, S., Korniliev, P., Falcão, A., Ismail, A., Gregorio, G., Mezey, J., & McCouch, S. (2016). Genome-wide association and high-resolution phenotyping link Oryza sativa panicle traits to numerous trait-specific QTL clusters. *Nature communications*, *7*(1), 1-14.

Grieve, S. W. (2017). spatial-efd: A spatial-aware implementation of elliptical Fourier analysis. *Journal of Open Source Software*, *2*(11), 189.

Das Choudhury, S., Samal, A., & Awada, T. (2019). Leveraging image analysis for high-throughput plant phenotyping. *Frontiers in plant science*, *10*, 508.

Dinneny, J. R., Weigel, D., & Yanofsky, M. F. (2005). A genetic framework for fruit patterning in Arabidopsis thaliana.

Donati, G., Santini, L., Eppley, T. M., Arrigo-Nelson, S. J., Balestri, M., Boinski, S., . . . Carrai, V. (2017). Low levels of fruit nitrogen as drivers for the evolution of Madagascar's primate communities. *Scientific Reports*, *7*(1), 1-9.

Dong, Y., & Wang, Y.-Z. (2015). Seed shattering: from models to crops. *Frontiers in Plant Science*, *6*, 476.

Doust, A. N., Devos, K. M., Gadberry, M. D., Gale, M. D., & Kellogg, E. A. (2005). The genetic basis for inflorescence variation between foxtail and green millet (Poaceae). *Genetics*, *169*(3), 1659-1672.

Doust, A. N., Mauro-Herrera, M., Francis, A. D., & Shand, L. C. (2014). Morphological diversity and genetic regulation of inflorescence abscission zones in grasses. *American Journal of Botany*, *101*(10), 1759-1769.

Elgersma, A. (1985). Floret site utilization in grasses: definitions, breeding perspectives and methodology. *Journal of Applied Seed Production*, *3*, 50-54.

Elgersma, A. (1990). *Genetic, cytological and physiological aspects of seed yield in perennial ryegrass (Lolium perenne L.)*. Wageningen University and Research.

Elgersma, A. (1990a). Heritability estimates of spaced-plant traits in three perennial ryegrass (Lolium perenne L.) cultivars. *Euphytica*, *51*(2), 163-171.

Elgersma, A. (1990b). Seed yield related to crop development and to yield components in nine cultivars of perennial ryegrass (Lolium perenne L.). *Euphytica*, *49*(2), 141-154.

Elgersma, A., Leeuwangh, J., & Wilms, H. J. (1988). Abscission and seed shattering in perennial ryegrass (Lolium perenne L.). *Euphytica*, *39*(3), 51-57.

Ervin, E. H., & Koski, A. (1998). Growth responses of Lolium perenne L. to trinexapac-ethyl. *HortScience*, *33*(7), 1200-1202.

Falconer, D. S. (1996). *Introduction to quantitative genetics*. Pearson Education India.

Feldmann, M. J., Gage, J. L., Turner-Hissong, S. D., & Ubbens, J. R. (2021). Images carried before the fire: The power, promise, and responsibility of latent phenotyping in plants. *The Plant Phenome Journal*, *4*(1), e20023.

Feldmann, M. J., Hardigan, M. A., Famula, R. A., Lopez, C. M., Tabb, A., Cole, G. S., & Knapp, S. J. (2020). Multi-dimensional machine learning approaches for fruit shape phenotyping in strawberry. *GigaScience*, *9*(5), giaa030.

Ferreira, T., & Rasband, W. (2012). ImageJ user guide. *ImageJ/Fiji*, *1*, 155-161.

Ferrándiz, C., Liljegren, S. J., & Yanofsky, M. F. (2000). Negative regulation of the SHATTERPROOF genes by FRUITFULL during Arabidopsis fruit development. *Science*, *289*(5478), 436-438.

Frei, D., Veekman, E., Grogg, D., Stoffel-Studer, I., Morishima, A., Shimizu-Inatsugi, R., . . . Studer, B. (2021). Ultralong Oxford Nanopore reads enable the development of a reference-grade perennial ryegrass genome assembly. *Genome biology and evolution*, *13*(8), evab159.

Friedman, J., & Harder, L. D. (2004). Inflorescence architecture and wind pollination in six grass species. *Functional ecology*, 851-860.

Fu, G., Huang, M., Bo, W., Hao, H., & Wu, R. (2018). Mapping morphological shape as a high-dimensional functional curve. *Briefings in bioinformatics*, *19*(3), 461-471.

Fu, Z., Song, J., Zhao, J., & Jameson, P. E. (2019). Identification and expression of genes associated with the abscission layer controlling seed shattering in Lolium perenne. *AoB Plants*, *11*(1), ply076.

Furbank, R. T., & Tester, M. (2011). Phenomics–technologies to relieve the phenotyping bottleneck. *Trends in plant science*, *16*(12), 635-644.

Grafius, J. E. (1964). A Geometry for Plant Breeding 1. *Crop science*, *4*(3), 241-246.

Gregory, T. R. (2009). Artificial selection and domestication: modern lessons from Darwin's enduring analogy. *Evolution: Education and Outreach*, *2*(1), 5-27.

Gustavsson, A. M. (2011). A developmental scale for perennial forage grasses based on the decimal code framework. *Grass and Forage Science*, *66*(1), 93-108.

Hammer, K. (1984). Das domestikationssyndrom. *Die Kulturpflanze*, *32*(1), 11-34.

Hampton, J., & Hebblethwaite, P. (1985). The effect of growth retardant application on floret site utilisation and assimilate distribution in ears of perennial ryegrass cv. S. 24. *Annals of applied biology*, *107*(1), 127-136.

Hare, M., Lunpha, A., & Phengphet, S. (2008). Effect of foliar applications of trinexapac-ethyl plant growth regulator on seed yield in brachiaria hybrid cv. Mulato II and Paspalum atratum. *TG: Tropical Grasslands*, *42*(3), 181.

Harlan, J. R., De Wet, J., & Price, E. G. (1973). Comparative evolution of cereals. *Evolution*, *27*(2), 311-325.

Harun, R. R., & Bean, E. (1979). Seed development and seed shedding in North Italian ecotypes of Lolium multiflorum. *Grass and forage science*, *34*(3), 215-220.

Heineck, G., Watkins, E., & Ehlke, N. J. (2018). Exploring alternative management options for multiyear perennial ryegrass seed production in northern Minnesota. *Crop science*, *58*(1), 426-434.

Heineck, G. C., Ehlke, N. J., Altendorf, K. R., Denison, R. F., Jungers, J. M., Lamb, E. G., & Watkins, E. (2020). Relationships and influence of yield components on spaced-plant and sward seed yield in perennial ryegrass. *Grass and Forage Science*, *75*(4), 424-437.

Hintze, C., Heydel, F., Hoppe, C., Cunze, S., König, A., & Tackenberg, O. (2013). D3: the dispersal and diaspore database–baseline data and statistics on seed dispersal. *Perspectives in Plant Ecology, Evolution and Systematics*, *15*(3), 180-192.

Ishii, T., Numaguchi, K., Miura, K., Yoshida, K., Thanh, P. T., Htun, T. M., . . . Terauchi, R. (2013). OsLG1 regulates a closed panicle trait in domesticated rice. *Nature genetics*, *45*(4), 462-465.

Jannink, J.-L., Lorenz, A. J., & Iwata, H. (2010). Genomic selection in plant breeding: from theory to practice. *Briefings in functional genomics*, *9*(2), 166-177.

Ji, H.-S., Chu, S.-H., Jiang, W., Cho, Y.-I., Hahn, J.-H., Eun, M.-Y., . . . Koh, H.-J. (2006). Characterization and mapping of a shattering mutant in rice that corresponds to a block of domestication genes. *Genetics*, *173*(2), 995-1005.

Jia, Y., & Jannink, J.-L. (2012). Multiple-trait genomic selection methods increase genetic value prediction accuracy. *Genetics*, *192*(4), 1513-1522.

Jiang, L., Ma, X., Zhao, S., Tang, Y., Liu, F., Gu, P., . . . Sun, C. (2019). The APETALA2-like transcription factor SUPERNUMERARY BRACT controls rice seed shattering and seed size. *The Plant Cell*, *31*(1), 17-36.

Joaquin, T., Trejo, C., Hernandez-Garay, A., Perez, P., De G. Garcia, S., & Quero, C. (2007). Effects of ethephon, salicylic acid and cidef-4 on the yield and quality of guinea grass seed. *Tropical Grasslands*, *41*(1), 55.

Jofuku, K. D., Den Boer, B., Van Montagu, M., & Okamuro, J. K. (1994). Control of Arabidopsis flower and seed development by the homeotic gene APETALA2. *The Plant Cell*, *6*(9), 1211-1225.

Jubery, T. Z., Shook, J., Parmley, K., Zhang, J., Naik, H. S., Higgins, R., . . . Ganapathysubramanian, B. (2017). Deploying Fourier coefficients to unravel soybean canopy diversity. *Frontiers in Plant Science*, *7*, 2066.

Kadkol, G. (2009). Brassica shatter-resistance research update. Proceedings of the 16th Australian research assembly on brassicas conference, Ballarat Victoria,

Kadkol, G. P., Halloran, G. M., MacMillan, R. H., & Caviness, C. (1989). Shatter resistance in crop plants. *Critical reviews in plant sciences*, *8*(3), 169-188.

Keith, R. A., & Mitchell-Olds, T. (2019). Antagonistic selection and pleiotropy constrain the evolution of plant chemical defenses. *Evolution*, *73*(5), 947-960.

Kellogg, E. A., Camara, P. E., Rudall, P. J., Ladd, P., Malcomber, S. T., Whipple, C. J., & Doust, A. N. (2013). Early inflorescence development in the grasses (Poaceae). *Frontiers in Plant Science*, *4*, 250.

Klein, L. M., & Harmond, J. E. (1971). Seed moisture--a harvest timing index for maximum yields. *Transactions of the ASAE*, *14*(1), 124-0126.

Klingenberg, C. P., & Monteiro, L. R. (2005). Distances and directions in multidimensional shape spaces: implications for morphometric applications. *Systematic Biology*, *54*(4), 678-688.

Koeritz, E. J., Watkins, E., & Ehlke, N. J. (2013). A split application approach to nitrogen and growth regulator management for perennial ryegrass seed production. *Crop Science*, *53*(4), 1762-1777.

Konishi, S., Izawa, T., Lin, S. Y., Ebana, K., Fukuta, Y., Sasaki, T., & Yano, M. (2006). An SNP caused loss of seed shattering during rice domestication. *Science*, *312*(5778), 1392-1396.

Kuhl, F. P., & Giardina, C. R. (1982). Elliptic Fourier features of a closed contour. *Computer Graphics and Image Processing*, *18*(3), 236-258.

Lamo, J., Tongoona, P., Okori, P., Derera, J., Hendricks, R., & Laing, M. (2011). A New Cheap and Efficient Single-Grain Shatter Tester for Use in Rice Breeding. *Crop science*, *51*(2), 651-655.

Larson, S. R., & Kellogg, E. A. (2009). Genetic dissection of seed production traits and identification of a major-effect seed retention QTL in hybrid Leymus (Triticeae) wildryes. *Crop science*, *49*(1), 29-40.

Law, R. (1979). The cost of reproduction in annual meadow grass. *The American Naturalist*, *113*(1), 3-16.

Lee, S.-K. (2006). Plant growth regulators and shattering control in cool-season perennial grasses.

Lee, T.-C., Kashyap, R. L., & Chu, C.-N. (1994). Building skeleton models via 3-D medial surface axis thinning algorithms. *CVGIP: Graphical Models and Image Processing*, *56*(6), 462-478.

Li, L.-F., & Olsen, K. (2016). To have and to hold: selection for seed and fruit retention during crop domestication. *Current topics in developmental biology*, *119*, 63-109.

Li, M., Frank, M. H., Coneva, V., Mio, W., Chitwood, D. H., & Topp, C. N. (2018). The persistent homology mathematical framework provides enhanced genotype-to-phenotype associations for plant morphology. *Plant Physiology*, *177*(4), 1382-1395.

Li, M., Shao, M. R., Zeng, D., Ju, T., Kellogg, E. A., & Topp, C. N. (2020). Comprehensive 3D phenotyping reveals continuous morphological variation across genetically diverse sorghum inflorescences. *New Phytologist*, *226*(6), 1873-1885.

Li, W., & Gill, B. S. (2006). Multiple genetic pathways for seed shattering in the grasses. *Functional & Integrative Genomics*, *6*(4), 300-309.

Liljegren, S. J., Ditta, G. S., Eshed, Y., Savidge, B., Bowman, J. L., & Yanofsky, M. F. (2000). SHATTERPROOF MADS-box genes control seed dispersal in Arabidopsis. *Nature*, *404*(6779), 766-770.

Lin, Z., Li, X., Shannon, L. M., Yeh, C.-T., Wang, M. L., Bai, G., . . . Clemente, T. E. (2012). Parallel domestication of the Shattering1 genes in cereals. *Nature genetics*, *44*(6), 720-724.

Mathiassen, S. K., Rabølle, M., Boelt, B., & Kudsk, P. (2007). Factors affecting the activity of Moddus M in red fescue. *Seed Production in the Northern Light*, 197.

Matzrafi, M., Preston, C., & Brunharo, C. A. (2021). evolutionary drivers of agricultural adaptation in Lolium spp. *Pest Management Science*, *77*(5), 2209-2218.

Mir, R. R., Reynolds, M., Pinto, F., Khan, M. A., & Bhat, M. A. (2019). High-throughput phenotyping for crop improvement in the genomics era. *Plant Science*, *282*, 60-72.

Momen, M., Bhatta, M., Hussain, W., Yu, H., & Morota, G. (2021). Modeling multiple phenotypes in wheat using data-driven genomic exploratory factor analysis and Bayesian network learning. *Plant Direct*, *5*(1), e00304.

Moore, K., Moser, L. E., Vogel, K. P., Waller, S. S., Johnson, B., & Pedersen, J. F. (1991). Describing and quantifying growth stages of perennial forage grasses. *Agronomy Journal*, *83*(6), 1073-1077.

Nathan, R., Schurr, F. M., Spiegel, O., Steinitz, O., Trakhtenbrot, A., & Tsoar, A. (2008). Mechanisms of long-distance seed dispersal. *Trends in Ecology & Evolution*, *23*(11), 638-647.

Neto, J. C., Meyer, G. E., Jones, D. D., & Samal, A. K. (2006). Plant species identification using Elliptic Fourier leaf shape analysis. *Computers and Electronics in Agriculture*, *50*(2), 121-134.

Nilsen, E. T., & Orcutt, D. M. (1996). Physiology of plants under stress. Abiotic factors. *Physiology of plants under stress. Abiotic factors.*

Obraztsov, V., Shchedrina, D., & Kadyrov, S. (2018). Film agents as an effective means of reducing seed shattering in Festulolium.

Onishi, K., Takagi, K., Kontani, M., Tanaka, T., & Sano, Y. (2007). Different patterns of genealogical relationships found in the two major QTLs causing reduction of seed shattering during rice domestication. *Genome*, *50*(8), 757-766.

Otsu, N. (1979). A threshold selection method from gray-level histograms. *IEEE transactions on systems, man, and cybernetics*, *9*(1), 62-66.

Oury, F.-X., & Godin, C. (2007). Yield and grain protein concentration in bread wheat: how to use the negative relationship between the two characters to identify favourable genotypes? *Euphytica*, *157*(1), 45-57.

Patterson, S. E. (2001). Cutting loose. Abscission and dehiscence in Arabidopsis. *Plant physiology*, *126*(2), 494-500.

Peleg, Z., Fahima, T., Korol, A. B., Abbo, S., & Saranga, Y. (2011). Genetic analysis of wheat domestication and evolution under domestication. *Journal of experimental botany*, *62*(14), 5051-5061.

Philipp, I., & Rath, T. (2002). Improving plant discrimination in image processing by use of different colour space transformations. *Computers and electronics in agriculture*, *35*(1), 1-15.

Rebolledo, M. C., Peña, A. L., Duitama, J., Cruz, D. F., Dingkuhn, M., Grenier, C., & Tohme, J. (2016). Combining image analysis, genome wide association studies and different field trials to reveal stable genetic regions related to panicle architecture and the number of spikelets per panicle in rice. *Frontiers in plant science*, *7*, 1384.

Roberts, J. A., Elliott, K. A., & Gonzalez-Carranza, Z. H. (2002). Abscission, dehiscence, and other cell separation processes. *Annual review of plant biology*, *53*(1), 131-158.

Robledo-Arnuncio, J. J., Klein, E. K., Muller-Landau, H. C., & Santamaría, L. (2014). Space, time and complexity in plant dispersal ecology. *Movement ecology*, *2*(1), 1-17.

Rolston, P., Trethewey, J., Chynoweth, R., & McCloy, B. (2010). Trinexapac-ethyl delays lodging and increases seed yield in perennial ryegrass seed crops. *New Zealand Journal of Agricultural Research*, *53*(4), 403-406.

Ross-Ibarra, J., Morrell, P. L., & Gaut, B. S. (2007). Plant domestication, a unique opportunity to identify the genetic basis of adaptation. *Proceedings of the National Academy of Sciences*, *104*(suppl_1), 8641-8648.

Saastamoinen, M., Bocedi, G., Cote, J., Legrand, D., Guillaume, F., Wheat, C. W., . . . Husby, A. (2018). Genetics of dispersal. *Biological Reviews*, *93*(1), 574-599.

Sampoux, J. P., Baudouin, P., Bayle, B., Béguier, V., Bourdon, P., Chosson, J., . . . Ghesquière, M. (2013). Breeding perennial ryegrass (L olium perenne L.) for turf usage: an assessment of genetic improvements in cultivars released in E urope, 1974–2004. *Grass and Forage Science*, *68*(1), 33-48.

San-Miguel, A., Kurshan, P. T., Crane, M. M., Zhao, Y., McGrath, P. T., Shen, K., & Lu, H. (2016). Deep phenotyping unveils hidden traits and genetic relations in subtle mutants. *Nature communications*, *7*(1), 1-13.

Sartie, A., Easton, H., Matthew, C., Rolston, M., & Faville, M. (2018). Seed yield in perennial ryegrass (Lolium perenne L.): comparative importance of component traits and detection of seed-yield-related QTL. *Euphytica*, *214*(12), 1-19.

Sartie, A. M. (2006). *Phenotypic assessment and quantitative trait locus (QTL) analysis of herbage and seed production traits in perennial ryegrass (Lolium perenne L.): a thesis presented in partial fulfilment of the requirements for the degree of Doctor of Philosophy (Ph. D.) in Plant Science, Institute of Natural Resources, College of Sciences, Massey University, Palmerston North, New Zealand* Massey University].

Schulthess, A. W., Reif, J. C., Ling, J., Plieske, J., Kollers, S., Ebmeyer, E., . . . Ganal, M. W. (2017). The roles of pleiotropy and close linkage as revealed by association mapping of yield and correlated traits of wheat (Triticum aestivum L.). *Journal of Experimental Botany*, *68*(15), 4089-4101.

Shah, S., Pearson, C., & Read, J. (1990). Variability in habit, flowering and seed production within the Kangaroo Valley cultivar of Lolium perenne when grown in a range of environments. *Australian Journal of Agricultural Research*, *41*(5), 901-909.

Shearman, R., & Beard, J. (1975). Turfgrass Wear Tolerance Mechanisms: I. Wear Tolerance of Seven Turfgrass Species and Quantitative Methods for Determining Turfgrass Wear Injury 1. *Agronomy journal*, *67*(2), 208-211.

Silberstein, T., Mellbye, M., Chastain, T., & Young III, W. (2004). Response of seed yield to swathing time in annual and perennial ryegrass. *SEED PRODUCTION RESEARCH*, 20.

Silberstein, T. B., Mellbye, M. E., Chastain, T. G., & Young, W. C. (2010). Using seed moisture as a harvest management tool.

Silberstein, T. B., Mellbye, M. E., III, W. C. Y., & Chastain, T. G. (2007). Using seed moisture to determine optimum swathing time in annual ryegrass (Lolium multiflorum Lam.) seed production. *Seed production in the northern light*, 270.

Simon U, Hare MD, Kjaersgaard B, Clifford PTP, Hampton JG, & MJ, H. (1997). Harvest and post harvest management of forage seed crops. *Forage Seed Production. 1. Temperate Species (Fairey DT, Hampton JG eds.)*, 181-217.

Simons, K. J., Fellers, J. P., Trick, H. N., Zhang, Z., Tai, Y.-S., Gill, B. S., & Faris, J. D. (2006). Molecular characterization of the major wheat domestication gene Q. *Genetics*, *172*(1), 547-555.

Spengler III, R. N. (2020). Anthropogenic seed dispersal: Rethinking the origins of plant domestication. *Trends in plant science*, *25*(4), 340-348.

Studer, B., Jensen, L. B., Hentrup, S., Brazauskas, G., Kölliker, R., & Lübberstedt, T. (2008). Genetic characterisation of seed yield and fertility traits in perennial ryegrass (Lolium perenne L.). *Theoretical and Applied Genetics*, *117*(5), 781-791.

Tackenberg, O., Poschlod, P., & Bonn, S. (2003). Assessment of wind dispersal potential in plant species. *Ecological Monographs*, *73*(2), 191-205.

Tang, H., Cuevas, H. E., Das, S., Sezen, U. U., Zhou, C., Guo, H., . . . Paterson, A. H. (2013). Seed shattering in a wild sorghum is conferred by a locus unrelated to domestication. *Proceedings of the National Academy of Sciences*, *110*(39), 15824-15829.

Taylor, J. E., & Whitelaw, C. A. (2001). Signals in abscission. *New Phytologist*, *151*(2), 323-340.

Team, R. C. (2013). R: A language and environment for statistical computing.

Teramura, A. H., & Sullivan, J. H. (1994). Effects of UV-B radiation on photosynthesis and growth of terrestrial plants. *Photosynthesis research*, *39*(3), 463-473.

Terrell, E. E. (1968). *A taxonomic revision of the genus Lolium*. Agricultural Research Service, US Department of Agriculture.

Thomson, F. J., Moles, A. T., Auld, T. D., Ramp, D., Ren, S., & Kingsford, R. T. (2010). Chasing the unknown: predicting seed dispersal mechanisms from plant traits. *Journal of Ecology*, *98*(6), 1310-1318.

Thorogood, D. (2003). Perennial ryegrass (Lolium perenne L.). *Turfgrass biology, genetics, and breeding. New York: Wiley*, 75-105.

Thorwarth, P., Liu, G., Ebmeyer, E., Schacht, J., Schachschneider, R., Kazman, E., . . . Longin, C. F. H. (2019). Dissecting the genetics underlying the relationship between protein content and grain yield in a large hybrid wheat population. *Theoretical and applied genetics*, *132*(2), 489-500.

Topp, C. N., Iyer-Pascuzzi, A. S., Anderson, J. T., Lee, C.-R., Zurek, P. R., Symonova, O., . . . Galkovskyi, T. (2013). 3D phenotyping and quantitative trait locus mapping identify core regions of the rice genome controlling root architecture. *Proceedings of the National Academy of Sciences*, *110*(18), E1695-E1704.

Trethewey, J., & Rolston, M. (2008). Is the flag leaf important in perennial ryegrass seed production? *NZGA: Research and Practice Series*, *14*, 67-73.

Tubbs, T. B. (2021). Topometric analysis for high-throughput phenotyping of seed shattering in Perennial Pyegrass (*Lolium perenne* L.).

Ubbens, J., Cieslak, M., Prusinkiewicz, P., Parkin, I., Ebersbach, J., & Stavness, I. (2020). Latent space phenotyping: automatic image-based phenotyping for treatment studies. *Plant Phenomics*, *2020*.

Valenta, K., & Nevo, O. (2020). The dispersal syndrome hypothesis: how animals shaped fruit traits, and how they did not. *Functional Ecology*, *34*(6), 1158-1169.

Van der Walt, S., Schönberger, J. L., Nunez-Iglesias, J., Boulogne, F., Warner, J. D., Yager, N., . . . Yu, T. (2014). scikit-image: image processing in Python. *PeerJ*, *2*, e453.

van Nocker, S. (2009). Development of the abscission zone. *Stewart Postharvest Review*, *5*(1), 5.

Virtanen, P., Gommers, R., Oliphant, T. E., Haberland, M., Reddy, T., Cournapeau, D., . . . Bright, J. (2020). SciPy 1.0: fundamental algorithms for scientific computing in Python. *Nature methods*, *17*(3), 261-272.

Wang, X., Xuan, H., Evers, B., Shrestha, S., Pless, R., & Poland, J. (2019). High-throughput phenotyping with deep learning gives insight into the genetic architecture of flowering time in wheat. *GigaScience*, *8*(11), giz120.

Warringa, J. W. (1997). *Physiological constraints to seed growth in perennial ryegrass (Lolium perenne L.)*. Warringa.

Wilkins, P. (1991). Breeding perennial ryegrass for agriculture. *Euphytica*, *52*(3), 201-214.

Wolde, G. M., Trautewig, C., Mascher, M., & Schnurbusch, T. (2019). Genetic insights into morphometric inflorescence traits of wheat. *Theoretical and Applied Genetics*, *132*(6), 1661-1676.

Wood, B. W., Lombardini, L., & Heerema, R. J. (2009). Influence of aminoethoxyvinylglycine on pecan fruit retention. *HortScience*, *44*(7), 1884-1889.

Wu, W., Liu, X., Wang, M., Meyer, R. S., Luo, X., Ndjiondjop, M.-N., . . . Cai, H. (2017). A single-nucleotide polymorphism causes smaller grain size and loss of seed shattering during African rice domestication. *Nature Plants*, *3*(6), 1-7.

Yadav, S. P., Ibaraki, Y., & Dutta Gupta, S. (2010). Estimation of the chlorophyll content of micropropagated potato plants using RGB based image analysis. *Plant Cell, Tissue and Organ Culture (PCTOC)*, *100*(2), 183-188.

Yao, N., Wang, L., Yan, H., Liu, Y., & Lu, B.-R. (2015). Mapping quantitative trait loci (QTL) determining seed-shattering in weedy rice: evolution of seed shattering in weedy rice through de-domestication. *Euphytica*, *204*(3), 513-522.

Yoon, J., Cho, L.-H., Antt, H. W., Koh, H.-J., & An, G. (2017). KNOX protein OSH15 induces grain shattering by repressing lignin biosynthesis genes. *Plant Physiology*, *174*(1), 312-325.

Yu, Y., & Kellogg, E. A. (2018). Inflorescence abscission zones in grasses: diversity and genetic regulation. *Annual plant reviews online*, 497-532.

Yu, Y., Leyva, P., Tavares, R. L., & Kellogg, E. A. (2020). The anatomy of abscission zones is diverse among grass species. *American journal of botany*, *107*(4), 549-561.

Yuan, R., & Carbaugh, D. H. (2007). Effects of NAA, AVG, and 1-MCP on ethylene biosynthesis, preharvest fruit drop, fruit maturity, and quality of 'Golden Supreme'and 'Golden Delicious' apples. *HortScience*, *42*(1), 101-105.

Zhang, G., & Mergoum, M. (2007). Developing evaluation methods for kernel shattering in spring wheat. *Crop science*, *47*(5), 1841-1850.

Zhang, Y., Ran, Y., Nagy, I., Lenk, I., Qiu, J. L., Asp, T., . . . Gao, C. (2020). Targeted mutagenesis in ryegrass (Lolium spp.) using the CRISPR/Cas9 system. *Plant biotechnology journal*, *18*(9), 1854.

Zhou, Y., Lu, D., Li, C., Luo, J., Zhu, B.-F., Zhu, J., . . . Zhou, B. (2012). Genetic control of seed shattering in rice by the APETALA2 transcription factor SHATTERING ABORTION1. *The Plant Cell*, *24*(3), 1034-1048.

Zhou, Y., Srinivasan, S., Mirnezami, S. V., Kusmec, A., Fu, Q., Attigala, L., . . . Schnable, P. S. (2019). Semiautomated feature extraction from RGB images for sorghum panicle architecture GWAS. *Plant physiology*, *179*(1), 24-37.

Zingaretti, L. M., Monfort, A., & Pérez-Enciso, M. (2021). Automatic fruit morphology phenome and genetic analysis: An application in the octoploid strawberry. *Plant Phenomics, 2021*.